Assessing Mold Risks in Buildings under Uncertainty

A Thesis
Presented to
The Academic Faculty

By

Hyeun Jun Moon

In Partial Fulfillment
of the Requirements for the Degree
Doctor of Philosophy in the
College of Architecture

Georgia Institute of Technology
August 2005

Assessing Mold Risks in Buildings under Uncertainty

Approved by:

Prof. Godfried Augenbroe, Advisor
College of Architecture
Georgia Institute of Technology

Dr. Linda Thomas-Mobley
College of Architecture
Georgia Institute of Technology

Dr. Andreas Holm
Hygrothermal Division
Fraunhofer-Institut Bauphysik (IBP)

Dr. Russell Gentry
College of Architecture
Georgia Institute of Technology

Dr. Charlene Bayer
Electro-Optics, Environment and Materials Laboratory
Georgia Tech Research Institute

Date Approved: May 19. 2005

In memory of *Chang-Bae Moon*

ACKNOWLEDGEMENTS

This dissertation would not have been realized without the support and help from everyone around me. Foremost I would like to thank Professor Godfried Augenbroe, who gave me this once-in-a-life-time opportunity to work with him at Georgia Tech. He opened my eyes to the building technology research area and encouraged me to keep up with the good work. I will never forget his words to me at the first year of my Ph.D. study "Think hard! Slowly but surely!" I would like to thank my dissertation committee members, who guided to complete this work: Dr. Linda Thomas-Mobley, Dr. Andreas Holm (IBP, Germany), Dr. Russell Gentry, and Dr. Charlene Bayer (GTRI). I am also indebted to the faculty in the Ph.D. program in the College of Architecture, especially professor Chuck Eastman (Ph.D. program director), Dr. Crag Zimring, Dr. Ruchi Choudhary, and my minor advisor Dr. Sham Navathe (College of Computing) for their advice and support.

It would not have been such a great and pleasurable experience at Georgia Tech without my friends and colleagues whom I spent most of my time with at school both day-and-night. In particular, I wish to thank Dr. Cheol-Soo Park, Mate Thitisawat, and all my colleagues in the building technology and design computing programs.

I cannot thank enough my former mentor Dr. Jang-Yeul Sohn at Hanyang University who first introduced me to the research area of building technology. He guided me through the new world and taught me everything to become a successful researcher, more than I ever dreamed of.

My family deserves special thanks for their support and understanding throughout the years I was a student, patiently watching my me progress. I thank my parents and parents-in-law who always trusted and supported me in any circumstances. I, of course, would like to express the deepest appreciation to my wife Eun Kang Kim and my daughter Christina Doyun Moon. They always made me smile when I came home at night and motivated me to study hard the next morning. They are the ones who deserve resounding and eternal praise for help me finish this dissertation.

Above all, thank God! With you, I have been at peace throughout the entire course of my study.

TABLE OF CONTENTS

LIST OF TABLES

LIST OF FIGURES

SUMMARY

Microbial growth in indoor spaces has been identified as the main moisture-related cause of Indoor Air Quality (IAQ) problems. Although studies in the past several decades have been conducted to identify ways to assess, mitigate, and predict mold problems in buildings, quantified mold growth risk assessment is not yet available. In many cases, mold occurrence involves local, situational, and sometimes idiosyncratic aspects of a building during its operation. These unexpected behaviors cannot be captured by current deterministic performance evaluation methods. Hence, this study has attempted to develop a probabilistic performance indicator for mold growth risk by treating mold as a risk and a limit state phenomenon. This new approach requires a reliable aggregation method to arrive at quantified mold growth risk and the extension of standard simulation capacity to account for additional mechanisms of the mold phenomenon. It also implicates uncertainty in building parameters, including natural variation of hygrothermal properties in building materials, deviation between "as-designed" values, and the actual "in-use" values of the parameters.

In this study, the mold germination stage is considered a limiting criterion for risk, realized by using the mold germination graph method based on local environmental conditions calculated from hygrothermal models and a standard mold germination graph. This method keeps track of the environmental conditions (i.e., surface temperature, relative humidity) at previous time steps so that the effect of the fluctuating conditions can be considered. A comparative study using the mold limitation curves in ESP-r

showed that the mold germination graph method could provide quantitative evaluation results in terms of mold growth risk.

The current standard moisture simulation was extended to account for additional mechanisms of the mold phenomenon (e.g., thermal bridge, workmanship, infiltration), based on four identified cause categories that represent the four areas in which an extension of simulation capabilities would be needed in order to produce accurate assessments. These extensions were realized using a mix of existing simulation tools, each specialized in a particular domain of heat, air, and moisture transport. The effects of thermal bridge and potential bad workmanship in a particular building construction technology are expressed with the temperature factor. By including the temperature factor at certain building details in the mixed simulation approach, the mold growth risky days can be approximately represented at a specific trouble spot.

The uncertainties of each building parameter are expressed as upper/lower values with a probability distribution based on available data in the literature, different models, and field measurements. The uncertainty associated with the temperature factor is investigated by establishing an empirical relationship between an idealized thermal bridge and potential bad workmanship. The quantified uncertainties of the parameters are propagated through the mixed simulation approach using the Latin Hypercube Sampling method, which is particularly suited for this purpose. The results of the uncertainty analysis provide the distribution of mold growth risk at a trouble spot in a particular building. The identification of dominant parameters that have a major influence on mold risk is performed using a parameter screening technique suggested by Morris(1991). Knowledge of these dominant parameters is vital, as they point to the areas that require

special attention during design and construction in order to guarantee a mold free environment over the life cycle of the facility.

The application of the developed mold risk indicator (MRI) is reported in three case studies: one virtual office building in Miami and two existing buildings with mold problems in Atlanta. The results of each case study are encouraging. They indicate that a reliable distribution of mold growth risk may result from the uncertainty analysis, as the actual mold growth occurrence could be related to the established mold risk in each case. The new approach thus seems capable of explaining unexpected and non-deterministic mold growth occurrences. Moreover, it identifies the parameters that have dominant effects on the increase in mold risk. Identification of these parameters leads to recommendations and guidelines for designers and engineers to guarantee better building performance.

The new performance indicator for mold risk is capable to reveal the actual mold risks going beyond the deterministic assessment. The identification of the parameters that have a major influence on mold risk may provide a long-awaited breakthrough for early control of mold risk, i.e., during design, commissioning, and A/E procurement. More calibration and validation will be necessary but the early results reported in this thesis indicate that the new mold risk indicator provides a foundation for establishing building performance criteria that will prevent mold in buildings.

CHAPTER 1

INTRODUCTION

1.1 OBJECTIVES OF THE STUDY

Microbial growth in buildings has been identified as the main moisture-related cause of Indoor Air Quality (IAQ) problems. Mold causes warping and twisting of framing members, deterioration of the building finish, structural damage, a reduction in the effectiveness of thermal insulation, paint peeling, and nail popping. More importantly, recent research has shown that the growth and spread of mold is related to adverse health effects such as asthma, coughing, wheezing, and upper respiratory tract symptoms. These mold-related health problems have created liability issues in the building industry. Due to increased public interest in health issues and the recent discovery of the adverse effects of mold infestation, preventing mold problems in the building industry is currently a high priority in the A/E/C research community.

In an effort to reduce mold problems in the building industry, national and international standards define upper limits on acceptable relative humidity in buildings. Unfortunately, this descriptive approach has failed to provide a mold-free environment, and many modern buildings continue to suffer from harmful levels of mold growth. Despite several decades of research aimed at preventing mold growth in buildings, the relationships between the probability of mold growth and certain types of building systems and usage parameters have not yet been fully established. While it is easy to associate low energy performance with certain parameters (high U-values of the

enclosure, low HVAC efficiency, and others), this is not so in the case of mold as the causalities with respect to the performance of a building system to avoid favorable mold growth conditions is more complex. Recent research has shown that mold occurrence is influenced by a multitude of parameters with complex physical and biological interactions (Burge 2002; Moon and Augenbroe 2003). As a result, mold problems are not well anticipated in the design stage. Moreover, once they occur in an operational building, it is difficult to determine the real causes and propose the best remedial actions.

Indoor mold growth is likely to occur when a combination of relatively high humidity and temperature on building material surfaces constitutes favorable conditions for mold germination. Recent experimental research on mold growth has revealed the relationships between the physical-biological conditions (involving relative humidity and temperature) and occurring mold growth. These relationships are now used in a "standard" simulation to assess mold growth risk on a local or whole building scale. Currently available evaluation methods use hygrothermal models based on the first-order physical principles of heat and mass transfer. A good example is WUFI (Kuenzel, Karagiozis 2000) which solves the non-linear coupled heat and mass transfer equations in local one-dimensional (1D) and two-dimensional (2D) geometries.

Although these models are accurate and validated with experimental results, they typically use as-designed building information in simulations. This information is based on an "idealization of the building," i.e., the building is assumed to be constructed and operated as designed and specified. These assumptions do not reflect the local, situational, and sometimes idiosyncratic aspects of building use and operation, which contribute to mold growth in existing buildings. For example, when a building is specified to be

operated at 22 °C with 50% of RH in a space, mold should not be found to be present in the building when an idealized mold growth analysis is used. However, in reality, most actual buildings undergo changes in building operation and usage, resulting in some specific cases to mold growth. Thus, the assumption of idealization of the building has proven inadequate for assessing mold risk in real-life, "in-use" buildings because important "non standard" factors related to building operation characteristics, envelope details, HVAC operational schedules, local ventilation conditions, cleaning regimes, and others are left outside the equation.

With a "design-interpreted idealization" of a building as input model, current building performance evaluation methods typically only provide a deterministic result of building performance. This approach does not include uncertainties related to natural variation of building material properties, physical and biological parameters, operational deviation from design specifications, and so on. The assessment of uncertainties is particularly relevant when a certain effect cannot be explained deterministically. In fact mold growth typically occurs unexpectedly and, in many cases, inexplicably due to unanticipated deviations from the assumed idealized operation point of the building. Capturing the effect of these deviations calls for the development of a new performance indicator that expresses the likelihood that a certain deviating circumstances will occur during the service life of a building.

The deviations between design specification and in-use building parameters involve all stages of a building project from early design to operation. In fact, all design decisions and activities in building construction and management affect the eventual mold growth risk. Examples of such decisions and activities are inappropriate building

component design, faulty construction and installation of the envelope and ventilation systems, selection of unsuitable building materials, mismanagement of building materials on the construction site, inadequate operation of HVAC system and improper building maintenance, and so on.

The unexpected occurrence of mold problems in existing buildings has triggered a number of research questions. One obvious question is whether a special performance indicator for mold, i.e. a mold risk indicator, can be established that will alert in cases where an increased risk is present. This study is an attempt to answer this question.

Mold growth is a continuous phenomenon from non-visible fungi states to visible mold infestation on building surfaces. Recent research has shown a general link between mold and adverse human health. It is however not easy to answer the following questions. What is the acceptable level regarding mold presence in built environment? How could the health risk of mold be quantified and measured to support a mold risk analysis?

Mold growth involves various causes and complex bio-physical mechanisms that take place at a certain location with certain building details. These locations will be referred to generically as "trouble spots." To study the mold phenomenon at these trouble spots, the following questions arise. What are the main causes or mechanisms of "unexpected" occurrences of mold in buildings? What are the additional mechanisms that should be included in an extension of current standard simulation model capabilities?

No systematic analyses have been conducted to quantify the deviations between as-designed idealization of buildings and their in situ reality. This leads to the question how the uncertainties in simulation model parameters can be quantified in a systematic way. A corollary question is, after we know what the main deviations are, how we could

reduce these deviations by enforcing an improved design and procurement process? But first it needs to be established what the potential role of the deviations are in the potential occurrences of mold growth. If certain types of (uncertain) deviations can be prioritized, these should obviously be targeted first in the improvement of the A/E procurement process.

Before a mold analysis under uncertainty can be conducted, there are a range of issues that need to be addressed. Can a building be guaranteed to be mold-free under uncertainty and what confidence level can be given to mold growth assessments? What could be an ultimate measure of mold growth risk, and would this lead to an indicator that could be used in a future standard? How could this lead to a normative indicator and how could such a normative measure be used to guarantee better building performance over the entire life cycle of a building from the design and procurement processes to construction and building operation?

This dissertation addresses these questions in a development of a novel measure of mold growth risk under uncertainty. By incorporating uncertainty in mold risk analysis, one can achieve probabilistic results that reflect the natural variation in building materials, variation in internal heat and moisture loads, errors in construction, bad workmanship in the installation of building components, and so on. This approach enables realistic predictions for mold problems in buildings. The primary objective of this study is therefore to establish a probabilistic performance measure for mold growth avoidance. Such a measure will take the form of a mold risk indicator, i.e. a probability distribution of a measure of mold occurrence. The importance of the probabilistic outcome for mold growth analysis was confirmed at a recent workshop about the future research needs,

organized by HUD in 2004. The report stated as one of its outcomes the "urgent research need to develop stochastic moisture models using probabilistic outputs (ranges) to reflect errors due to weather (external loads), material variations, and internal load variations."(HUD 2004)

The main idea of the new probabilistic performance indicator is discussed in the next section. The issues and the requirements for each component of the indicator are described in the following chapters. The merits of the new approach are elucidated on three case studies later.

1.2 A New Approach for Mold Growth Analysis

If the construction and operation of buildings would be fully predictable, and be realized without any errors, it would be possible to predict its environmental conditions over time with a high level of certainty and hence predict any potential mold growth at surfaces where favorable conditions may occur over its service life. However, in reality, all buildings and subsystems deviate from their design specifications, their programmed usage and expected operating points. Moreover, many specifics of the building and the physical processes that occur in it, cannot be known with certainty and therefore add additional uncertainty, such as natural variations in material properties and variations in flow conditions near obstacles, not perfectly calibrated ventilation systems, the role of dust, aerosol movement processes, complex temperature stratification patterns, etc. It is important to distinguish sources of uncertainty as will be explained in the next chapters. One general source of uncertainty is the fact that buildings are not delivered as expected. Another major source of uncertainty is that our knowledge and representation of the physical processes in the building are imperfect. In general, most deviations between the idealized expectation and reality stem from design errors, bad workmanship in installation of building components, change of building use and operation schedule, lack of maintenance, and so on. All of them contribute to unexpected situations during operation of the building. This study starts from the hypothesis that it is exactly this type of unexpected situations that leads to building failure or below-standard performance of building systems, which, among others, can eventually lead to mold growth problems. It is concluded that the deterministic use of the current simulation models is therefore not adequate for making a full assessment of mold risks in real -life buildings.

A risk based performance indicator uses estimates (probability distributions) of random deviations between "as-designed" values of design and operation specifications and the actual "in-use" values of these parameters. The parameters in question may represent building component properties, HVAC ad other device and building component parameters, construction detailing parameters, operation set points, maintenance event and efficiency parameters, and others. By considering the combined effects of these random parameter deviations in the simulation of the physical states of the building, the indicator of a performance aspect of a building and its systems (e.g., their combined performance to prevent a certain deterioration or pathological effect) can be analyzed and expressed as a quantified risk factor under the assumed randomness of the parameter values.

Following earlier work on uncertainty analysis of buildings (De Wit 2001), this analysis will identify three separate sources of uncertainty: (1) building behavior and operation uncertainty, (2) scenario uncertainty and (3) model uncertainty. In this study, we focus on the first source of uncertainty whereas we will deal with the second in an explicit fashion, repeating the analysis for a set of plausible usage scenarios. The third source of uncertainty is not deeply explored in this study. It is assumed that the mix of simulation tools used in this study is sufficiently accurate and validated to not introduce a major additional source of uncertainty in the calculation of material surface conditions which are used as the "drivers" of the mold occurrence. Modeling uncertainty will be discussed in more detail in chapter 5.

A brief description of the general set-up of uncertainty analysis follows: Depending on the specific building case, a relevant set of N causal parameters (causal is

used here to mean that a parameter is significant effect on the material surface temperature and humidity) is selected. The estimated potential deviations of the selected parameters from their as-designed values are quantified for specific building cases. This can be expressed as

$$Pi = Pi^* \pm \Delta i \tag{1.1}$$

Where P_i = range of actual value of a parameter (i=1…N)

P_i^* = design value of the parameter, i.e. representing the best expected value for the "design case"

Δ_i = random deviation in relation to the design value

The governing conditions for mold growth can be considered the result of a "standard" evaluation method, such as computer simulation (based on a set of agreed assumptions), with the superimposed effect of a deviation from the parameters. The resulting performance indicator (PI) can be mathematically expressed as follows:

$$PI = PI^* + X \tag{1.2}$$

where we have introduced PI* as the result of a standard simulation of the design case and X as the combined effect of all parameter uncertainties.

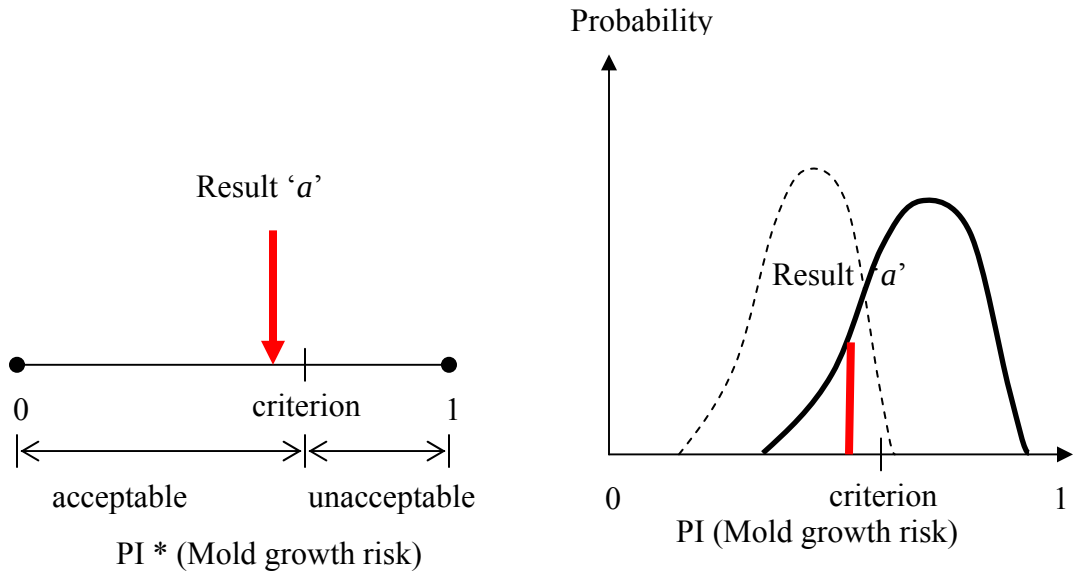

(a) deterministic PI*

(b) probabilistic PI

Figure 1.1 Current deterministic performance indicator (a) and a performance indicator based on an uncertainty analysis (b).

Figure 1.1 shows the basic approach. Current deterministic evaluation methods provide a deterministic result (e.g., '*a*') based on the idealized building representation, as shown in Figure 1.1 (a). If we assume that an acceptable mold avoidance criterion can be introduced, the result of the deterministic PI* may fall into the acceptable (regulated) range, depending on the choice of parameter values used in the simulation. The result from the deterministic approach can be easily changed and biased from the nonlinear effect of the combination of parameters in the simulation models.

Actual mold growth risk may lead to different interpretations by considering uncertainty. Figure 1.1. (b) shows two hypothetical results (solid and dashed line) that both correspond with the deterministic result but would lead to vastly different

interpretations of the mold risk. This example supports the view that the deterministic result is useless for mold risk assessment. A closer inspection of the figure explains this. The solid line would indicate that the actual risk far exceeds the performance criterion. Whereas the dotted line would indicate that the risk is very tolerable. If one would only do a deterministic simulation one would have no knowledge whether one is dealing with the solid or the dashed line and any distribution for that matter.

The figure suggests a mold risk criterion. It should be noted that such a criterion (risk threshold) has not yet been developed. It is plausible that such a criterion could be developed based on the mold risk indicator (MRI) which is the main focus of this thesis. It will be discussed that the MRI provides a foundation for a normative risk-based performance criterion for mold.

The figure above can also be interpreted in another way. It could be used to show how redesign (or better management of uncertainties in A/E procurement contracts) must attempt the transition of the solid line to the dotted line, indicating the reduction of the mold risk. It will be shown in Chapter 5 that a parameter screening technique can be used for this purpose. This technique identifies the set of dominant parameters that contribute the most to the increased risk of a performance indicator, potentially causing it to fall outside the acceptable range. Knowledge of these dominant parameters is vital, as they point to the systems that require special attention to guarantee acceptable performance.

1.3 ORGANIZATION OF THE THESIS

The outline of this thesis is as follows. Chapter 1 describes the objective of the study and the new approach for mold growth analysis. Chapter 2 focuses on the mold

phenomenon, reviews the required conditions for mold germination, and develops a new aggregation method. Chapter 3 provides an overview of the performance indicators and different approaches for each functional aspect of a building, introduces a risk view of mold and discusses the development of a probabilistic performance indicator for mold. Chapter 4 investigates the cause of mold problems in buildings and discusses the required extensions of the capacity of the current simulation methods and describes the mixed simulation approach in detail, providing the calculations for local environmental conditions. Chapter 5 introduces uncertainty in mold growth analysis and addresses the identification and quantification of uncertain parameters. Chapter 6 presents three case studies in which the approach is tested. The case studies include one virtual office building and two existing buildings, all of which show the merits of the developed new approach and its implications for the building industry. Chapter 7 evaluates the developed MRI and discusses its limitations. Chapter 8 completes the thesis with conclusions and an outlook towards future work.

CHAPTER 2

MOLD GROWTH IN BUILDINGS

2.1 MOLD PHENOMENON IN BUILDINGS

Mold growth in buildings, a phenomenon that has occurred as long as humans have lived inside of built environments, is not a new problem. However, the incidence of mold growth has increased as buildings have become more air tight due to higher energy costs. Mold growth problems can also be attributed to the use of new building materials. Thus, the control of this phenomenon has become a major concern to architects and builders. To control the mold phenomenon appropriately, we must first understand what mold actually is and what should be done to prevent mold growth during the course of building service life. This section addresses the consequences of mold problems and environmental conditions favorable to mold growth in buildings.

2.1.1 Consequences of mold growth in buildings

Various studies have reported the consequences of mold growth in buildings. It has been shown that indoor mold growth can cause adverse health effects and building damage, both of which lead to liability issues.

Recent research has revealed that mold is linked to adverse health effects such as asthma symptoms, coughing, wheezing, and upper respiratory track symptoms (Clark, Ammann 2004). Moreover, Bornehag (2001) found a strong relationship between damp buildings and a risk of respiratory symptoms, respiratory infections, allergies, and asthma.

Some fungi species are involved in producing mycotoxins, considered toxic to occupants (Robbins, Swenson 2000). The research community has generally agreed that mold occurrences in a building should be treated as causes of harmful health conditions and thus eliminated. However, the causal agents, underlying mechanisms, and the threshold level at which mold becomes a threat to human health, have not yet been fully established.

Moisture and its subsequent effects, i.e., mold infestations, have been issues of great concern in building deterioration. Building structural and property damage due to mold and moisture problems include defacement of building enclosure finishes, warping and twisting of framing members, deterioration of wood products and building materials, reduction in the effectiveness of thermal insulation, electrochemical corrosion of metal components, paint peeling, and nail popping (Straube 2002; TenWolde 2000).

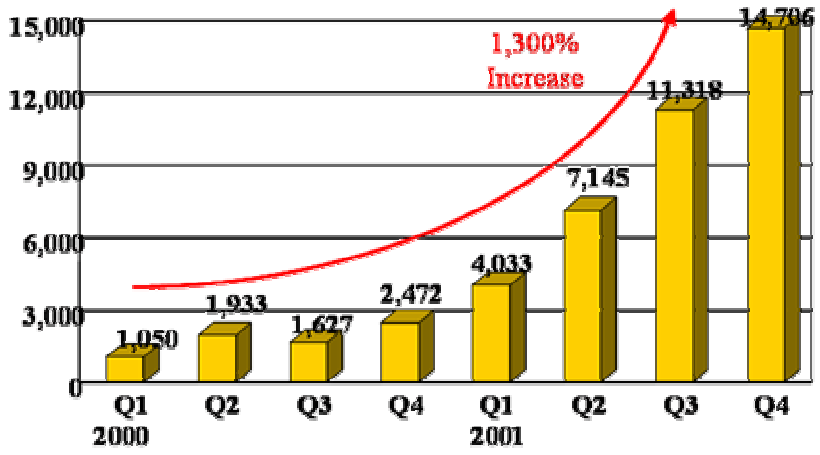

Figure 2.1 Increased number of mold claims in Texas houses

Mold problems lead to liability issues and often high profile litigation. Recently, the amount of litigation related to mold or moisture problems has risen dramatically in the United States (U.S. Chamber Institute for Legal Reform 2003). A special study by the

Texas Department of Insurance found that the number of such claims increased by 1,300 percent between the beginning of 2000 and the end of 2001 as shown in Figure 2.1 (Hartwig and Wilkinson 2003). High-profile mold- related lawsuits involve different types of defendants, including contractors, subcontractors, construction managers, property managers, architects, building component suppliers, building owners, and insurers.

Aside from the direct cost to mold remediation and loss of property, the period of vacancy of rentable space increases financial risk to owners as well. Reduced worker productivity is also an issue due to poor indoor air quality (Fisk and Rosenfeld 1997). However, once mold contamination occurs in an operational building, it is difficult to determine the real causes and propose the best remedial actions. It is still uncertain whether the building can be guaranteed to be mold-free after the remediation.

Although the above consequences related to mold contamination in buildings have been studied for decades, quantified risk assessment is not yet available. Thus, socially acceptable levels of risk have not been established. Biological fungal spore behavior and physical interactions of heat, air, and moisture transport in buildings and subsystems require a holistic approach to evaluate the mold growth risk, which involves harmful health effects and building damage. Strong scientific correlations, such as the dose response relationship between mold and human health should be established as well. However, all these studies require understating the characteristics of mold phenomenon.

2.1.2 Life cycle of mold

It has been reported that over 1.5 million of fungal species exist on earth, 65,000 of which have been identified (FWCI 2002). Although they are all slightly different, mold species that grow in building spaces exhibit a similar life cycle. The typical life cycle of fungi consists of four stages: the spore, germination, hyphal growth (vegetative growth), and reproduction (Figure 2.2). Each stage is briefly discussed below, and further information can be found in Burnett(1976), Burge(1995), Jennings and Lysek (1996), and Harriman and Nelson (2001).

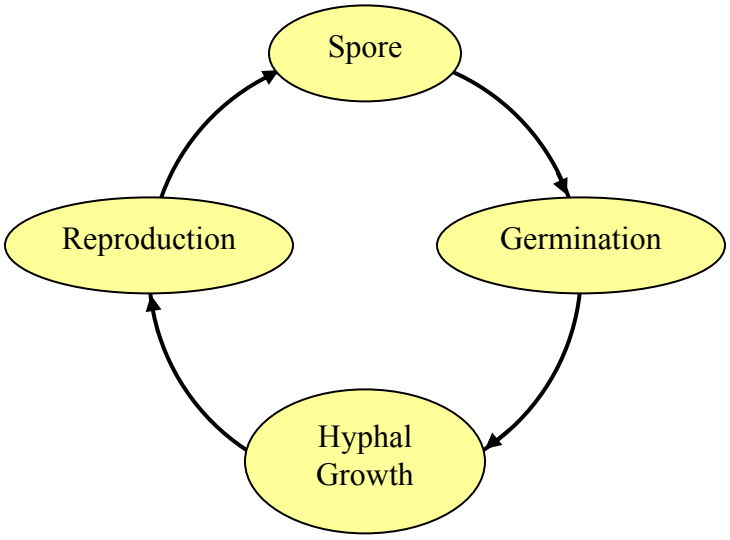

Figure 2.2 Typical life cycle of mold in building environment

In the germination stage, spores that have settled on surfaces remain dormant until they absorb enough moisture and liquid nutrients that enable them to germinate. If a substrate does not provide enough moisture and nutrients, however, the spore will not germinate. Hence, prevention of mold growth relies on the control of environmental

conditions before the spore germination. Once a spore germinates, the immediate consequence of germination is the production of short germ tubes, called hyphae. In the next stage, the hyphae (fungal filaments) begin to grow at their tip and produce lateral branches. As the hyphae thicken with the available moisture, they form a mass of hyphae, called mycelium. At this stage, the fungi metabolize and retain enough moisture to maintain growth. Limiting surface moisture does not effectively prevent the hyphae from growing. Since they ramify through the substrate, the fungus will re-grow after removal of its upper part. As a last step, the fungi form reproductive units and produce spores.

In the area of building physics research, mold growth is often categorized into visible or non-visible states. Viitanen (2000) has developed a seven-levels mold growth index. Sedlbauer (2003) used another index for mold growth intensity with six levels, as shown in Table 2.1. The mold growth index can be matched with fungus life stages, as previously described.

Table 2.1 Mold growth index and growth intensity

Mold Growth Index	**Growth rate**	**Growth Intensity**	**Features**
0	No growth (Spore not activated)	0	No growth detectable
1	Some growth detected only with microscopy (Initial stages of hyphae growth)	1	Growth visible only under the microscope
2	Moderate growth detected with microscopy (Coverage more than 10%)	2	Growth visible with the naked eye
3	Some growth detected visually (New spores produced)	3	Noticeable growth
4	Clear visually detected growth (Coverage more than 10%)	4	Strong growth
5	Plenty of visually detected growth (Coverage more than 50%)	5	Total over growth
6	Very heavy and tight growth (Coverage of more than 100%)		

From the study on the life cycle of mold, it is found that the control of environmental conditions (i.e. avoiding favorable conditions for mold germination) is critical for mold prevention in buildings. Such favorable environmental conditions for mold growth are discussed in the next section.

2.1.3 Environmental conditions for mold growth

Mold problems in buildings are observed across all climate regions regardless of the types of buildings, including residential and commercial (HUD 2004; Rousseau 1983). Design teams, engineers, and building maintenance professionals should always consider the possibility of mold growth in buildings and provide appropriate means to protect occupants and properties against mold infestation.

To proliferate, mold requires a favorable combination of environmental conditions in which to germinate, grow, and sporulate. These conditions include fungal spores settling on the surface, oxygen, appropriate temperature, nutrients in the substrate, and moisture or water activity (Hens 1999). Krus (2001e) studied these five conditions, plus a more comprehensive range of factors that can influence mold growth. Additional contributing factors are pH-value, light, roughness of the surface, biotic interactions, and exposure time. The level of indoor airborne spores, one of the required conditions for mold growth, is dependant on the seasons and the outdoor environment (Adan 1994a). Four important requirements for mold germination are illustrated in Figure 2.3.

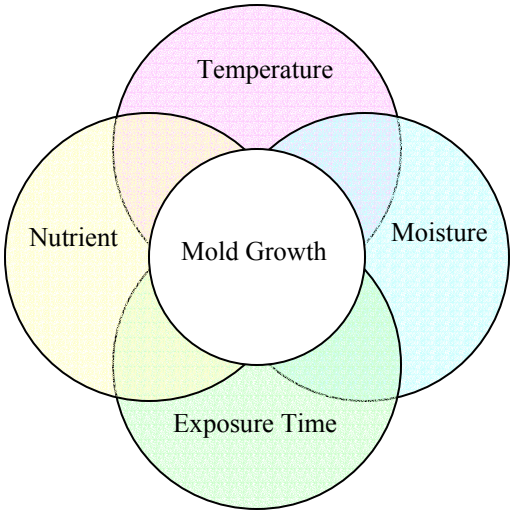

Figure 2.3 Requirements for mold germination

Depending on the species, mold spores require different optimal temperatures and different levels of relative humidity in order to germinate. Although mold can grow in temperatures ranging from 0° C to 40° C, a temperature range of 22° C to 35°C is considered the optimal temperature range for most species (Baughman and Arens 1996). As Adan (1994b) discussed, most buildings provide a favorable temperature range for mold to germinate/grow on building materials and interior finishes.

Different mold species also require different minimum moisture levels. The measure of moisture on a substrate is referred to as "water activity (a_w)" or the "equilibrium relative humidity (ERH)," which is an expression of the water activity as a percentage. Water activity is defined as the ratio of water vapor pressure at the substrate to that of pure water at the same temperature and pressure(Ayerst 1969; Baughman and Arens 1996). Ayerst (1969) have conducted experiments to find the differences between species in optimum and minimum moisture content. These experiments showed the limit of equilibrium relative humidity of 71% to 94% for mold growth depending on species.

Mold species can be categorized as primary colonizers (xerophilic), secondary colonizers, and tertiary colonizers (hygrophilic): xerophilic species require grow 80% of ERH or less, and hygrophilic species require more than 90% of ERH (Baughman and Arens 1996). Clarke and Johnstone (1999) developed six categories of mold species found in buildings with respect to temperature and relative humidity.

Regardless of the moisture preference of each mold species, the International Energy Agency (IEA) recommends an average relative humidity of 80% as the critical threshold for mold growth. Although it may be reasonable and conservative to set the moisture content of a material at 80% RH as a threshold level for preventing mold occurrences in buildings, it must be acknowledged that the actual threshold level varies with temperature, relative humidity, length of time that certain conditions were maintained (i.e., exposure time), types of building material, and so on.

Each building material contains a different level of nutrients that affect the germination of mold and the rate of mold growth. Some building materials can be a good substrate for mold growth, providing carbon and nitrogen. The relationships between building materials and mold growth have been studied in laboratory settings, but only limited results are available due to the large variety of building materials and other factors such as the aging of materials, the presence of fungal species, the cleaning and maintenance of the materials, varying environmental conditions in real buildings. Sedlbauer (2001) categorized building materials as category 0: optimum culture medium; Category Ⅰ: biologically recyclable building materials; Category Ⅱ: building materials with a porous structure; and Category Ⅲ: building materials that are not degradable nor contain any nutrients. Based on these four building material categories with different

fungal spores, he developed the generalized isopleth systems in non-fluctuating temperature and relative humidity conditions. Ritschkoff and Viitanen (2000b) conducted experiments using various wood-based materials (particle board, fiber board, plywood), stone-based materials (cement screed, gypsum board, concrete) and insulation materials (glass wool, fiber wool) under different temperature and relative humidity conditions. The results showed that all building materials are conducive to mold growth in high relative humidity (90%), even on stone-based building materials. However non-organic materials require higher relative humidity and longer exposure time for mold to germinate and grow.

Although metals or plastics cannot be used as substrates directly, dust containing microorganisms, debris, or fatty matter can settle on their surfaces, where they are sources of nutrition for fungi. In existing buildings, a number of mold growth problems have been reported on non-organic building materials even on the surface of concrete blocks and non-organic insulation materials inside ducts (Kowalski, Bahnfleth 1999). Experiments by Gertis (1999) proved that strong contamination of non-organic building materials supported mold germination. Therefore, it can be concluded that the nutrient effects of the building materials can be minimal in in-use buildings since deposited particles on surfaces and their subsequent contamination provide enough nutrients for mold to grow if the surfaces are not properly cleaned and maintained.

Depending on the environmental conditions of building materials, the required exposure time varies significantly. To elucidate the phenomenon of mold growth in real building cases, experimental research has been conducted on various building materials that have different nutrient effects under different environmental conditions (Pasanen,

Kasanen 2000; Ritschkoff, Viitanen 2000b). Non-organic building materials showed higher moisture requirements and longer exposure time than the optimum medium for mold germination. In favorable environmental conditions (surface temperature and relative humidity), shorter exposure time is required for mold germination. Figure 2.4 schematically illustrates the relationship between environmental conditions, nutrient content, and required exposure time, depending on fungal species. Dotted lines represent different fungal species in the figure.

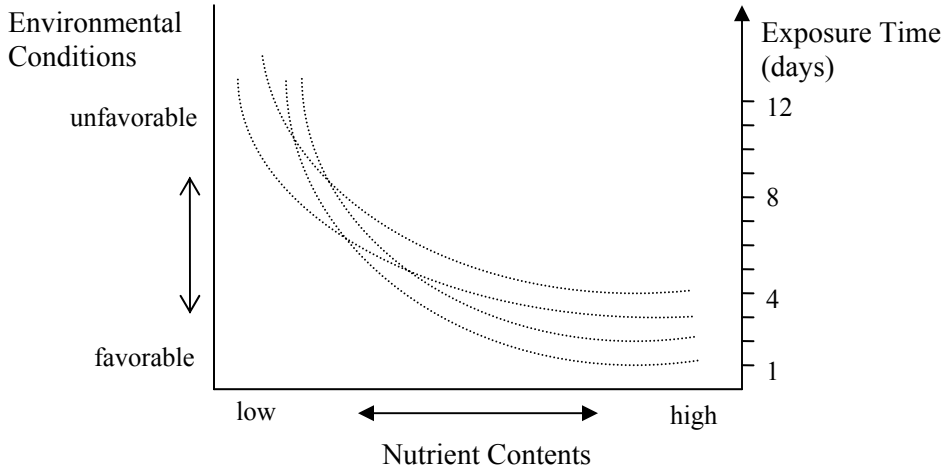

Figure 2.4 Schematic drawing for the relationship between environmental conditions, nutrient contents, and the required exposure time depending on fungal species

In summary, surface temperature, moisture contents, and nutrient contents in building materials are the most important factors for mold growth in the built environment. Most office and residential buildings meet the mold growth conditions except for the moisture requirement. Appropriate moisture control can prevent mold growth in buildings. Indoor relative humidity varies across a broad range over time, and

is dependant on building location and design, HVAC operation and maintenance schedule, occupants' behavior, and so on. However, mold growth is dominated by relative humidity (or moisture content) and temperature on the surfaces of building materials, not by ambient relative humidity (Pasanen, Juutinen 1992). Surface conditions can vary significantly within the same building space due to thermal bridges, cracks on the wall, local flow phenomena, and so on. Therefore, the local and micro-environmental conditions on the surface of a specific building detail should receive the focus of attention in the prevention of mold growth in buildings. The next section describes the current standards and evaluation methods for mold control in buildings.

2.2 REVIEW OF THE STANDARDS AND GUIDELINES FOR MOLD GROWTH

National and international standards have set upper limits on acceptable relative humidity in buildings, such as a range of 60% to 80%, as specified in ASHRAE (1992). This standard focuses mainly on providing or maintaining human comfort, not on preventing mold inside buildings. Although mold growth is affected by other factors such as those discussed in the previous section, current research has focused on the limiting criteria of moisture for preventing mold growth. Mold limiting-criteria have been developed based on laboratory experiments to find the minimum relative humidity for fungi spores to germinate. Such experiments have been conducted in various countries using environmental chambers that provide constant temperature and relative humidity on the Malt Agar medium (Adan 1994b; Ayerst 1969; Rowan, Johnstone 1999; Smith and Hill 1982). The purpose of the experiments, conducted on this optimum medium, provided the minimum requirements for each type of fungi (e.g., xerophilic or

hygrophilic species) in terms of constant relative humidity and temperature. However, these experiments produce different relative humidity criteria (65~80% RH), depending on the use of fungi species, substrates, temperature, and exposure time.

From the review on relative humidity and mold germination, Adan (1994b) concluded that susceptible surfaces should not be exposed to conditions with over 80% relative humidity if mold growth is to be prevented. The IEA also set a threshold of 80% relative humidity for preventing mold germination (IEA 1991). Later on, ASHRAE adopted the IEA criterion (ASHRAE 2001b), but it did not led to a general consensus on an acceptable level of relative humidity that would prevent the growth of indoor mold.

The above prescriptive standards/guidelines have proven unable to provide a mold-free built environment. One reason is that the standards deal only with relative humidity and do not consider the effect of temperature, exposure time, and nutrition of building materials on mold growth. Such a phenomenon is influenced by a multitude of parameters with complex physical and biological interactions.

The current prescriptive standards and codes have been studied to develop a more flexible and technically non-prescriptive framework for building design and construction. The worldwide interest in and acceptance of the performance-based, building methods endorsed by organizations such as CIB has given rise to global and regional initiatives, such as a working group (W060) and the PeBBu Thematic Network by CIB (2005). With respect to indoor environment, performance criteria have been relatively well established related to building material emissions and air handling unit cleanliness (Seppanen 2001). However, standards and codes regarding mold growth have not been published yet. One currently available performance-based standard is the ICC performance code for

buildings and facilities (ICC 2003). This code defines objective, functional statements and performance requirements regarding internal moisture, as shown in Table 2.2.

Table 2.2 Descriptive and performance-based standards/code regarding mold and moisture in buildings

	Organizations/Authors	**Moisture Criteria**	**Remarks**
Descriptive standards/code	IEA (IEA 1991)	80% of relative humidity	
	ASHRAE Fundamental (2001)	80% of relative humidity	
	ASHRAE (ASHRAE 1992; 1999a)	60~80% of relative humidity	Focused on human comfort
	ISO (ISO 1994)	30~70% of relative humidity	
Performance-based standards/code	ICC performance code(ICC 2003)	Objective: "to safeguard people against illness or injury…" Functional statement: "Buildings shall be constructed *to avoid the likelihood of fungal growths* or the accumulation of contaminants…" Performance requirement: "An adequate means shall be provided to remove excess moisture, or protect the structure from the effects of excess moisture …"	

2.3 EXISTING HYGROTHERMAL MODELS

2.3.1 Simplified hygrothermal models

Current descriptive standards and guidelines focus on moisture or water activity in a building envelope system, such as 80% of RH. To verify that prescribed values are met, many moisture transport calculation methods have been developed, ranging from simple manual analysis to sophisticated computational models. This section reviews manual analysis methods and simple steady-state calculation tools developed for moisture transportation. More sophisticated computational models are discussed in chapter 4.

Traditional manual analysis methods have been widely used in design practice for exterior walls. These methods are based on the comparison of vapor pressure inside the wall and saturation pressure at temperature within the wall. The dew point method, the Glaser diagram, and the Kieper diagram methods are variations of the manual analysis (TenWolde 2001). All three manual analysis methods use vapor diffusion theory, as shown in equation (2.2)

$$w = -\mu \frac{\Delta p}{d}, \tag{2.2}$$

where w = vapor flow [$kg / m^2 \cdot s$]

μ = water vapor permeability [$kg / m \cdot s$]

p = vapor pressure [Pa]

d = thickness of the material [m]

The manual analysis method focuses only on surface condensation within the building material. Thus, the accuracy of results is questionable due to lack of information about other moisture transportation mechanisms, such as liquid capillary transportation and moisture transportation functions in porous building materials. Nonetheless, current building codes for controlling moisture in a wall are based on manual analysis methods. Although all three manual analysis methods appear in the ASHRAE *Handbook of Fundamentals* (ASHRAE 2001b), they should not be used for the evaluation of mold growth on a wall, which can occur in the absence of condensation problems.

Simplified steady state computational tools have been developed using Glaser scheme of heat conduction and vapor diffusion. Examples of steady state models are WAND, HYGRO, and BRECON (Hens and Sneave 1996). Many extended models for moisture transportation in a wall have been developed by adding additional mechanisms, such as airflow, liquid flow, and vapor convection. However, these simplified steady state models should be used with caution as some fundamental flow phenomenons are not (well) represented. For example, models without convective vapor transport should be used only in airtight envelope evaluation. Due to the limitation to steady state calculation, hourly or daily calculations of moisture transport are not recommended (TenWolde 2001).

More detailed models are transient hygrothermal computational models with hygroscopic material properties. The entire list of models can be found in Hens and Sneave (1996). These models, validated by experimental data, have provided accurate results of moisture content within a wall if the boundary condition is known accurately. The next section discusses these detailed hygrothermal models with respect to their potential use in mold growth analyses.

2.3.2 Detailed hygrothermal models

Determining surface environmental conditions requires the calculation of the moisture flow between porous building materials and adjacent air, and moisture flow within multi-layered building materials. For this purpose, a set of first-principles-based heat and mass transport models have been developed (Clarke, Johnstone 1997; Karagiozis and Salonvaara 2001; Kunzel and Kiessl 1997; Liesen and Pedersen 1999; Mendes 2002; Nakhi 1995; Rode and Grau 2001). Straube (2001) reviewed recent developments of hygrothermal models and described the features of each model, including WUFI and LATENITE. The international energy agency (IEA) reviewed the heat, air, and moisture (HAM) transport models for buildings as well and identified 37 different models of various complexity. The IEA divided the HAM models into nine types, ranging from very simple to the most complete, according to the complexity of the model (Hens and Sneave 1996). However, this classification was not based on the applicability of the models for accurate mold growth prediction in buildings. In fact, most of these models are not suited for mold growth prediction, even in idealized situation, because complete HAM models have to combine the flow equations of the mass and energy, i.e., three flow components - energy, air, and moisture (vapor and water) - should be considered.

The hygrothermal models are hard to solve due to the nonlinearity in simultaneous heat and mass transfer. Additional nonlinearity is introduced through the sorption isotherms, the moisture dependent thermal properties of materials, and the coupling to the significant energy quantities involved in the sorption process (Liesen and Pedersen 1999; Rode and Grau 2001). A “complete” hygrothermal simulation should

include the Navier-Stokes equations for air flow in building zones. There are no studies as yet that have attempted to establish the coupling between mold growth predictions and computational fluid dynamics (CFD).

Hygrothermal simulation requires a number of material properties. One of the important properties is the sorption/desorption curve, which represents the relationship between the vapor pressure (or, more often, the relative humidity (RH)) of the surroundings and the moisture content in the material. Critical moisture content is established by using the sorption isotherms for each building material. Thus, critical moisture content can be defined as the lowest moisture content necessary to initiate moisture transport in the liquid phase. Below this level, moisture is transported only in the vapor phase. For many building materials, hygroscopic properties such as vapor permeability, moisture capacity, the thermal moisture diffusion coefficient, as well as the sorption curves, are still being developed. Because different hygrothermal models require different hygroscopic properties depending on the driving forces for moisture transport, some of the hygroscopic properties are not applicable for all hygrothermal models (Kumaran 1996).

With the intrinsic complexity of the hygrothermal models, the author has investigated state-of-the-art hygrothermal models to identify those that can be used in mold growth analysis. Some of the models, which predict moisture behavior within a building material, especially as part of the building envelope, help researchers or practitioners to identify the moisture transport behavior of building components. Other models, which incorporate moisture transfer modules into existing thermal models that operate mostly on a whole building scale, simulate whole building performance by

calculating thermal and moisture behavior simultaneously. The researched models were categorized into either "hygrothermal envelope models" (e.g., 1-D HAM, WUFI-pro, MOIST) or "hygrothermal models within a whole building energy simulation" (e.g., ESP-r, BSIM2002, EnergyPlus). The features and limitations of the models in both categories are summarized in Table 2.3.

Table 2.3 Characteristics of the hygrothermal models in the two categories

Category	**Hygrothermal envelope Models**	**Hygrothermal models within a whole building energy simulation**
Target	One building envelope	One or multi- building zones
Features and limitations	• Detailed moisture transfer (vapor diffusion, vapor convection, liquid diffusion, rain penetration, etc.) • Predefined indoor boundary conditions • Non reciprocal moisture transfer from/to an interior surface and indoor air • Limitation of the fluctuating surface conditions	• Whole building simulation • Multi-zone simulation • Ability to calculate fluctuating surface conditions • Various moisture sources • HVAC operation and control • Moisture transport between zones by airflow (infiltration, ventilation) • Simplified moisture flows within the building envelopes (vapor diffusion)
Examples of the models	1-D HAM, WUFI, MOIST	ESP-r, BSIM2002, EnergyPlus

These hygrothermal models deliver deterministic physical states at building material surfaces (i.e., temperature and relative humidity) as a function of time. These states are the determining input for mold growth assessment.

2.4 EXISTING MOLD GROWTH ANALYSIS METHODS

A few mold growth analysis methods have been developed recently, which can predict the mold occurrences or growth rates of molds on the surfaces of building materials. Existing analysis methods are reviewed in this section.

2.4.1 ESP-r

ESP-r is a computer simulation tool that calculates the local surface temperature and relative humidity at a surface of concern, while taking into account the moisture flow in porous material and local air movement. The results of the local conditions are superimposed on growth limit curves contained in the ESP-r database. The concentration of the data points over the curves indicates relative mold growth risk and its persistence over time(Clarke, Johnstone 1999; Rowan, Johnstone 1999). In this approach, the principal mold species affecting U.K. dwellings were identified and their minimum growth requirements, in terms of temperature and relative humidity, were established. The identified mold species were then assigned to one of six categories, A-F. The six categories and example mold species are as follows:

A: Aspergillus repens

B: Aspergillus versicolor

C: Penicillium chysogenum

D: Cladosporium sphaerospermum

E: Ulocladium consortiale

F: Stachybotrys atra

Figure 2.5 presents an example of the ESP-r simulation results for mold growth.

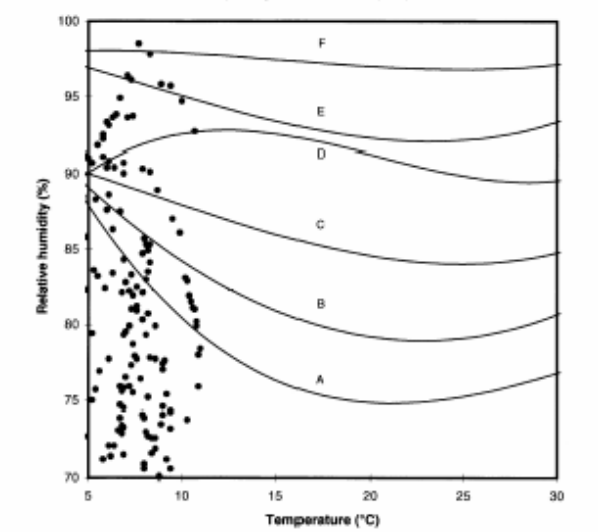

Figure 2.5 Predicted surface temperature and relative humidity with mold growth curves

It is important to note that the mold growth curves were generated from experiments under constant temperature and relative humidity and did not account for the required exposure time for mold to germinate. This limitation can lead to misinterpretation of data points that fall above the mold growth curve; not all data points that exceed the curve are associated with mold growth.

2.4.2 LATENITE

A mold growth prediction model was embedded in LATENITE VTT (Hukka and Viitanen 1999; Viitanen, Hanhijarvi 2000). The quantification of mold growth in the model is based on the mold growth index used in the experiments for visual inspection, as introduced in Table 2.1. The mold growth model is based on the mathematical relations

between the mold growth rate and different environmental conditions, including the effects of temperature, relative humidity, exposure time, and dry periods. This model generates the largest possible value of the mold growth index that has a parabolic form:

$$M_{\max} = 1 + 7\frac{RH_{crit} - RH}{RH_{crit} - 100} - 2\left(\frac{RH_{crit} - RH}{RH_{crit} - 100}\right)^2 \tag{2.1}$$

The critical relative humidity for mold growth depends not only on temperature but also on the stage of mold development, i.e., the mold index itself. This result is depicted in Figure 2.6.

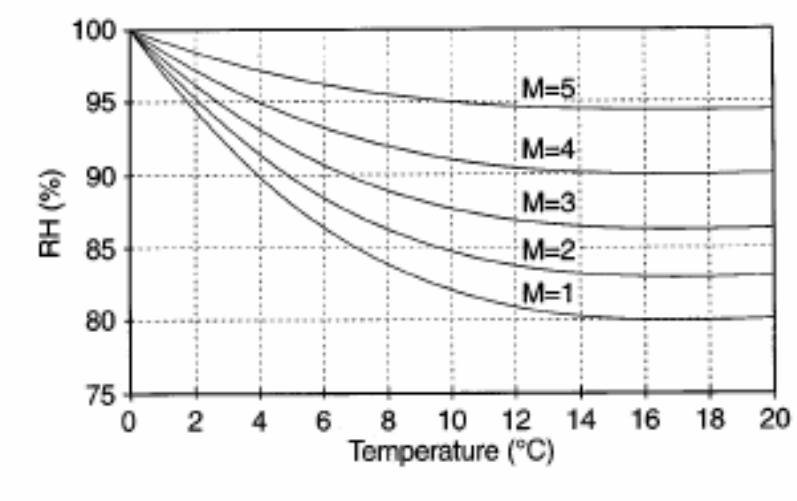

Figure 2.6 Temperature dependent critical relative humidity needed for mold growth at different values of mold index

The complete model for mold growth in favorable conditions is expressed as follows:

$$\frac{dM}{dt} = \frac{1}{7\exp(-0.68\ln T - 13.9\ln RH + 0.14W - 0.33SQ + 66.02)} k_1 k_2 \qquad (2.2)$$

The input parameters are ambient temperature, ambient relative humidity, wood species (W), surface quality (SQ) and two coefficients representing response time for the initiation of mold growth (k_1, k_2). As a basis for the growth model, a regression equation was developed for the response time and the initiation of mold growth on wooden material in constant temperature and humidity conditions. The numerical values of the parameters have been established for pure pine and spruce sapwood. This model focused on the visual appearance of mold spread and the maximum value of the mold index. However, Viitanen showed that mold growth can be retarded and slower at fluctuating humidity conditions than at constant conditions.

2.4.3 Biohygrothermal model

The biohygrothermal model was developed by Krus and Sedlbauer, who described the hygrothermal behavior of the spore(Krus, Sedlbauer 2001; Sedlbauer 2002; Sedlbauer, Krus 2003). They, first, developed the isopleth systems that represent the requirements for mold germination and growth as a function of temperature and relative humidity in different fungal spores. From the isopleth systems, the lowest isopleth for mold (LIM), which is the lowest occurring limit of growth, was derived in order to consider the combined growth conditions of all fungus species, as shown in figure 2.7. A

set of isopleth systems has been developed for health risk classes of fungal spores and substrate group.

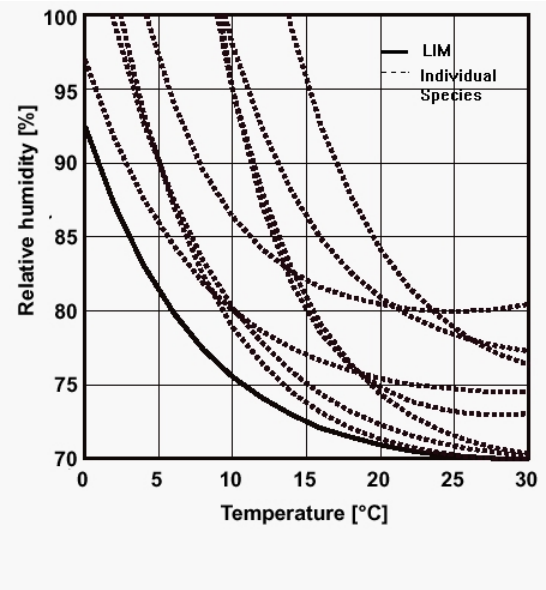

Figure 2.7 Development of the LIM from isopleths of different species

Sedlbauer developed the biohygrothermal model for transient environmental conditions. This model predicts the moisture balance inside a spore with fluctuating boundary conditions. In this model, the spore is treated as a biological wall. The moisture transfer through the spore wall is assumed vapor diffusion. The required properties of the spore include the moisture retention curve and the vapor diffusion resistance. The model uses the moisture retention curve for bacteria with slight modification. The calculated moisture content inside the spore is then compared to the limiting water content for spore germination based on the lowest relative humidity from the LIM and the moisture retention curve. Figure 2.8 shows an example of the result from the biohygrothermal

model used in two building materials. This model provides a good indication of relative mold growth risk in different building materials.

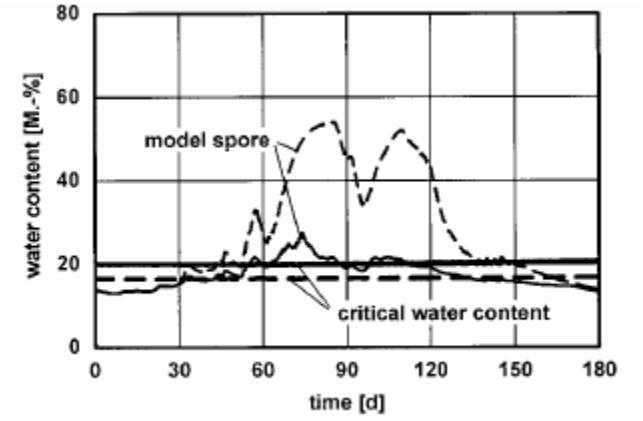

Figure 2.8 Calculated results of water content inside the spore on two different building materials (paper and smart vapor retarder)

2.4.4 Discussion

Table 2.4 presents an overview of three state-of-the-art mold growth analysis methods. Most of the existing methods have established mold growth limitation curves called “critical relative humidity” in LATENITE or “lowest isopleth for mold (LIM)” in the biohygrothermal model. These analysis methods are in good agreement with experimental results and enable the qualitative evaluation of mold growth risk. However, the applicability of these methods to real buildings is still limited since the boundary conditions are always assumed to be known. This assumption leads to a situation in which important parameters for mold phenomena such as an imperfect envelope system, a thermal bridge, or moisture generation inside the building, are ignored in real situations. Despite all the mechanisms that govern moisture and heat transfer at a specific location in

a building are considered, the uncertainty associated with building parameters, e.g., natural variation of material properties, should be included in the analysis to provide a more relevant picture of mold growth. This realization drives the development of a new performance indicator for mold growth in Chapter 3.

Table 2.4 Overview of existing mold growth analysis methods

	ESP-r (Clarke, Johnstone 1999)	**LATENITE** (Hukka and Viitanen 1999)	**Biohygrothermal Model** (Krus, Sedlbauer 2001)
Method	Mold growth limitation curve	Critical relative humidity based on mold index	Lowest Isopleth for Mold (LIM)
Features	• Superimposition of the calculated surface conditions on the mold growth limitation curves	• Calculation of the largest possible mold index	• Calculation of moisture content in a mold spores • Spores as a biological wall in WUFI
Limitations	No quantified results available	Applicable only to pure pine and spruce sapwood	Hard to acquire the required moisture properties for a spore

Before the investigation of a new performance indicator for mold growth, an objective method that quantifies mold growth risk should first be developed. Thus, the next section describes a new mold growth analysis method that uses hygrothermal models and a mold germination graph.

2.5 MOLD GERMINATION GRAPH METHOD

The earlier study discussed the main environmental requirements for mold growth to occur, and introduced hygrothermal models that calculate the local environmental conditions in an undisturbed, plain wall. We can now proceed to develop a new mold growth analysis method that generates quantified results of mold risk. This method uses a standard germination graph showing the relationship between temperature, relative humidity, and exposure time.

2.5.1 Development of the mold germination graph method

The mold germination graph method keeps track of the environmental conditions at previous time steps so that the effect of fluctuating conditions can be considered. This is important because certain conditions can be viewed as inductive to mold growth only if they persist long enough. However, in fluctuating humidity conditions, germination does not occur outside a certain range of conditions that are favorable to mold growth. In this unfavorable range, some delay in the rate of mold growth will occur if mold has already germinated (Hukka and Viitanen 1999; Pasanen, Kasanen 2000). In terms of germination conditions, it is assumed that germination will not occur if environmental conditions are outside the favorable range. In this case, the accumulated exposure time is set at zero. In order to provide reliable data, more experimental research is required to observe mold growth in fluctuating conditions.

Figure 2.9 shows the standard "mold germination graph" for the new mold growth analysis method. This graph was established based on the isopleths of Aspergillus restrictus, which were derived from the experiments reported by Smith(1982) and Ayerst

(1969). In this graph, the surface condition in the group Ⅰ should be maintained at least one day for initiation of mold germination to occur. Depending on the calculated surface relative humidity and surface temperature, each state condition can be assigned to one of the groups in the mold germination graph. After this step, accumulated exposure time for each group can be recorded. An accumulated exposure time greater or equal to the required exposure time indicates mold growth risk. The resulting "mold growth risk" is expressed in the following metric "number of mold risky days over a standard simulation period."

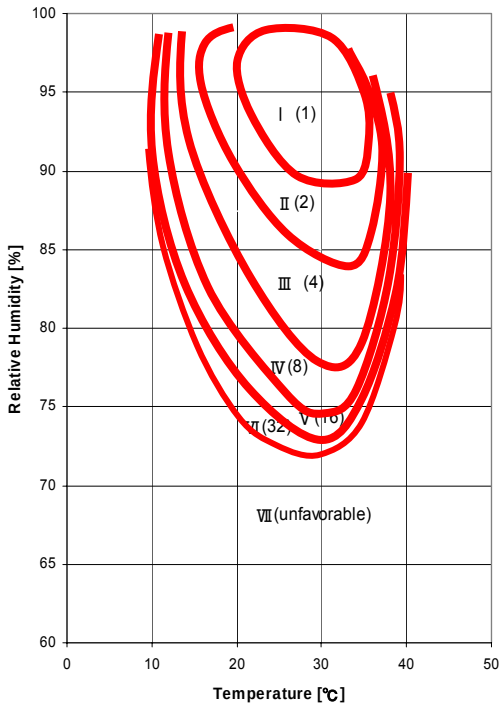

Figure 2.9 Mold germination graph showing each group with temperature, relative humidity and required exposure time for the initiation of mold germination, modified from Smith and Hill (1982)

Table 2.5 illustrates the use of the germination graph in the mold growth analysis method. The surface temperature and relative humidity are assumed to be available as a result of hygrothermal simulation. In this example, the mold germination graph method generated five risky days out of 12 days.

Table 2.5 Example of the application of the germination graph method

Day	Surface		Group	Accumulated exposure time	Required exposure time	Mold growth risk	
	Temp	RH				Each group	Day
1	20	70	Ⅶ	-	-	x	x
2	25	80	Ⅲ	1	4	x	x
3	23	85	Ⅲ	2	4	x	x
4	26	90	Ⅱ	1	2	x	x
			Ⅲ	3	4	x	
5	30	95	Ⅰ	1	1	o	o
			Ⅱ	2	2	o	
			Ⅲ	4	4	o	
6	22	85	Ⅲ	5	4	o	o
7	18	97	Ⅱ	1	2	x	o
			Ⅲ	6	4	o	
8	25	80	Ⅲ	7	4	o	o
9	18	97	Ⅱ	1	2	x	o
			Ⅲ	8	4	o	
10	20	70	Ⅶ	-	-	x	x
11	25	80	Ⅲ	1	4	x	x
12	18	97	Ⅱ	1	2	x	x
			Ⅲ	2	4	x	

('x' represents no mold growth and 'o' represents mold growth risk)

Critical humidity and exposure time for the initiation of mold growth vary for different building materials. For example, wood-based materials require a lower critical humidity level and exposure time than stone-based materials do (Ritschkoff, Viitanen 2000a). The effect of different building materials as substrates can be taken into account by either modifying the mold germination graph for each. However, the nutrient effects

from different building materials are ignored in this study, since the contamination of the building surface and dust settlement are sufficient for mold to grow in an existing building environment.

Although the germination graph has been developed using one of the common fungal species (i.e., Aspergillus), a certain restriction applies to the germination graph method in the mold growth analysis. Certain fungal species can germinate and grow outside of the favorable environmental conditions that are specified in the germination graph (Figure 2.9). Such species are not assumed to be common in the built environments and thus ignored in the current approach. However, when a specific fungal species are of concern in a mold growth analysis, one should replace the germination graph accordingly.

We use the germination graph of Aspergillus in the mold growth analysis throughout the remainder of this thesis and refer to it as the "standard germination graph". The next section describes two comparative studies using this germination graph.

2.5.2 Comparative study

Two case studies were conducted to compare the results from the mold germination graph method with those of the embedded mold prediction method in ESP-r. For the first case study, a one-zone building model was made in ESP-r. The building model included a simple HVAC plant with a specified humidity ratio, a heating coil, and a supply fan. The HVAC system ran with an on-off control law, and the zone temperature was set at 20 to 24°C during working hours (8:00 to 18:00). The simulation was implemented for one week in the winter with Atlanta weather data. The results of the

temperature and the relative humidity on the interior surface of the south facing wall are shown in Figure 2.10.

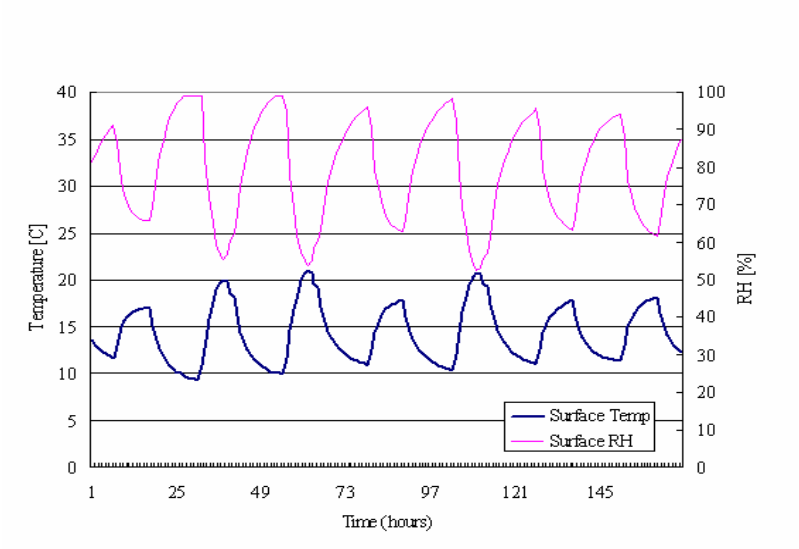

Figure 2.10 Results for interior south surface temperature and relative humidity in ESP-r.

As a consequence of the zone temperature set points, the surface temperature occasionally reaches 20°C (leading to low RH in the 60% range at the surface). On the other hand, the relative humidity on the surface can reach values close to 100% at night. Figure 2.10 shows the variations in surface conditions in response to fluctuating indoor conditions. Figure 2.11 presents the results of mold growth conditions as used in ESP-r. In the figure, the surface temperature and relative humidity points are superimposed on the generic mold growth limitation curves that are embedded in a database within ESP-r. As can be seen, the distribution of data points affects all growth curves. On this basis, it can be concluded that mold infestation would have occurred in all growth categories. As ESP-r does not generate quantitative results, the results of this method are difficult to compare with those of other methods.

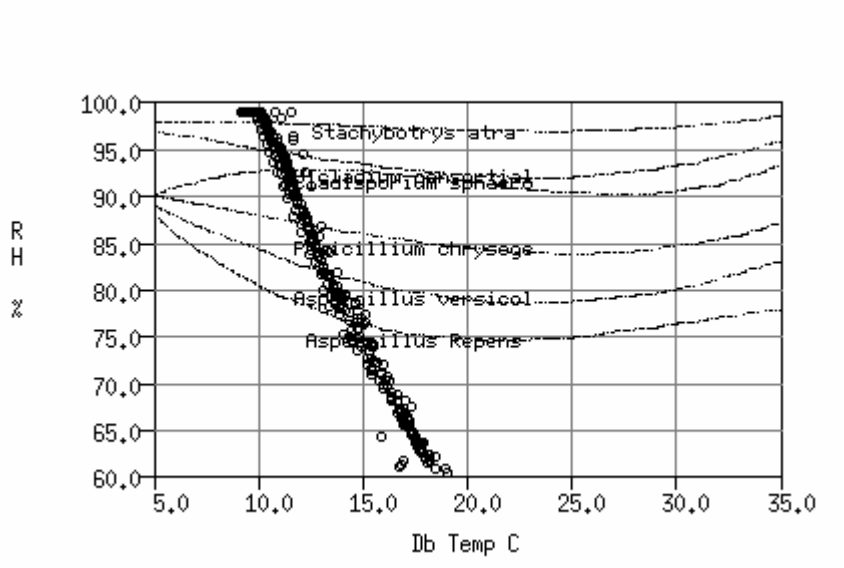

Figure 2.11 Mold growth prediction using ESP-r.

The results of mold growth risk are shown in Table 2.6, based on the calculated environmental conditions and the germination graph method. Daily surface temperature and relative humidity are calculated using the same model as used in the ESP-r simulation. Although the simulation ran for only one week, interestingly, it showed that five days fell within the favorable ranges (Group 5 and 6), which require 16 days and 32 days, respectively, for the initiation of mold germination. The results indicated that mold growth would not occur during that period. The ESP-r model as presented in Figure 2.11 would not have come to the same conclusion. For more accurate results, the germination graph method requires a longer period of simulation.

Table 2.6 Mold growth risk analysis using a germination graph method

Day	Surface		Group	Accumulated exposure time	Required exposure time	Mold growth risk	
	Temp	RH				Each group	Day
1	13.9	79.5	Ⅵ	1	32	x	x
2	13.8	84.7	Ⅴ	1	16	x	x
3	14.7	78.0	Ⅵ	3	32	x	x
4	14.0	85.1	Ⅴ	1	16	x	x
5	14.9	76.8	Ⅶ	-	-	x	x
6	14.0	79.9	Ⅵ	1	32	x	x
7	14.3	78.7	Ⅶ	-	-	x	x

('x' represents no mold growth and 'o' represents mold growth risk)

The second case study for the same one-zone building, conducted for a one-year simulation using EnergyPlus (figure 2.12), analyzed mold growth risk with the mold germination graph method. In this study, two identical buildings were situated in Atlanta and Hawaii in order to investigate the effect of infiltration in different locations. Case A represents the same control of the building that was used in the previous case study. In case B, additional outside air infiltration of one air change per hour (ACH) was applied. In the Atlanta climate, the number of risky days decreased significantly from 129 to 11 with the introduction of infiltration. By contrast, for Hawaii, the number of risky days increased from 71 to 108 when infiltration was introduced. These results show that infiltration can increase or decrease the mold growth risk depending on the climates.

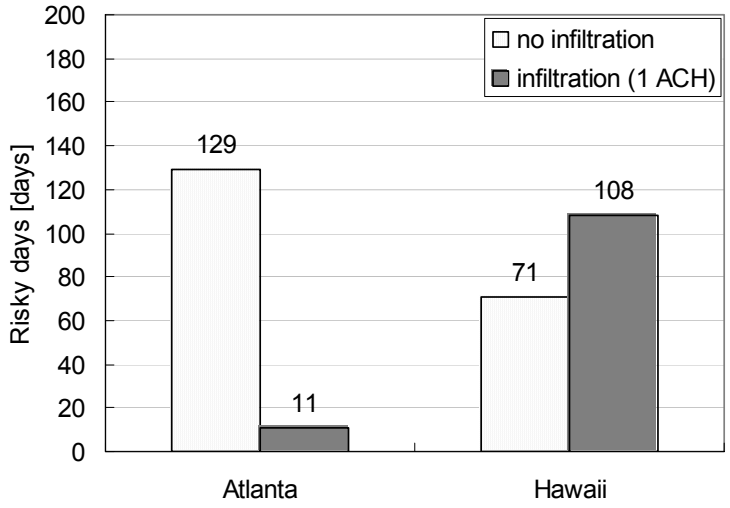

Figure 2.12 Effect of infiltration in two different locations.

The purpose of this exercise is two-fold. First, it shows the case dependent sensitivity to certain parameters, which is a strong motivation for performing an uncertainty analysis. Even with the same building (same design, building materials, and operation), mold growth risk is very sensitive to local climate and occurring infiltration. This study regulates only one building parameter, but the building model is composed of many additional parameters which for this preliminary study have been assumed fixed. The infiltration rate is a good example of an uncertain parameter as it can significantly deviate in buildings that are facing seaside or inner city because of the major difference in local microclimate. The simple study in two locations reveals some important conclusions. It confirms that buildings should be designed and operated differently in different climates to reduce mold growth risk something that is not immediately obvious from a deterministic simulation, but becomes obvious when one takes into account that the margins of uncertainty varies from one situation to the other. Obviously, a full and

realistic mold risk assessment should include all the building parameters and appropriate range of these values. Another conclusion is that the uncertainty analysis is by necessity always case specific. The reason is that the estimate of parameter uncertainties is heavily dependent on local circumstances and specific details of the design and its realization and use. Hence "generic" uncertainty analyses performed on standard design cases make little or no sense.

Second, the above study shows how a more sophisticated mold growth analysis model provides better resolution in the study of the effect of certain parameters (in this case, infiltration). The Atlanta case showed negative correlation between infiltration rate and mold growth risk, and positive correlation in the Hawaiian case. Finding these relationships for each building parameter is important input for the management of the building design process and facility operation. It provides teams with important relationships between what uncertainty may impact the most on the indoor environment. In this case it is obvious that the building located in Hawaii needs to find a way to decrease infiltration. The mold germination graph method identifies the relationship between a building parameter and resulting mold growth risk in a specific case of the building. The sensitivity of a parameter can be quantified using the germination graph method. The identification of dominant parameters that have a major influence on mold risk is vital, as they point to the areas that require special attention during design and construction in order to guarantee a mold free environment over the life cycle of the facility. A larger set of building parameters will have to be studied in a sensitivity analysis that identifies the dominant parameters.

Inclusion of the above issues in a mold growth analysis in buildings calls for the development of a new performance indicator for mold growth. This indicator aims to capture the effect of the deviations of building parameters and include additional mechanisms for local environmental conditions in trouble spots. It also intends to provide the outcome of the indicator that expresses the likelihood of mold growth risk during the service life of a building and identify dominant parameters. The development of the performance indicator is discussed in the next chapter.

CHAPTER 3

A NEW PERFORMANCE INDICATOR FOR MOLD GROWTH

As discussed in Section 2.2, current prescriptive standards and guidelines fail to ensure a mold-free environment. Accordingly, current deterministic performance evaluation methods are inadequate for assessing mold growth risks in buildings, mainly because mold growth is dependant on multivariate building parameters, and the correlations between mold growth and each building parameter can be positive or negative in each specific building case, as shown in the previous chapter.

The new performance indicator utilizes a performance-based approach that focuses on the performance of a certain performance aspect of the building (system) as a whole instead of prescribing the properties of certain building components. For this purpose the building is regarded as an interacting set of systems and occupant processes that determine the conditions within the building. The conditions in turn can be post analyzed to find out whether they produce risks for mold growth. Based on this approach the development of a probabilistic performance indicator for mold growth under uncertainty is undertaken. This chapter describes the core concept of the approach and identifies the requirements for the development of the mold indicator.

3.1 OVERVIEW OF PERFORMANCE INDICATORS

3.1.1 Performance-based building and performance indicator

The performance-based building concept provides a flexible and technically non-prescriptive framework for building design and construction. The core concept is that all building activities should be based on the performance of the building rather than on the description of the building/subsystem construction. The performance concept forces the building industry to move from the providers' specifications to the client/stake holders' performance requirements. Furthermore, this approach encourages innovative solutions and guarantees high quality building performance over the life cycle of the building within the target budget. Application and implementation of the performance concept throughout the building process has gained worldwide interest. Endeavors in implementing this approach in regulatory settings are currently taking place in many countries and international organizations (Becker 1996; Lee and Barrett 2003). However, without adequate performance evaluation tools and methods (e.g., embodied in the definition of so-called performance indicators, PI), the performance concept cannot be implemented properly (Foliente, Leicester 1998).

In the performance-based regulatory framework shown in Figure 3.1, the top level [objectives] represents the essential interests of the community and the needs of the user. The second level [functional requirements] addresses one specific aspect of the building or a building element that achieves the stated goal. The third level [performance requirements] specifies the actual requirements that must be satisfied in order to meet the functional requirements, and the bottom level [verification methods] deals with the specifics of meeting the goal. Appropriate evaluation or verification methods should be

introduced to verify the performance of the building on this level. The performance-based verification methods include testing (experiments), calculation (mathematical models and computer procedures), or a combination of both, depending on the aspect of building performance.

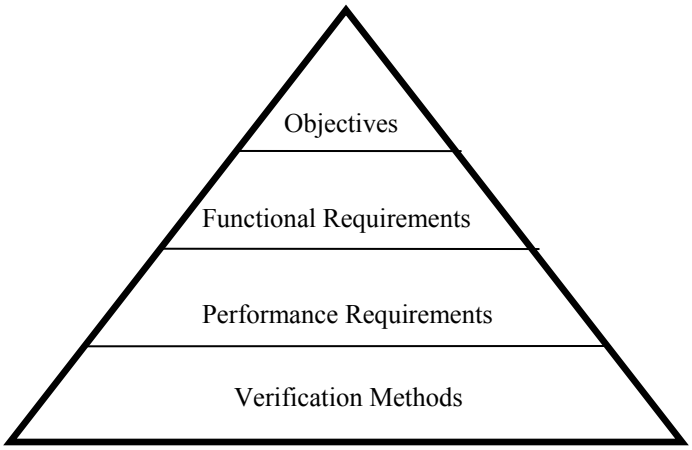

Figure 3.1 Four-level regulatory framework (Foliente, Leicester 1998)

The development of reliable and accurate building performance models is critical for each function of a building, such as thermal comfort, structure, or fire safety. These performance models can be used to quantify the performance requirements for building codes and standards and to evaluate the performance of a specific building in service life. The outcome (observed state variable) of a performance model should be aggregated to indicate the performance of a building. These performance indicators provide a quantified method for evaluating specific functions of buildings (Augenbroe and Park 2005).

Many types of performance indicators have been developed, even for the same aspect of the buildings, based on aggregation methods and metrics. For example, for thermal comfort, Fanger developed the PMV (Predicted Mean Vote) and PPD(Predicted

Percentage Dissatisfied) by calculating six state variables and aggregating them over time. They use a static comfort model that represents the physical/physiological state variable, i.e., "thermal load," and then generate a human response distribution for various thermal loads (Fanger 1970). Another performance indicator, the TO, has commonly been used in Dutch design practice for thermal comfort. The TO performance indicator determines the number of hours for which more than 10% of the people would be dissatisfied. Based on a one-year simulation period, the common target value for offices is 100 hours (De Wit 2001).

3.1.2 Normative performance calculation

In the performance-based approach, uncertainty and risk analysis play a key role in the specification of target performance level(s). In the establishment of target performance and the development and validation of performance evaluation/grading tools, probabilistic methods should be applied in developing performance criteria (Foliente, Leicester 1998). After all, the risk of failure to meet a specific building performance always exists. Although it is hard to establish an acceptable level of risk, the initial quantification of such risk, which will set a target performance level, is crucial. The most advanced disciplines in which risk is implemented in performance evaluations are both the structural and fire safety engineering fields, where safety is the central issue.

As mentioned earlier, the performance of a building can be verified using test and/or calculation procedures (i.e., mathematical models and computer procedures). However, full dynamic simulations or experiments are costly and time consuming. In addition, most computer simulations and small-scale experiments generate biased results

because of simplified models, assumptions in the mathematical model, uncertainty in the natural variability of building parameters, and unknown data for the building. Considering all these uncertainties associated with the evaluation models and parameters for each building case requires substantial effort and time. These problems can be avoided if a performance indicator is based on normative calculations whenever possible.

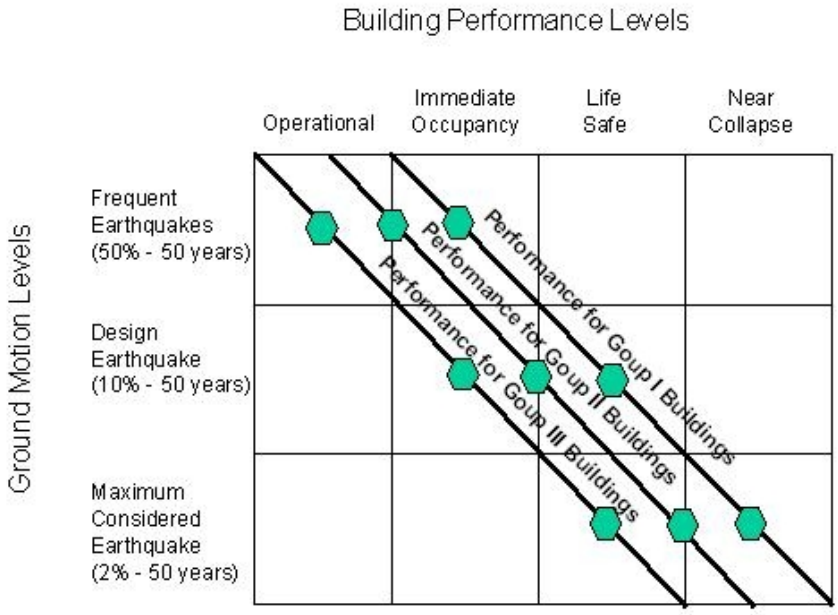

Figure 3.2 Multi-level performance targets in building structure design against earthquakes (FEMA 1997b)

One good example of a normative performance evaluation can be found in the discipline of seismic rehabilitation of buildings. The performance-based criteria in this area will be described briefly. In building structure design against seismic earthquakes, a multi-level performance target has been developed based on building function and earthquake hazard intensity/frequency, as shown in Figure 3.2.

The graphic representation of an objective performance matrix matches the chosen earthquake hazard levels with selected target building performance levels. Four building performance levels are defined, i.e., operational, immediate occupancy, life safety, and collapse prevention. The three diagonal lines represent the performance objectives for different groups of buildings. Group I is representative of a basic commercial structure, while Groups II and III represent structures that require a higher level of protection such as hospitals, fire stations, data centers, key manufacturing facilities, and so forth. Each cell in the above figure represents discrete rehabilitation.

The general analytical approach is to calculate the demand (i.e., force, moment, deformation, or any combination of these variables) on individual components, which results from the design level of ground motion, and to compare that demand with the calculated capacity of the component at the specified rehabilitation objective. If the demand is equal to or less than the capacity, the component is acceptable (Capacity ≥ Demand). If not, the rehabilitation design must be modified until the component demonstrates sufficient capacity. The demands are calculated using the appropriate analytical procedure (i.e., Linear Static, Linear Dynamic, Nonlinear Static, and Nonlinear Dynamic Procedures), and then the capacities are computed for each component using the criteria outlined in the Guidelines (FEMA 1997a). As an example of an acceptance criteria for the linear procedure, deformation-controlled actions in components and elements should satisfy the below equation (FEMA 2000):

$$mkQ_{CE} \geq Q_{UD}, \tag{3.1}$$

where

m = The component or element demand modifier factor that accounts for expected ductility associated with this action at the selected structural performance level. m-factors are specified for each type of construction (e.g., steel, concrete, masonry)

k = The knowledge factor defines the required level of knowledge considering the selected objectives and analytical procedure

Q_{CE} = The expected strength of the component or element at the deformation level under consideration for deformation-controlled actions

Q_{UD} = The deformation-controlled design action due to gravity and earthquake loads

Note that this approach uses a finite set of parameters and factors in the analysis according to the selected level of the performance objective and analytical procedures. In the guidelines, the procedures according to which the appropriate deterministic value for each parameter and factor are selected are as follows. These values are the result of a study in uncertainty and risk analyses of different building types and components, hazard levels, damages, cost, and so forth. After the uncertainty study and consideration of all kinds of safety factors and assumptions, a set of parameters can be constructed for a specific analytical method that is most sensitive to the outcome (risk). This study also leads to appropriate values for each parameter and factor. These parameters and values generate a deterministic result for the performance evaluation of a building. These results can now be compared to the selected performance criteria, and if the analytical results are less than a certain threshold, the building design is considered safe (as in the example

above against seismic damage at a level of the selected objective). This approach is considered a normative procedure that calculates a certain performance of a building aspect with a limited set of building parameters and a simplified, standardized (normative) model. Although it does not generate accurate results, the outcome provides indicative information for comparison. The normative building performance evaluation can be used easily in practice with a simple acceptance criterion.

3.1.3 Types of performance indicators

From a review of performance indicators, three types of performance indicators can be identified depending on the function of a building under consideration: the result of the PI, the parameters used for evaluation, and the performance criteria. The identified types of PIs include a deterministic PI, a probabilistic PI, and a risk-based normative PI. Although a risk-based normative PI is considered the most advanced, specific building aspects require different types of PIs (see Table 3.1 at the end of this section).

Deterministic performance indicator

The deterministic performance indicators are the simplest and most widely used in the discipline of building physics. The performance evaluation models try to represent a physical phenomenon in a building as accurately as possible and then generate an absolute number for it. The main concern about this approach is the accuracy of the results. Usually, the phenomenon does not involve a risk that leads to design failure. For example, many deterministic PIs for building energy and lighting, such as for building energy consumption (KWh/m^2) and for luminous efficacy of luminaries (lumens/watt),

have been developed. The performance evaluation using deterministic PIs generates a number, depending on the building configuration, the (sub)systems, local outdoor conditions, and building usage/operation. The PI results can be compared with the PI results of other reference buildings, as in the EnergyStar labeling program (www.energystar.gov). However, interpreting the results versus a desired value for a performance criterion can be difficult, as the number of parameters used in the evaluation model generally increases, as the complexity of a building increases and higher accuracy is required.

Probabilistic performance indicator

Unlike energy and lighting performance, some functions of buildings can be considered a limit state phenomenon. If a building exhibits specific performance that does not meet a certain threshold (i.e., the performance criterion), then the design "fails." In this case, the design team has to modify the building so that it performs below the threshold. One good example is thermal comfort. A certain threshold exists, which triggers discomfort in individual occupants. Using Fanger's comfort model, individual discomfort levels can be aggregated to provide the distribution of overall thermal discomfort level of the occupants in the building, which are the PMV and PPD. From the relationship between the PMV and PPD, one can set a performance criterion such as maximum10% of PPD, which corresponds to the PMV range of ± 0.5. Although the distribution depends on all the parameters used for the performance evaluation, determining which parameters are most sensitive to the outcome is important. This set of parameters and the uncertainty associated with them should be part of the analysis. From

the uncertainty and sensitivity analysis, the probabilistic PIs produce a confidence level of specific building performance that meets the required performance criteria.

Risk-based normative performance indicator

The risk-based normative performance indicator calculates the risk failure of a specific building performance. When a phenomenon is considered a risk, clear and unambiguous levels of socially acceptable risks need to be constructed. The acceptable criteria can be developed based on risk analysis that considers the possibility of an unwanted outcome and the resulting loss or harm to something that is valued. In building performance evaluation, these acceptance criteria are compared with an outcome of a performance evaluation. The performance indicators in this category calculate the risk of the failure. These performance indicators employ normative calculation procedures that provide indicative information that show whether or not the design meets the target performance criteria. A normative PI uses a limited set of building parameters in a standardized calculation routine. The routine may be developed using on uncertainty and sensitivity analyses considering all assumptions, safety factors, and uncertain parameters. The routine is calibrated and validated for its purpose and clear specifications give the value of the input parameters. This approach thus enables direct performance evaluation. The normative PIs are based on simplified procedures and generate deterministic results. They provide indicative performance evaluation results that can be compared with the performance criteria in a selected level of objective.

Table 3.1 Three types of performance indicator

	Parameter space	Performance Evaluation Model	PI results
1) Deterministic Performance Indicator			
	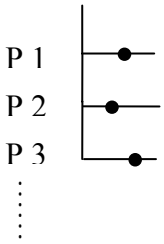	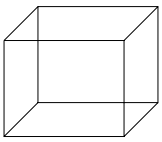 ex) Heat balance model (E+, ESP-r, etc)	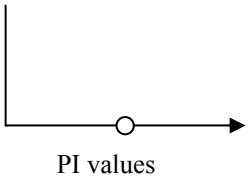 ex) Energy consumption per m^2 (KWh/m^2)
2) Probabilistic Performance Indicator			
	Set of parameters 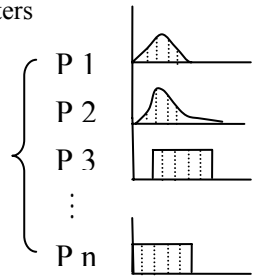	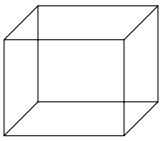 ex) Fanger's comfort model	Probability 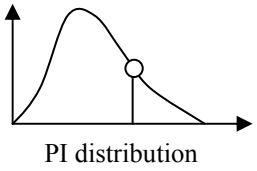 ex) PMV, PPD, TO
3) Risk-based Normative Performance Indicator			
	Set of parameters with normatively defined deterministic values 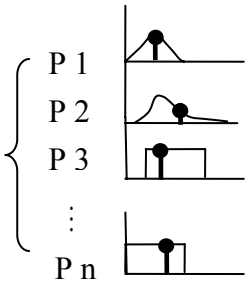	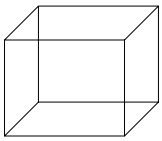 Ex) Seismic analysis model (Constructed for normative quantification)	Acceptance Criteria 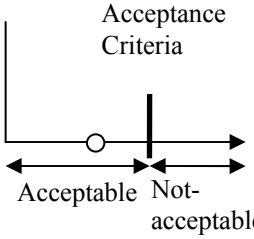 ex) capacity-demand ratio

The next section deals with the mold phenomenon and determines the type of performance indicator appropriate for development within the context of the performance-based building approach.

3.2 A RISK VIEW OF MOLD

Unlike energy or lighting performance in building design, mold occurrence is considered a limit state phenomenon. In this approach, the limiting conditions, the mold phenomenon and environmental conditions, can be considered a "load" similar to that in structural engineering. This similarity implies that once it is shown that a building has unacceptable mold occurrence risk, the design fails and must be fixed. When the combination of relatively high humidity and temperature on building material surfaces constitutes favorable conditions for mold germination, i.e., exceeding a certain threshold during a certain period, mold will occur. In that case, we regard the building as no longer safe against mold. When the building environmental load reaches the threshold level, the occupants feel discomfort and complain about visible or hidden mold, and certain structure damage occurs.

The mold phenomenon can be compared with thermal comfort, as described in the previous section. In PMV, four environmental properties (i.e., air temperature, relative humidity, air velocity, and mean radiant temperature) and an estimate of clothing and activity constitute an environmental load, and a certain aggregated duration of discomfort is used as a limiting state. The same approach can be applied to the mold phenomenon.

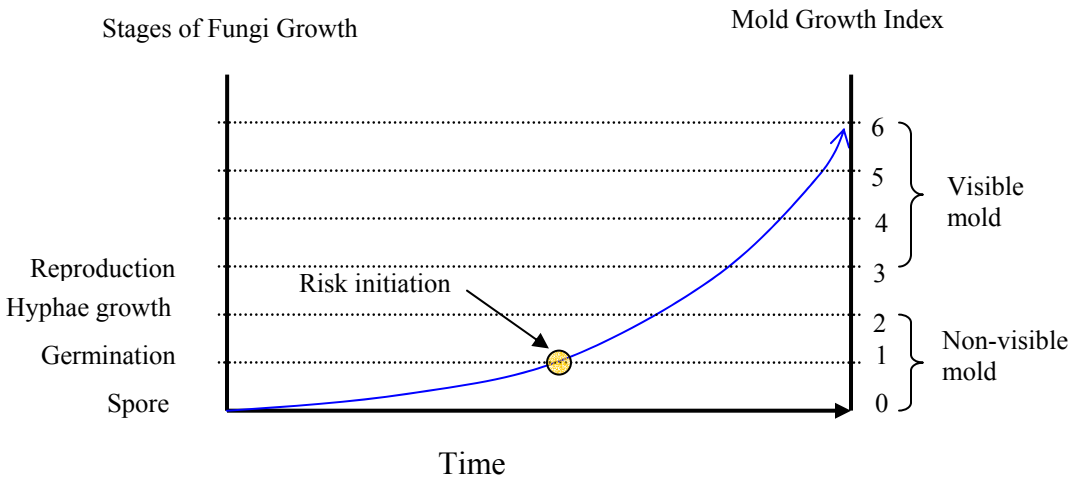

Figure 3.3 Relationship between fungus life stages, mold growth index, and risk initiation

Figure 3.3 shows the relationship among fungus life stages, the mold growth index, and risk initiation. In this particular study, mold growth risk is initiated at a point of the mold germination stage in a sense of a limiting phenomenon. In other words, once a mold spore germinates on a building material surface, the building has a mold risk. This definition of mold growth risk is used throughout the remainder of this thesis. As Harriman(2001) pointed out, after mold spores germinate, the fungi survive because of the moisture and nutrients inside the body, and the hyphae cannot be eliminated inside the substrate. This has been confirmed empirically under fluctuating moisture and temperature conditions (Pasanen, Kasanen 2000). The experimental results showed that fungal flora transforms to tolerate fluctuating temperature and relative humidity conditions, and relative drying conditions do not affect the viability of fungi, once they germinate.

The risk view of mold will be used as a foundation for the development of the intended performance indicator for mold.

3.3 DEVELOPMENT OF A PROBABILISTIC PI FOR MOLD GROWTH

3.3.1 Probabilistic mold risk indicator (MRI)

Although the hygrothermal simulation models are accurate, they are limited in that they typically operate on input models that are derived from as-designed information, producing deterministic results for a "design-interpreted idealization" of a building. This idealization, however, does not reflect the local, situational, and sometimes idiosyncratic aspects of a building during its operation. The lack of consideration of uncertainty and risk associated with mold growth and the complex physical, biological interaction necessitates the re-examination of appropriate evaluation methods for mold growth risk analysis.

Our approach treats mold phenomenon as a risk impacted by different sources of uncertainty. As explained earlier, the development of a risk-based performance indicator requires risk assessment composed of hazard identification, exposure assessment, dose response assessment, and risk characterization (Williams 2001). In engineering fields, risk is often defined as a numerical value that is a function of probability and consequences. This definition combines the potential for an undesired consequence with the likelihood that such a consequence will occur. It can be expressed mathematically (Meacham 2001) as follows:

Risk (consequence/unit time)

$$= \text{Probability(event/unit time)} \times \text{Magnitude(consequence/event)} \quad (3.2)$$

In the risk analysis for mold, both components of equation 3.2 have not been developed yet. First, we need to develop a reliable evaluation method that provides the probability of mold growth (based on germination as indicated above) in a building. The second component requires the study on the quantification of the impact of mold growth to individuals, property, and society. This thesis focuses on the development of a probabilistic performance indicator for mold based on the use of hygrothermal simulation models. We need to verify the reliability of input data, simulation tools, and methods used for mold assessment. All three interject uncertainty (issues regarding uncertainty will be discussed in more detail later in this thesis) into the analysis. The consideration of uncertainty in mold growth risk analysis leads to the second type of performance indicator in Table 3.1. In this study, the resulting performance indicator is called a mold risk indicator (MRI). Once the MRI is developed, a complete risk-based performance indicator for mold growth can be accomplished with a study of risk assessment. The next section addresses a roadmap and requirements for the development of the MRI.

3.3.2 Roadmap and requirements for the MRI

As discussed in Chapter 3.1, a performance indicator is based on experiments, calculation procedures including computational simulation, or a combination of both. Figure 3.4 shows the typical components and process for a performance indicator using

mathematical models. Depending on the target aspect of a building, an appropriate mathematical model is constructed, e.g., a thermal building model for thermal comfort evaluation. This model results in outcomes of state variables that are aggregated by a post process in which a performance indicator is generated.

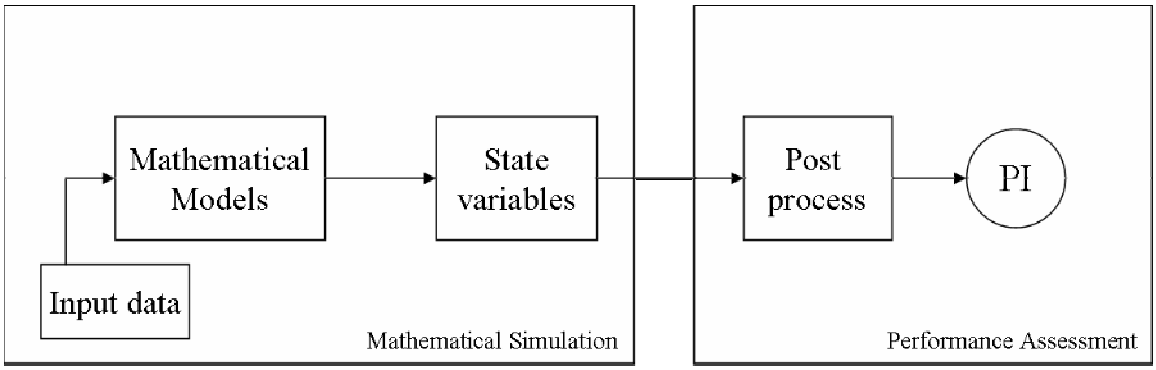

Figure 3.4 Schematic drawing of components and procedure for a typical performance indicator using mathematical models

In the development of an MRI, a similar process is followed with additional considerations specific to the mold phenomenon (Figure 3.5). The mathematic model should be constructed so that it encompasses all related mechanisms for the calculation of local environmental conditions (state variables). A probabilistic performance evaluation becomes available when uncertainty associated with the simulation process (mathematical models and input data) is taken into account. Input data consists of a scenario, building model data, building behavior and operation and a detailed discussion about associated uncertainties, discussed in Chapter 5. A new aggregation method will quantify the risk of mold growth for a specific building case. The results in the MRI are expressed as mold risk with a probability distribution over a certain measure, i.e. number of risky mold days.

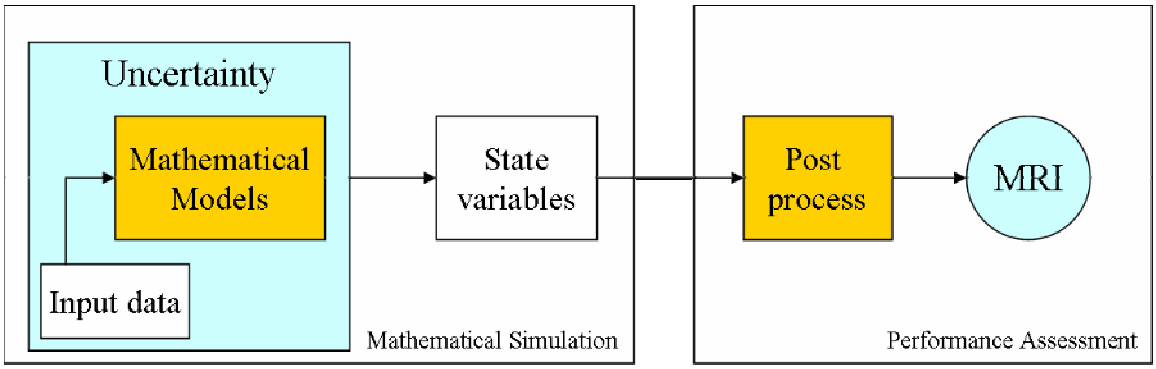

Figure 3.5 Schematic drawing of components and procedure for a new mold risk indicator (MRI) using mathematical models

To ensure reliable results from the MRI, three main issues must be addressed and studied: the extension of the simulation model, identification of uncertain parameters and quantification of uncertainty, and an aggregation method of state variables. These main issues are described in detail in subsequent chapters. The developed approach will be implemented in three cases, and the merits of the new method will be discussed. The three issues will be briefly introduced below.

First, current hygrothermal simulations do not treat all mechanisms in a coupled way and do not treat them at different levels of granularity. Identifying the relationship among all the complex causes and related parameters of mold growth could theoretically be accomplished by coupling all heat, air, and mass transfer equations in a new simulation code that treats all equations simultaneously at whole building and local component level. However, this approach is not advisable as long as there is no clear evidence that such development (and large amounts of research dollars) is warranted by quantified evidence that shows such a new simulation tool will indeed enable better and more secure mold risk assessments. This study, therefore, does not attempt to develop

such an extended simulation tool. Instead, it chooses best of breed tools that account for the major mechanisms that govern local environmental conditions for mold growth. The choice of tools is based on the identification of the causes of actual mold occurrences in real buildings. Each tool requires input models, derived from a conceptualization of the building case. An extension of the simulation model is thoroughly discussed in Chapter 4.

Second, uncertainty in the building model parameters is captured as probability distributions of model parameters. Depending on the building cases (i.e., building model and exposed scenario) each parameter may affect mold growth negatively or positively. Since the selection of a value may be a critical step for mold growth assessment, the mean values of uncertain parameters cannot be used as representative design values in mold growth analysis. Varying only a few of the parameters will have a significant effect on the outcome of a mold analysis. Since not all the building-related parameters have a significant effect on mold growth, the identification of a set of dominant parameters whose uncertainty range has a dominant effect on an increase in mold risk is useful. Thus, identifying the critical influence of building components, building operation, and maintenance factors on the increase in risk will lead to appropriate actions during building design, and the procurement process can be set up to address these risks. The issues related to uncertainty are discussed in Chapter 5.

Third, a reliable method that aggregates the physical conditions at material surfaces over time should be developed. Although 80% relative humidity seems a reasonable and conservative threshold level for preventing mold occurrence in buildings, it must be acknowledged that the actual threshold level varies with temperature, relative humidity, length of time that certain conditions were maintained (i.e., exposure time),

types of building materials, and so on. In this study, a germination graph method that accounts for surface relative humidity, temperature, and exposure time has been developed. The applicability of the germination graph method will be discussed first in the next section.

3.4 A UNIT OF MOLD RISK

By considering uncertainty in the process of the MRI, the results can provide probabilistic outcomes of mold growth risk as shown in Figure 3.6. The X-axis of the graph represents the normalized mold growth risk (between 0 to 1). "0" indicates no mold risk, and "1" indicates mold risk over the entire simulation period. The objective and quantified measure of mold risk can be calculated from the mold germination graph method that has been established in an earlier chapter. Since this method aggregates all important state variables calculated from hygrothermal simulation, it can be used in the post process stage to arrive the MRI result.

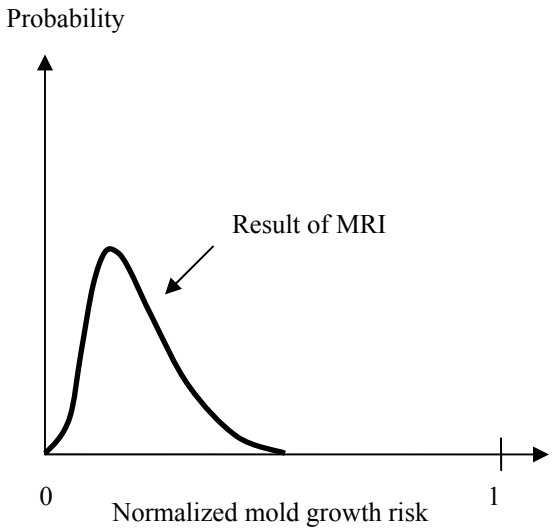

Figure 3.6 Distribution of mold growth risk using uncertainty analysis

The mold germination graph method provides “number of mold risky days” as a result within the period of simulation. The normative mold growth risk is now calculated as:

$$\text{Normalized mold growth risk} = \frac{\text{mold risky days}}{\text{days in simulation period}} \tag{3.3}$$

Based on the normalized mold growth risk, the MRI results are comparable between building cases or trouble spots within the same buildings. The next chapter deals with issues of the simulation extension to calculate local environmental conditions.

CHAPTER 4

MIXED SIMULATION APPROACH

The mold growth phenomenon is influenced by a multitude of parameters with complex physical and biological interactions. The proper calculations of local environmental conditions and the consideration of the biological effects of substrates on mold growth can be accomplished in mathematical models. Each model for physical and biological phenomena requires a deep understanding of mold occurrences and causes. A proper combination of these models will result in state variables on a specific location at a material surface, referred to as “trouble spot”. The extended simulation models serve as a simulation engine in the process of the MRI. This chapter discusses related issues in the extension of the simulation models starting with a study of the causes of mold problems in existing buildings and then providing so-called cause categories (section 4.1). Section 4.2 identifies the required simulation capacities for mold growth risk analysis based on the identified cause categories. Implementation of the extended simulation is described in section 4.3. The deployment of a particular simulation tool in the modeling procedure for simulation extension is discussed in the following sections respectively (i.e., hygrothermal models, building details and thermal bridges, local environmental condition).

4.1 CAUSE CATEGORIES

Although current hygrothermal models include heat and moisture transfer, the lack of capability of the models to include the deviation from the idealized building specifications may lead to academic and rather sterile results for mold growth risk analysis. To obtain meaningful result from the simulation procedure in existing buildings, our simulation capabilities need to include the impact of all physical processes in a building during its operation. In order to find the potential impact of non considered processes, a study of the main causes of reported mold problems and locations of mold occurrences was undertaken. This was done primarily to identify those cause that would require new simulation approaches and models, surpassing the capabilities that current simulation models offer. This study started with a review of the literature on reported mold cases.

Many researchers have reported possible causalities between building parameters and mold occurrences in existing buildings. The causes range from accidental and obvious water leakages and spills to unidentified sources. Recently, Sedlbauer (2001) described seven causes of mold growth in buildings: 1) moisture production indoors, 2) production of condensation water due to bad heat insulation, 3) insufficient heating, 4) inadequate ventilation behavior on the part of the occupants, 5) leaks in the building wall, 6) penetration of driving rain, and 7) construction moisture. A more comprehensive study was conducted as a review of building pathology literature(Moon and Augenbroe 2003). This study identified a wide range of causes of mold and moisture-related problems in residential, commercial, and school buildings as shown in Table 4.1.

Baughman reported that interior dampness problems are usually related to construction faults such as inadequate insulation, thermal bridges, inadequate ventilation,

certain patterns of building use, interior sources of humidity, improperly weatherproofed outside walls, or inadequate drainage (Baughman and Arens 1996). These and other sources were used in the literature review to categorize the causalities that were studied. It was found that common causes of moisture problems in different type of buildings can be attributed to a set of common causes, summarized in Table 4.1.

Table 4.1 Causes of mold problems from literature review

Causes	**Real building examples from literature review**	**Buildings***
HVAC defect	Direct infiltration of humid air	1,2,3
	Negative pressures across the envelope	1,2
	Inadequate moisture removal (return duct)	1
	Inadequate ventilation	1,2,3
Design defect	Low permeability of the exterior weather barrier	1
	Vapor retarder in the wrong location	1,2
	Leakage of precipitation	3
	Defective drainage	1,2,3
	Impermeable surfaces (vinyl flooring, vinyl wall paper)	1,2
	Inadequate insulation, thermal bridges	1,2
Building usage	High occupant density	1
	Pattern of use, cooking habits	1,2
	Low air conditioner thermostat setting	1
	Stock of wood, papers, books	1
Maintenance/ operation	Inadequate maintenance and operation of equipment	1
	Cleaning	2
	Aging of construction materials	3
Construction defect	Poor site drainage	1
	Location and orientation	1,2
	Water leakage from piping, roof, basement.	1,3

(* 1: residential 2: commercial 3: school)

Investigations of mold problems in buildings have revealed a variety of trouble spots of mold. Mold prefers to grow where insulation materials are improperly designed or installed, which contributes to condensation problems due to thermal bridge effects.

Possible places for condensation include window frames and sills, ceilings, the backs of furniture, duct insulation, the interior corners of exterior walls, and 3-D joints (e.g., corners between ceiling and exterior walls), behind impermeable wallpaper or under vinyl flooring, and so on. Table 4.2 summarizes the reported locations of mold problems and types of buildings. Although mold can grow in any location in which favorable environmental conditions are met, the mold risk analysis first concentrates on the locations where actual condensation or mold growth may occur faster than predicted by the idealized simulation.

Table 4.2 Mold growth locations

Locations	**Buildings***
Sheathing	1
Interior walls	1,2,3
Interior furnishing	3
Window frames, sills	1,2,3
Gable ends	1
Ceiling	1,3
Shoes	1
Wood fittings	1
Back of Furniture	1
Behind impermeable surfaces	1,3
Fixture	2
Building construction	1,2
Under carpet	1,3
Fan-coil units	3
Papers, books	1,3
Duct insulation	1,3

(* 1: residential 2: commercial 3: school)

The above study of the causes and effects of mold problems can be categorized into four major “non-standard” mold cause categories. These categories potentially can “explain” the anomalies found in actual buildings where mold has occurred without a

satisfactory explanation based on standard simulation assessments. The suggested four cause categories are: (a) spore availability, (b) substrate condition, (c) HVAC maintenance and operation, and (d) local building details. The physical aspects and situational dependence of the four categories are discussed below.

Cause category (a) - spore availability: This category considers the spore distribution in a building and in transportation from outside air through infiltration and ventilation. Cleaning activity removes the deposited spores on surfaces and reduces the concentration of airborne fungal spores. Thus, this category includes information about the type of ventilation system, the use of space and cleaning schedule, and the concentration of spores in the air and on surfaces.

Cause category (b) - substrate condition: The state aggregation required for quantification of mold risk is based on the isopleths for mold spores (see the mold germination graph). Since the experiments were not conducted on building materials but on optimum substrate for mold growth, appropriate germination graphs for each building material and fungal species need to be developed. Thus, this category includes the relationships between different building materials, environmental conditions, and mold occurrences.

Cause category (c) - HVAC maintenance and operation: Some researchers have reported that the maintenance and operation of the HVAC system can be important factors in mold occurrence in existing buildings. Past research has stressed the importance of air supply layout, ventilation efficiency, dead zones, maintenance and cleaning policies, as well as the HVAC operation schedule. Thus, this category includes

the risk of outside air infiltration related to pressurization, air tightness of facades, HVAC shutdown operation, and other factors related to HVAC.

Cause category (d) - building details: Mold prefers to grow in places where insulation materials are improperly designed or installed, causing condensation problems due to the thermal bridge effects. This category takes into account all building details in which actual condensation or mold growth may occur faster than predicted by the idealized simulation.

Table 4.3 Cause categories and preliminary list of parameters

Cause categories	**Parameters**
Spore availability	Number of outdoor spores Re-emission rate Indoor spore sources Deposition rate Cleaning frequency Cleaning efficiency
Substrate condition	Pore size of the surface Roughness of the surface Initial water content Thermo-physical properties of building materials (density, specific heat capacity, etc)
HVAC system operation and maintenance	Supply air volume Amount of outdoor air intake Surface air velocity Pressure difference Local outdoor temperature Local outdoor relative humidity HVAC filter efficiency Moisture generation rate
Building details	Structure of materialization (thermal bridge) Workmanship External heat transfer coefficients Internal heat transfer coefficients Precipitation Wind velocity and direction Infiltration (Cs, Cp, Cd) Exfiltration (Cs, Cp, Cd)

Table 4.3 presents a preliminary list of parameters and cause categories. Depending on building geometry and physical configuration, each building may have different parameters for mold growth analysis. For example, a building with a fan coil unit has different parameters than one with an air-based ventilation system. This information is captured in the building model that drives the simulation. Types of occupancy, operation schedule, and occupant profiles affect mold growth in buildings as well. These factors are described in a fixed "scenario" that is used for the building simulation. It will be described in detail later.

Experts have reported the most plausible causes in mold problem cases in which no obvious sources of water are found in the building. However, clear and unbiased scientific validation of causes has not been conducted due to the lack of a mold risk indicator that considers all related mechanisms and uncertainties. The referenced study of causes and locations of mold growth in existing buildings showed that more sophisticated simulation models are needed to assess or predict mold risk at specific trouble spots. The MRI for that purpose will have to be based on extended simulation capabilities and uncertainty analysis. The following section describes the use of simulation tools and discusses extension of their functionality to calculate all local environmental conditions for mold growth analysis.

4.2 SIMULATION EXTENSION

Current mold growth analysis approaches, based on the modeling of heat and mass transfer processes in buildings, emphasize the hygrothermal simulation of space enclosures. Hygrothermal models calculate detailed moisture content and temperature

within building envelops. However, these standard hygrothermal models assume the idealization of a building and known boundary conditions. Furthermore, the output of 1-D simulation does not represent a trouble spot where mold prefers to grow, such as line joints or thermal bridge locations. The required additional mechanisms that are important in mold growth are discussed in this section.

The extended simulation capabilities should include additional bio-physical mechanisms for accurate mold growth assessment. Physical mechanisms that affect the local environmental conditions at specific trouble spots include airflow in a space (poor ventilation and dead zones), heat and moisture transfer in 2-D or 3-D building details, additional local sources of heat and moisture, and so on. In actual buildings, these physical mechanisms govern the boundary conditions (the micro environment) at a specific trouble spot. The micro environment is affected by various factors in buildings, including HVAC system operation, infiltration and ventilation, and building usage. Meanwhile, moisture generation from the occupants and sources in a space are critical for moisture transfer. These issues should be therefore all be dealt with in the extended simulation capabilities.

Mold growth and germination are affected by biological mechanisms as well. Each building material provides different levels of nutrients for mold growth. Higher nutrients on the substrates increase the rate of mold growth and require less exposure times for germination. Furthermore, determining the severity of mold infestation on building surfaces require knowledge of the concentrations of indoor air spores and deposited spores on building surfaces. These biological relationships are complex and vary considerably among the fungal species.

The simulation extensions that account for most of non-considered (in standard simulations) physical and biological phenomenon in mold growth can be based on the four cause categories identified. The required four expanded capabilities are shown in Figure 4.1; each arrow represents one of the identified mold cause categories.

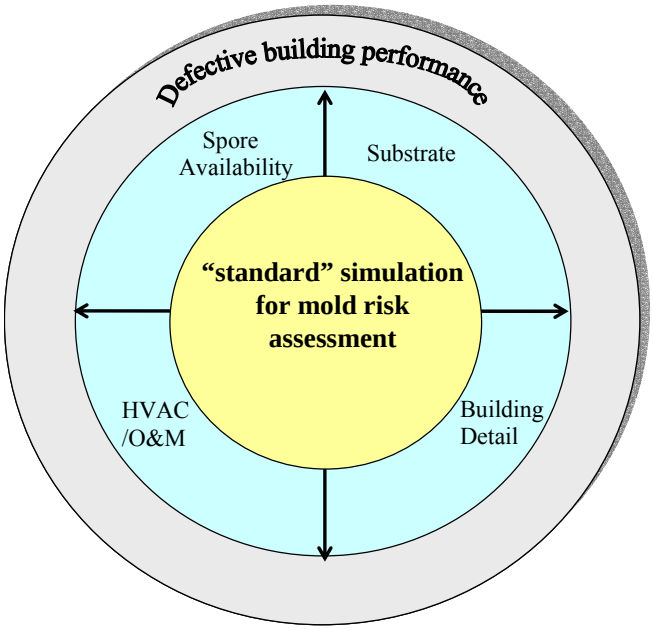

Figure 4.1 Additional simulation capabilities required for accurate mold growth assessment.

The upper half relates to biophysical mechanisms driving the germination in existing buildings (i.e., the behavior and settlement of fungal spores and the effects of building materials as substrates). The lower half of the figure relates to the detailed modeling of physical (heat, air, and mass) transport mechanisms that result from special HVAC features and local 2D and 3D building details. Issues for HVAC include types of heating and cooling system, infiltration, operation schedules, set temperature, and so on.

In “Building detail”, main issues are thermal bridge, workmanship, low airflows in corners, and certain obstacles in the proximity of wall surfaces.

The center of the figure shows the current simulation base for standard mold growth assessment. This study identifies the areas in which the base should be extended to encompass the (bio)physical processes related to one or more of the four mold-cause categories. It should be noted that mold is a phenomenon that results not only from (partly) predictable phenomena (in the middle concentric circle), but also from random events, such as building defects, extreme events, and abuse of building systems. Such causes are deemed to lie in the outer “defective building performance” circle and are not within the scope of this research. The next section describes the implementation of the simulation extension based on a mixed simulation approach.

4.3 MIXED SIMULATION APPROACH

4.3.1 Coupling methods

Identifying the relationship among all the complex causes and related parameters of mold growth could theoretically be accomplished by increasing the capabilities of current simulation models. Complete heat, air, moisture (HAM) models have to couple the flow equations of the energy and mass, including heat, air, and moisture components in various states. The ideal and most accurate coupling method is the algorithm coupling: coupling of all the transport equations, both on whole building as well as on local enclosure scale (Figure 4.2). However, this method would require a tremendous amount of work and would probably produce complex matrices beyond the capabilities of current mathematical solvers (Huang, Winkelmann 1999). This is not advisable as long as there

is no clear evidence that such extensions are warranted by quantified evidence that these extensions will indeed enable better and more secure mold risk assessments.

The other coupling method is to combine existing models sequentially for the calculation of the local environmental condition. This sequential coupling of current best of breed models is the simplest method (Figure 4.3). With this method, the first model runs and its output is used as input data for the second model. This approach eliminates the efforts to couple all heat, air, and moisture transfer equations. Depending on the required level of granularity, the modeling procedure can easily be changed.

However, the sequential coupling of method presents certain limitations. First, the calculation results from the sequential coupling are less accurate than those of the fully coupled method, since each flow equation is solved sequentially, and no feedback between the two models is accounted for. This approach should be used only if the objective of the simulation is to observe the relative performance evaluation.

It should be noted that the sequential approach introduces a source of (model) uncertainty due to the lack of feedback loops. Another major source of model uncertainty is the non representation of ignored mechanisms, such as indoor temperature stratification. As indicated before, the model uncertainty is not considered at this point of the research but is regarded as a refinement of the current study of downstream validation of the developed MRI gives rise to the need for more refined analysis. Accurate analysis of the model uncertainties will require very substantive research efforts (similar to the ones conducted in (de Wit 2001) for only two parameters.

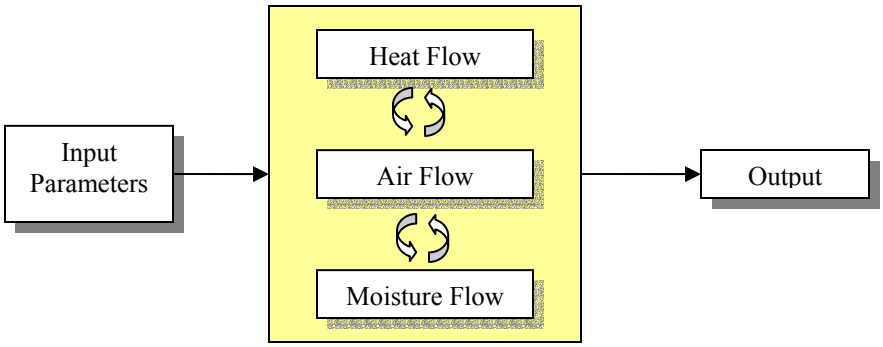

Figure 4.2 Schematic drawing for the algorithm coupling method

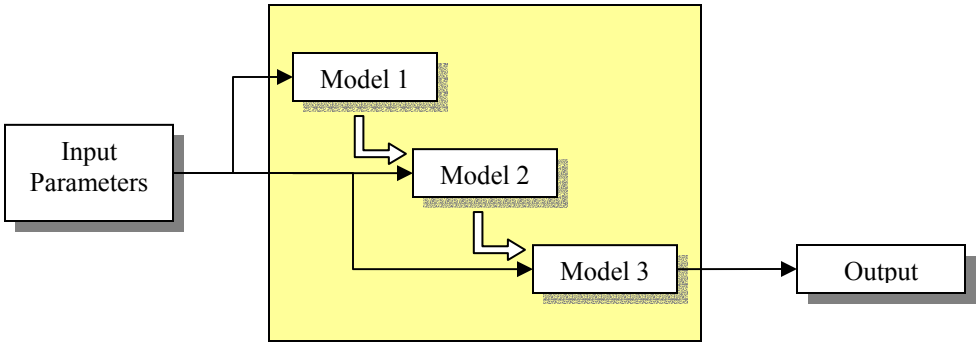

Figure 4.3 Schematic drawing for the sequential coupling method

Since this thesis focuses on the "first-pass" development of a performance indicator for mold growth risk and interests in relative performance evaluation, the sequential coupling method is used for the implementation of the simulation extension. As a result, it is not attempted to develop one big model that couples all equations and solves them simultaneously in the expanded matrix. Instead, the new performance indicator uses a mix of existing simulation tools, each specialized in a particular domain

of heat, air, and moisture transport with the sequential coupling method. The associated modeling uncertainty will be discussed in Chapter 5 with other sources of uncertainty. For the time being, the resulting model uncertainty is deemed of second order. The next section deals with the realization of the mixed simulation based on the sequential coupling.

4.3.2 Mixed simulation approach in mold growth analysis

Mold growth is mainly affected by local environmental conditions (i.e., surface temperature and relative humidity) on the surface of material. Local conditions are governed by heat and moisture transport in the material and at the air-material interface, boundary airflows, material composition and properties, HVAC system operation, outside air infiltration, building maintenance activities, and so on. These mechanisms vary in nature and need to be studied at different building granularities. The combined effect of relevant mechanisms can be studied using a mixed simulation approach. The judicious mix of tools to investigate the effect of critical building parameters on mold growth is demonstrated by the case studies presented in Chapter 6. Figure 4.4 shows a schematic drawing of the mixed simulation approach in mold growth analysis and an example of tools for each domain.

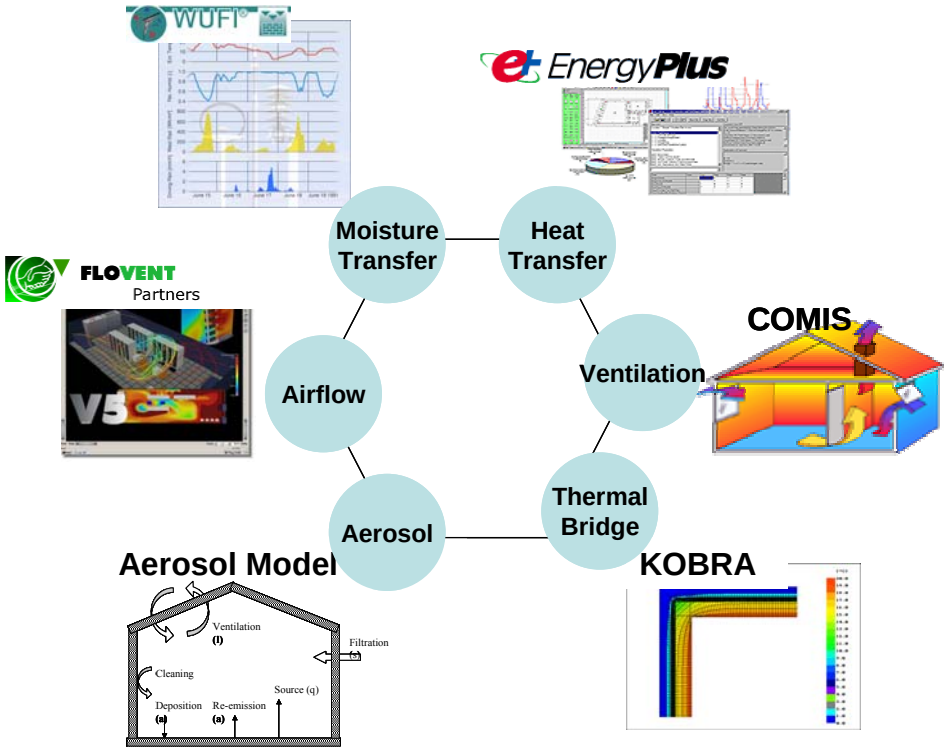

Figure 4.4 Schematic drawing for the mixed simulation approach in mold growth analysis

Figure 4.5 shows the modeling procedure and simulation tools that are used in this study for an interior corner wall. Their choice is driven by the need to cover every mechanism that affects the local conditions at material surfaces. Each box represents a step in the sequential simulation approach (i.e., the deployment of a particular simulation tool). The outcomes of the steps are combined to provide a full assessment, as shown in Figure 4.5. The objective is to simulate the mold growth conditions on a set of specific locations ("trouble spots") on interior surfaces at the end of the modeling procedure. Depending on the trouble spots, the mixed simulation modeling procedures can be modified with additional simulation models. For example, if the trouble spot is selected

as an interior corner wall behind furniture, one may include the CFD model to investigate the effect of poor ventilation around the corner that may increase mold growth risk.

The general procedures of the mixed simulation approach are described as follows. The mixed simulation is typically performed for a whole building or a large enough building zone in a given geographic location with known (micro-) climatic conditions. Within the simulated building zone, a set of trouble spots is identified, typically in corners, at edges, or at spots where deficient building detailing has been established or may be suspected. The latter distinction may need some explanation. In a given building case, a thermal bridge may actually exist in the design specification. In that case, it is treated as a deterministic input for the design reference case (or "base case" that uses best estimates of all variables, as they would be chosen in a standard deterministic simulation). The thermal bridge may also be the result of an uncertainty analysis, e.g., resulting from an analysis of the likelihood that bad workmanship would lead to certain deficient building details. One needs to model the probability that a deficient building detail of a certain type and severity will be present in the building. The probability would be derived from what is known about the occurrences of deficient details in similar buildings with similar technologies.

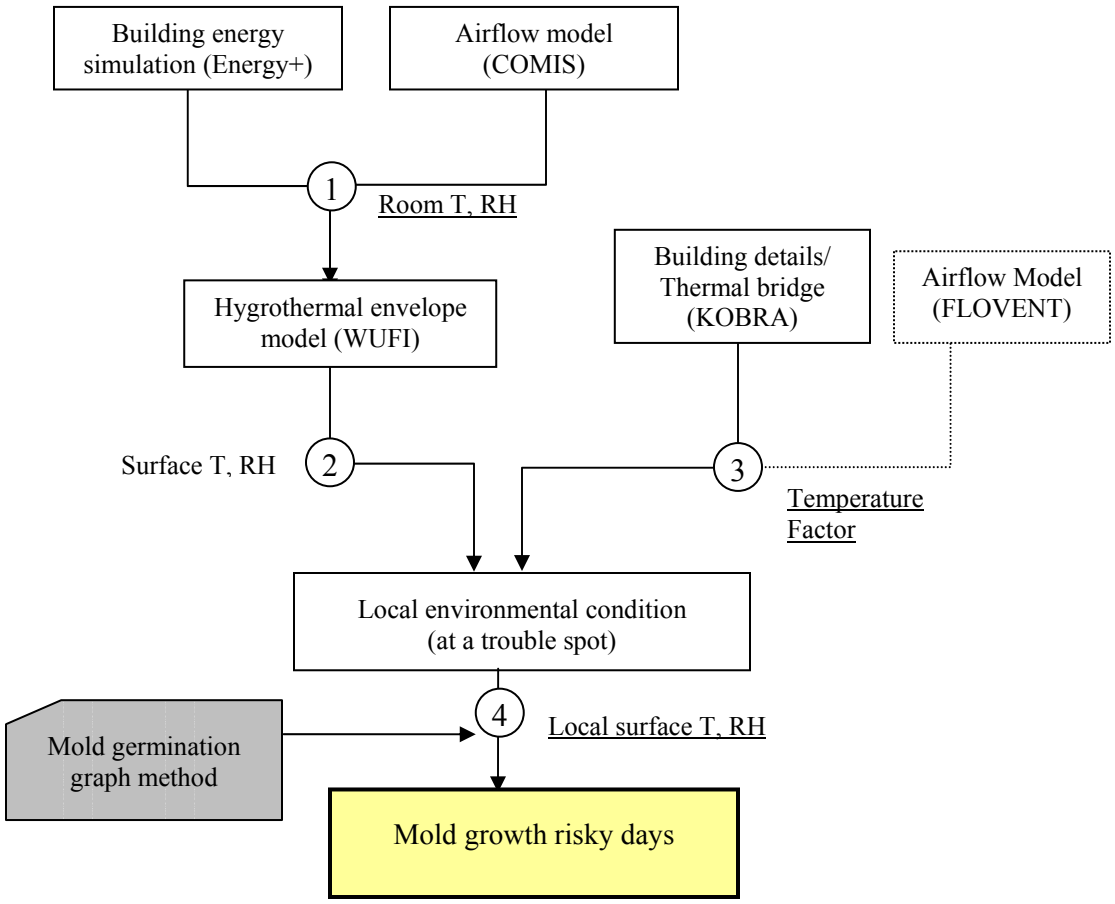

Figure 4.5 Flowchart of the mixed simulation approach and the outcome of each step

Each step in the above flowchart (Figure 4.5) is described in the following sections of this chapter. The developed mold germination graph method is used in step 4 to aggregate the calculated local environmental conditions.

4.4 HYGROTHERMAL MODELS

This section discusses the first and the second steps of the mixed simulation approach presented in Figure 4.5. In each step, the best breed model is selected and the simulation results are provided to the next detailed model. The analysis starts with a standard building energy simulation model that is capable to give zone level information with respect to temperature and relative humidity over time. Any whole building energy and moisture simulation model is a good candidate in this step. In Table 2.4, EnergyPlus, Esp-r, and BSIM 2002, were compared for this purpose. EnergyPlus and COMIS were chosen in our study for heat transfer and airflow models respectively, since both software tools can easily be combined. They have been intensively validated. The equations below show the heat balance equations used in EnergyPlus, at an outside wall surface, at an inside wall surface, and an air zone defined within the building (Strand, Pedersen 2001):

Outside surface:

$$Q_{SWrad} + Q_{LWrad} + Q_{conv} + Q_{cond} = 0 \tag{4.1}$$

Inside surface:

$$Q_{solar} + Q_{SWlight} + Q_{LWradExch} + Q_{LWrddIntGains} + Q_{conv} + Q_{cond} = 0 \tag{4.2}$$

Zone air:

$$C_z \frac{dT_z}{dt} = Q_{conv} + Q_{convIntGains} + Q_{infil} + Q_{sys}\,, \tag{4.3}$$

where $C_z \frac{dT_z}{dt}$ = energy stored in zone air

Q_{SWrad} = amount of solar radiation absorbed on the surface

Q_{LWrad} = thermal radiation exchanged between the surface and its surroundings

Q_{conv} = convection between the surface and the surrounding air

Q_{cond} = conduction into the wall materials

Q_{solar} = solar radiation absorbed on the inside surface

$Q_{SWlight}$ = short wavelength radiation from lights

$Q_{LWradExch}$ = long wavelength radiation exchanged with other surfaces

$Q_{LWrddIntGains}$ = long wavelength radiation from internal heat gains

$Q_{convIntGains}$ = heat convected from internal gains

Q_{infil} = heat gain or loss due to infiltration

Q_{sys} = heat added or subtracted from the space due to a space conditioning system

To predict detailed moisture behavior on specific locations on interior surfaces of the building envelope, hygrothermal envelope models such as 1-D HAM, WUFI and MOIST are good candidates. This particular research chooses WUFI for the purpose because it is ideally suited to simulate moisture transport in multi-layered envelopes and the surrounding environment. It provides a detailed moisture transfer analysis with additional functionality, such as the specification of initial moisture content in building materials and rainwater penetration.

The governing equations employed in WUFI for mass and energy transfer are as follows (Kunzel 1995):

Moisture transfer:

$$\frac{\partial w}{\partial \varphi}\frac{\partial \varphi}{\partial t} = \nabla \cdot \left(D_{\varphi} \nabla \varphi + \frac{\delta}{\mu} \nabla (\varphi P_{sat}) \right) \tag{4.4}$$

Heat transfer:

$$\frac{\partial H}{\partial T}\frac{\partial T}{\partial t} = \nabla \cdot (\lambda \nabla T) + h_v \nabla \cdot (\frac{\delta}{\mu} \nabla \varphi P_{sat}), \tag{4.5}$$

where φ = relative humidity [%]

T = temperature [°C]

$\frac{\partial H}{\partial T}$ = heat storage capacity of the moist building material

$\frac{\partial w}{\partial \varphi}$ = moisture storage capacity of the moist building material

λ = thermal conductivity of the moist building material [W/mK]

D_{φ} = liquid conduction coefficient of the building material [kg/ms]

δ_p = water vapor permeability of the building material []

δ = vapor diffusion coefficient in air [kg/msPa]

μ = vapor diffusion resistance coefficient in building material [-]

h_v = evaporation enthalpy of the water [J/kg]

P_{sat} = water vapor saturation pressure [Pa]

The coupled EnergyPlus/COMIS calculation results in zone air temperature and air relative humidity for the chosen simulation period. The results of the two models are

subsequently used as an interior time varying boundary condition in the WUFI's hygrothermal envelope model. The parameters in the above equations are considered uncertain parameters in an uncertainty analysis.

4.5 BUILDING DETAILS AND THERMAL BRIDGES

This section describes the modeling of building details and thermal bridges in mold growth analysis and discusses related issues, such as bad workmanship. Mold does not typically occur on an undisturbed wall. Instead, it prefers to grow at line or node joints, i.e., where certain building details negatively influence the surface conditions. These situations occur where insulation materials are improperly designed or installed with bad workmanship, causing condensation problems due to bad building detailing, leading, for instance, to unwanted thermal bridge effects. Heat transmission is much higher at a thermal bridge than at a plain wall, if the same film coefficient is used. This thermal bridge effect will lead to lower internal surface temperature and higher surface relative humidity, subsequently affecting the mold growth risk. The building details and thermal bridge effect are described here as step 3 in Figure 4.5.

Thermal bridges typically give rise to lower internal surface temperatures in cold climates and higher temperatures in hot climates, which may increase or decrease mold growth risk. Deficient building detailing usually occurs at wall/window connections, wall/floor intersections, and wall/foundation intersections, but many other types of thermal bridges may occur depending on the construction technologies used for the installation of the envelope components. ASHRAE (2001d) also report that mold often grow in exterior corners due to thermal bridge, wind washing, the fin effect, or poor

indoor air circulation. Figure 4.6 shows a typical temperature distribution result conducted in a building in Atlanta with an indoor/outdoor temperature difference of 20°C in the heating season. In the external corner wall, the lowest interior surface temperature is at the corner of the wall (16.3 °C) and the interior surface temperature increases as the distance from the corner increases.

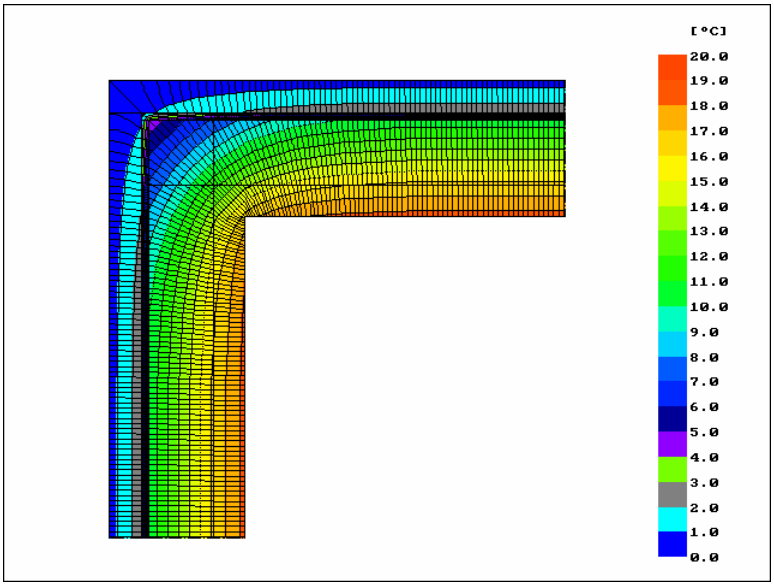

Figure 4.6 Temperature distribution due to the thermal bridge effect at the corner wall

To make the study feasible, this thesis focuses on a specific type of thermal bridge, which is an exterior wall corner in a cavity wall. The following section describes how to take into account building details in which actual condensation or mold growth may occur faster than predicted by the idealized simulation. The uncertainties associated with thermal bridges and bad workmanship during the installation of building components is discussed.

4.5.1 Thermal bridge assessment

Thermal bridge assessments can be based on simple steady state assumptions, which allow the straightforward classification of thermal bridges. This method uses a thermal bridge atlas that provides a simple and easy assessment of a thermal bridge in a steady state, which is supported by the European Standards Organization (CEN). A computational tool for this approach is EUROKOBRA, developed by PHYSIBEL (2002). Alternatively, one could opt for a detailed 3D simulation in a whole building model. The second approach enables a 3D, detailed, dynamic thermal bridge analysis, such as ESP-r (Ben-Nakhi 2003; Strachan, Nakhi 1995). Clearly, for the purpose of this study, such an integrated dynamic study would overkill the problem as it only need to assess the effect of the uncertain location and the uncertain severity of a set of (not precisely known) building details. It was decided to use the stand-alone tool KOBRA that offers flexible configuration of thermal bridge types and give a "temperature factor" which can easily be interpreted in the proposed combined simulation approach. It qualifies the severity of a thermal bridge using the "temperature factor" which is defined as the inside surface temperature that results from an indoor-outdoor temperature difference of 1°C. The temperature factor is considered the key building detail parameter that will be an input parameter in the simulation roadmap of Figure 4.2.

By definition, the temperature factor of an interior surface of a wall is expressed as

$$f = \frac{T_s - T_o}{T_i - T_o} \ , \tag{4.6}$$

where T_s : internal surface temperature

T_i : internal air temperature

T_o : external air temperature

The temperature factor does not depend on actual boundary conditions; it depends on inside surface resistance (R_{si}) and the thermal conductivities of the building materials (λ). The surface temperature can be calculated by the known boundary conditions and the temperature factor. The temperature factor is used to estimate the quality of the thermal bridge in the mold investigation. Case studies that use the temperature factor in mold investigation in buildings can be found in IEA (1990). The ISO (2001) standard also used the temperature factor to calculate the minimum acceptable surface temperature to avoid the critical surface humidity. However, ISO and other case studies did not specify the types of thermal bridges or consider workmanship that may increase mold growth risk.

4.5.2 Bad workmanship

Field investigation studies showed cases of mold infestations on the interior surfaces of exterior walls, which were caused by thermal bridges and bad workmanship in installing insulation. As an illustration, Sedlbauer (2002) investigated a house and found an extended mold infestation in the lintels area that had not been insulated. He also discovered a continuous gap of 3 mm (due to poor workmanship) between the insulation sheets, which caused circular patterns of the infestation to appear in the middle of the façade. In another study, Csoknyai (2001) reported an intensive mold growth problem at a thermal bridge in a room, especially in the corner. Observation showed that mold

always began to grow from the top of the corner and gradually descended. Mold infestation kept reoccurring at the same location after eradication. Mold growth on exterior surfaces caused by thermal bridges can be found in Kunzel and Sedlbauer (2001).

In this research, the author focuses on a specific type of wall construction technology and one type of thermal bridge associated with the wall construction. One of the popular wall construction technologies for small buildings is the cavity wall in the United States and European countries. The most common location of mold infestation is interior surfaces in the exterior wall corner. Thus, this research focuses on the cavity wall construction technique and an exterior wall corner as a thermal bridge.

A cavity wall consists of two walls separated by an air space. The purpose of the cavity is to break the capillary flow path and drain penetrating rain water into a controlled exit. The cavity can be empty, half filled, or fully filled with insulation materials. After the energy crisis of 1973, the filled cavity was common used to increase thermal performance of the wall in cold regions. However, the installation of insulation in the air gap complicates matters and causes construction problems, such as the corner of the walls not being filled in well. Figure 4.7 gives an exemplary section of a cavity wall with partial insulation.

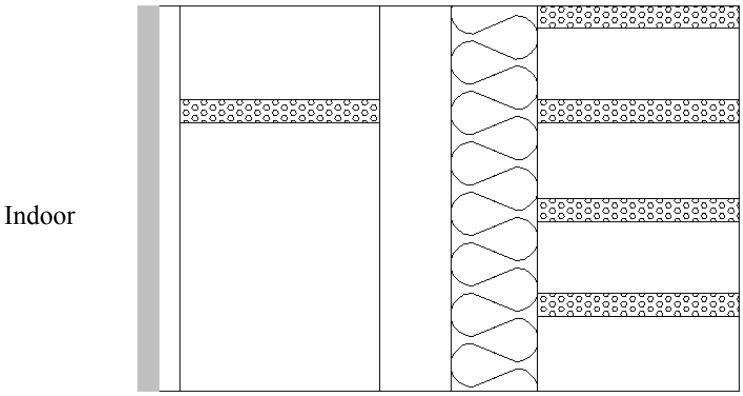

(a)

Building Materials	**Thickness (m)**
Brick	0.1
Mineral insulation	0.05
Air gap	0.05
Concrete block	0.1
Air layer	0.01
Gypsum board	0.01

(b)

Figure 4.7 Example of a cavity wall with partial insulation (a) section of the cavity wall (b) construction elements

Although manufacturer's guidelines or building standards (BIA 1999; BSI 1994) offer a guide for construction a cavity wall and installing insulation materials, thermal performance of cavity walls largely depends on workmanship and supervision during their construction. Inappropriate site practices in installation of insulation materials in the cavity wall include

- Wrong order of construction
- Installation in incorrect orientations
- Installation with wet or damaged insulation materials (poor storage)
- Badly fitted insulation materials or folded materials
- Lack of use of insulation materials
- Dirt or mortar droppings in the cavity

Hens (1995) also pointed out that partial and full-fill insulation of the cavity walls required critical view of workmanship, thermal bridges, and interstitial condensation. Knapen (1985) conducted experimental research on thermal bridges of filled cavity walls and showed the temperature factor on the edges falls to 0.78, while the value remains at 0.94 at the middle of the wall. The temperature factors at thermal bridges in existing buildings can fall far below those found in laboratory experiments due to bad workmanship.

Table 4.4 Field measurement of temperature factor on a partially filled cavity wall

Location	**Temperature Factor**	
	Measurement	Calculated
Middle of the façade wall	0.71	0.9
Façade wall at 40cm above floor level	0.67	0.9
Edge of floor and façade wall	0.35 – 0.46	0.6
Corner floor-gable wall-façade wall	0.28	-

Hens (1992; 1995) conducted field measurements for a partially filled cavity wall with poor workmanship and showed that the temperature factor goes down to 0.28 in the corner between the façade wall, the gable wall, and the floor on grade as shown in Table 4.4. These differences between the temperature factors of the idealized thermal bridge calculations and those of the actual measurements are assumed to be attributable to bad workmanship during construction. The uncertainty associated with the temperature factor due to thermal bridge and bad workmanship in the cavity wall in a real case can for instance be investigated through field measurements. The results will be discussed later in Chapter 6.

4.6 LOCAL ENVIRONMENTAL CONDITIONS

This section describes how to calculate local environmental conditions at a thermal bridge location based on the result from a hygrothermal envelope model and a temperature factor from KOBRA (step 4 in Figure 4.5). As Sedlbauer (2001) pointed out, the relative humidity at the thermal bridge increases because of locally increased heat transmission. The calculation of the hygrothermal envelope model provides the overall surface temperature and relative humidity at the interior surfaces of a wall. This result is derived for an undisturbed plane wall, assuming a uniform distribution of temperature and relative humidity. By mixing the temperature factor, which accounts for the disturbed temperature field at certain building details in this calculation, the local conditions at a trouble spot can be approximately represented. For this, it has to be assumed that the humidity ratio in a wall is uniformly distributed at the surface of the wall (i.e., at the surface not disturbed by the building detail). With this assumption, the adjusted local

surface temperature and relative humidity at the presumed trouble spot can be calculated by using only the temperature factor.

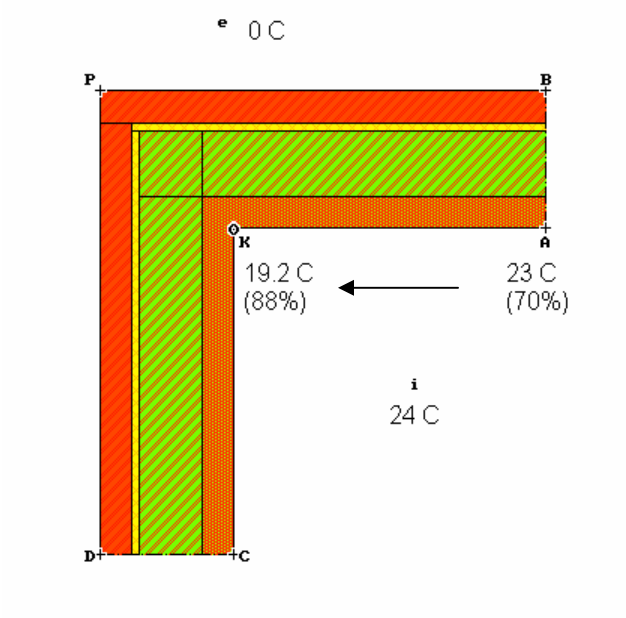

Figure 4.8 Schematic drawing for surface temperature and relative humidity at the thermal bridge location from undisturbed plain wall results

Figure 4.8 above shows a schematic drawing for surface temperature and relative humidity at the thermal bridge location and undisturbed plain wall. The surface temperature and relative humidity at the plain wall can be calculated by using the calculation procedures in Figure 4.5 (steps 1 and 2). With the known temperature factor, the local conditions at the thermal bridge are calculated as follows.

The equation (4.6) can be rewritten to calculate local surface temperature ($T_{s,l}$) with the known temperature factor at a specific location as equation (4.7):

$$T_{s,l} = f \times (T_i - T_o) + T_o \qquad (4.7)$$

The local relative humidity can now be calculated based on the local surface temperature and wall relative humidity (φ_s). Using a suitable psychometric charts, tables or an empirical formula, one can calculate the saturated vapor pressure of water as a function of temperature, such as equation (4.8) in ISO (2001). Vapor pressure at a local surface ($P_{s,l}$) can be calculated using equation (4.9).

$$\mathrm{P_{sat}} = 610.5 \times \mathrm{e}^{\frac{17.26 \times \mathrm{T}}{237.3+\mathrm{T}}} \text{ for } T \geq 0°\mathrm{C}$$

$$\mathrm{P_{sat}} = 610.5 \times \mathrm{e}^{\frac{21.875 \times \mathrm{T}}{265.5+\mathrm{T}}} \text{ for } T \leq 0°\mathrm{C} \quad (4.8)$$

$$P_{s,l} = \varphi_s \times P_{sat} \quad (4.9)$$

$$\varphi_{s,l} = \frac{P_{s,l}}{P_{sat,s,l}} \quad (4.10)$$

Finally relative humidity at local surface ($\varphi_{s,l}$) is calculated from equation (4.10). In general, a thermal bridge and bad workmanship lower the surface temperature but increase the surface relative humidity during the heating season, and vice versa during the cooling season. The effect of a thermal bridge may increase or decrease mold growth risk depending on the temperature and the relative humidity. This section has described the procedures of the mixed simulation approach (Figure 4.5). Next section addresses the implementation of the mixed simulation approach.

4.7 IMPLEMENTATION OF THE MIXED SIMULATION APPROACH

The implementation was driven by practicality and speed. No attempt was made to make a robust interoperable set of simulation tools. In stead most of the simulations were connected in a handcrafted way. Details are described in this section.

In the mixed simulation approach, the simulation inputs are initially prepared by hand. The transfer of output from one simulation to the boundary condition of the next model is hardwired into the simulation inputs. The models in the mixed simulation approach are not easily linked to each other. The input data exchange requires human intervention at each step between the models. It should be ensured that the same values of the input parameters are used in all the models involved. An Excel macro-based interface was used to facilitate the connection between the steps in the mixed simulation approach, as shown in Figure 4.9. This interface generates a kli file (boundary condition of WUFI), analyzes the results from WUFI, and calculates the surface temperature and the relative humidity at the thermal bridge location.

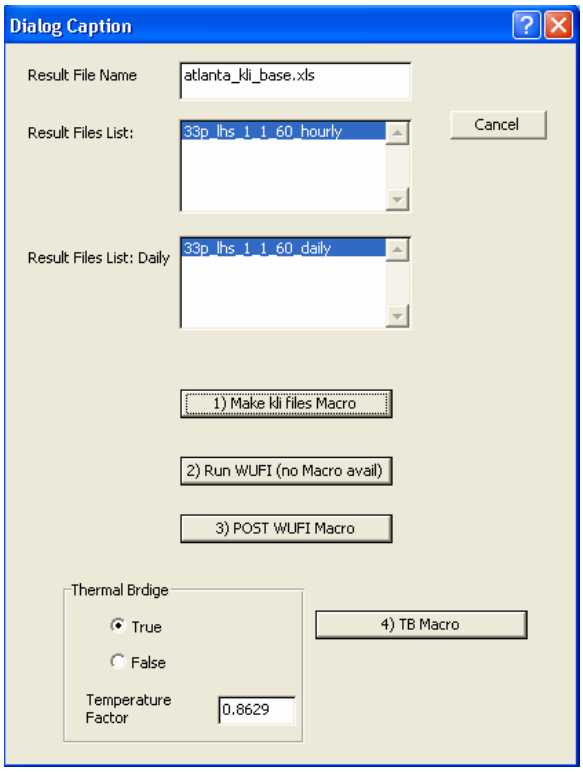

Figure 4.9 An Excel macro interface connecting each step of the mixed simulation approach

Using this interface, first, the outcome of the EnergyPlus and COMIS is prepared for WUFI boundary condition. With the specified boundary condition and building data, the WUFI simulation is then conducted by hand. The results of WUFI and the temperature factor are used to calculate the surface temperature and the relative humidity at a thermal bridge location. These local environmental conditions are then analyzed to arrive at mold risk days based on the mold germination graph method, as shown in Figure 4.10. If needed, different mold germination graphs can be replaced in the analysis. It also enables mold risk analysis using an alternative, simple 80% RH criterion.

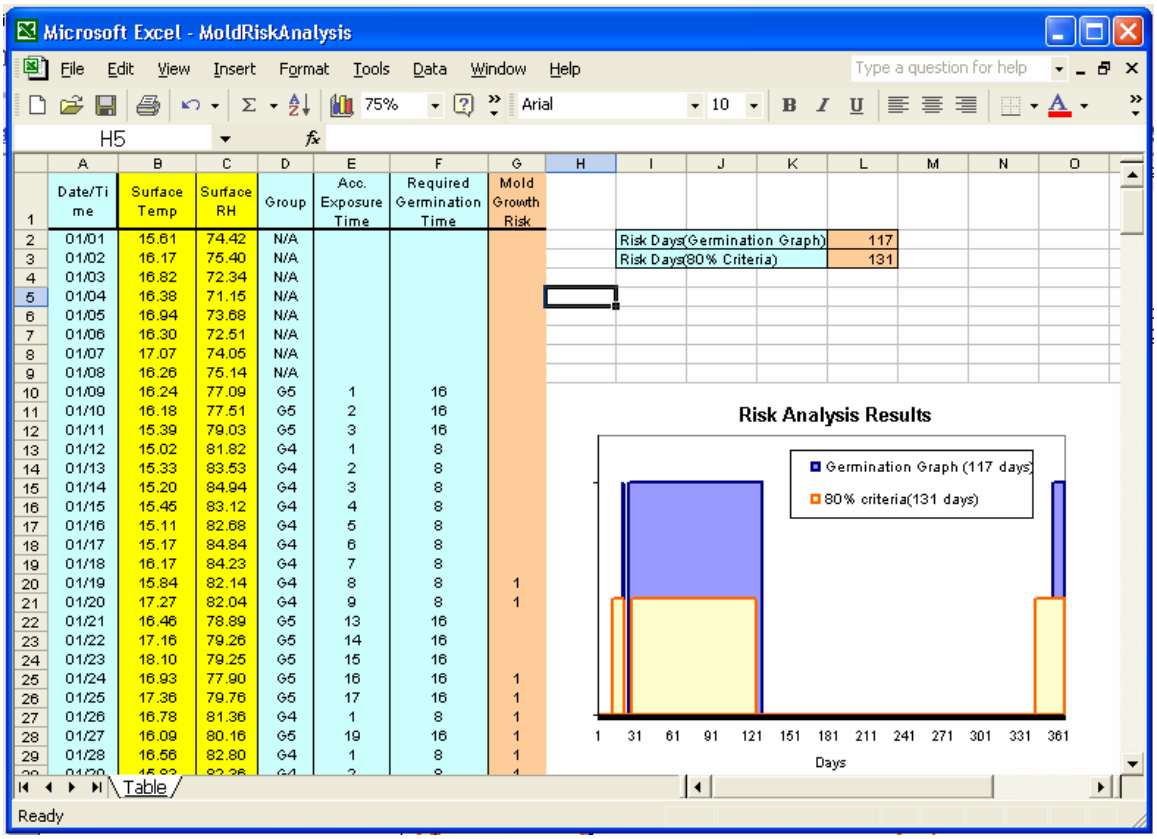

	A	B	C	D	E	F	G
1	Date/Time	Surface Temp	Surface RH	Group	Acc. Exposure Time	Required Germination Time	Mold Growth Risk
2	01/01	15.61	74.42	N/A			
3	01/02	16.17	75.40	N/A			
4	01/03	16.82	72.34	N/A			
5	01/04	16.38	71.15	N/A			
6	01/05	16.94	73.68	N/A			
7	01/06	16.30	72.51	N/A			
8	01/07	17.07	74.05	N/A			
9	01/08	16.26	75.14	N/A			
10	01/09	16.24	77.09	G5	1	16	
11	01/10	16.18	77.51	G5	2	16	
12	01/11	15.39	79.03	G5	3	16	
13	01/12	15.02	81.82	G4	1	8	
14	01/13	15.33	83.53	G4	2	8	
15	01/14	15.20	84.94	G4	3	8	
16	01/15	15.45	83.12	G4	4	8	
17	01/16	15.11	82.68	G4	5	8	
18	01/17	15.17	84.84	G4	6	8	
19	01/18	16.17	84.23	G4	7	8	
20	01/19	15.84	82.14	G4	8	8	1
21	01/20	17.27	82.04	G4	9	8	1
22	01/21	16.46	78.89	G5	13	16	
23	01/22	17.16	79.26	G5	14	16	
24	01/23	18.10	79.25	G5	15	16	
25	01/24	16.93	77.90	G5	16	16	1
26	01/25	17.36	79.76	G5	17	16	1
27	01/26	16.78	81.36	G4	1	8	1
28	01/27	16.09	80.16	G5	19	16	1
29	01/28	16.56	82.80	G4	1	8	1

Figure 4.10 Mold growth risk analysis based on surface temperature, relative humidity, exposure time at the thermal bridge location

4.8 LIMITATION

The developed mixed simulation approach did not deal with all biophysical mechanisms that affect mold phenomena. This section discusses two major physical phenomena that are not dealt with at this stage of the research: fungal spore transportation and local air flow around trouble spots. It is an open question at this point whether the phenomena should be dealt with through estimation of model uncertainties or through adding additional simulation components. A verdict on this could be reached after the first pass MRI developed in this thesis is validated on practical cases.

4.8.1 Fungal spore transportation

The developed mixed simulation procedure enables the calculation of a performance indicator (mold growth risk) on a specific location of an interior surface based on physical environmental condition. On the other hand, spore transportation is crucial to understand the transportation of outdoor spores to indoor environments and their deposition on the interior surfaces. It has been shown that fungal spore transportation in buildings can be described in a mathematical model that accounts for the concentration of airborne indoor spores and the amount of spores deposited on interior surfaces (Kulmala 1999; Kulmala, Raunemaa 1987; Nazaroff and Cass. 1991; Raunemaa, Kulmala 1989). Figure 4.3 shows a schematic drawing of spore transportation in a building and parameters in the model.

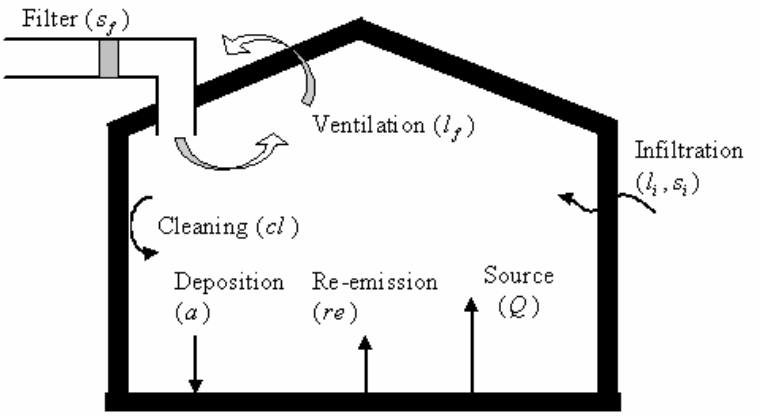

Figure 4.11 Schematic drawing of spore transportation in a building

The model parameters include the deposition rate, penetration factors, the re-emission rate, the indoor source, ventilation and infiltration rates, and outdoor spore

concentrations. The model also considers surface cleaning efficiency and frequency, which periodically removes a portion of deposited fungal spores on interior surfaces. Care should be taken for the values of parameters, since they are critically depend on the size of the aerosol. For example, the penetration of aerosols through a filter is a function of aerodynamic diameter.

Although the study of spore transportation can provide information of the concentration of indoor airborne spores and deposition, the relationship between the number of indoor airborne spores and mold growth risk has not been established. However, it is reasonable to assume that spores are available in any indoor building environments, which has been supported by various field measurement results. Shelton (2002) collected air samples for indoor fungal spores in 1,717 buildings located in the United States. Indoor spores were detected in all buildings regardless of building types and seasons. The research conducted by Burge (2000) for a building also showed that fungal spores exist in various locations of the building, e.g., occupied spaces and mechanical rooms. These field investigation results demonstrate that mold spores are ubiquitous in buildings. This thesis thus assumes that fungal spores already exist in the building. A fungal spore transportation model is hence not used in the local mold assessment.

4.8.2 Airflow model

Local indoor environmental conditions at envelope surfaces are also affected by indoor airflow characteristics. It is often reported that mold occurs behind furniture pieces and in internal room zones with poor air circulation such as behind cupboards or

inside wall closets; and it has been well established that adequate air circulation can effectively remove moisture from surfaces (Jing, Aizawa 2003). Indeed, good air circulation creates relative high boundary air velocities at material surfaces at trouble spots. Hence, a computational fluid dynamics (CFD) simulation is most adequate tool with which the effects of poor local ventilation can be studied. In the CFD simulation, different ventilation strategies can also be studied to give an indication of how bad pressure calibration or blockages of air ducts could lead to stagnant airflows around trouble spots. A fundamental analysis would require the full coupling of the CFD simulation with the heat, air, and moisture transfer models. For the purposes of this study, however, this full coupling would not be necessary as we are only interested in the probability that certain deficiencies in the ventilation flows will cause surface conditions to be more or less favorable to mold growth. For such a limited purpose one could try to add a non integrated CFD component (as suggested in Figure 4.4) to assess flow conditions around trouble spots and translate these flow conditions in effects on the convective and moisture diffusion coefficients at the material boundaries, as used in EnergyPlus and WUFI. The effect between flow field and these coefficients would warrant an extensive study. Therefore, at this stage of the research, no CFD coupling is attempted.

As a future research, the following approach is proposed: a set of CFD simulations is performed on the design reference case with varying assumptions about the quantity and placement of airflow obstructions, and with the assumption of potential deficiencies in the airflows that are produced by the HVAC system, due for instance to bad installation, stuck vents, inaccurate pressure calibration, and so on. The choice of

obstructions and deficient airflow regimes are based on observations in typical usage settings. The choice should represent the statistical distribution of obstructions and HVAC flow deficiencies as observed in similar settings. For each case, a CFD simulation is performed and the outcomes are interpreted for each trouble spot, leading to the derivation of reduced surface convection and surface moisture diffusion coefficients. It is expected that both outcomes can then be aggregated with the temperature factor as indicated in Figure 4.5. For reasons explained earlier, in the current stage of the research this approach is not attempted.

This section completes the mixed simulation approach that will be used as a core of the extended simulation engine in the MRI. The next chapter introduces uncertainty in mold growth analysis.

CHAPTER 5

UNCERTAINTY IN MOLD GROWTH ANALYSIS

5.1 INTRODUCTION

As discussed above, the main motivation for this study is that the phenomenon of mold growth in buildings typically occurs unexpectedly and in many cases remains unexplained by current standard simulations. The objective, therefore, is to express the relative risk that harmful levels of mold growth will occur. In order to quantify this risk, the study performs an uncertainty analysis on the basis of the mixed simulation approach discussed in the previous chapter. This analysis quantifies the uncertainties in the environmental conditions that govern mold growth and expresses the likelihood that mold will occur during the service life of a building. As pointed out in Sateri (2004), the prevention and control of moisture during the design stage must continually be addressed and sustained in the operation phase of the building.

5.1.1 Uncertainty in building simulation

Although, the building industry and the research communities have sought to employ computer simulation tools in the context of building evaluation at various stages of building services, many obstacles still prevent widespread use of computational tools in building performance evaluation. Among the obstacles, two relate to the performance concept discussed in this thesis.

The first obstacle is that unknown building information and uncertain input parameters are always a concern in the evaluation of an aspect of building performance. From the start of the building design to the operation of the building, lack of accurate information can lead to unrealistic evaluation. The magnitude of unknown information decreases as the design process proceeds. At the beginning of the building design, little information is available so most decisions cannot be informed about all their potential consequences. In the building operation stage, all building design information is available but his information deviates from the realized/and used state model of the building. Although the latter is (at least partly) observable few building performance models are constructed from ”as realized” information. If we would construct such a model and compare the as-designed information with the as-realized information we would find many differences. In other words, if we use a design model to represent the reality of the building we see that this introduces many uncertainties which actually increase as decisions are made during the course of the realization of the building project. These uncertainties arise from several sources, including the (unavoidable) natural variability of building materials, but also from other avoidable sources such as a faulty construction, lacking workmanship, modified building operation and management, and so on. For example, as soon as a design team makes a decision for a façade system, uncertainty associated with the system arises since the exact installation and operational performance of the system are uncertain. Uncertainty increases as other decisions are made, such as those related to HVAC system, building operation and maintenance schedules, the shape and dimensions of the building, and so on (Figure 5.1).

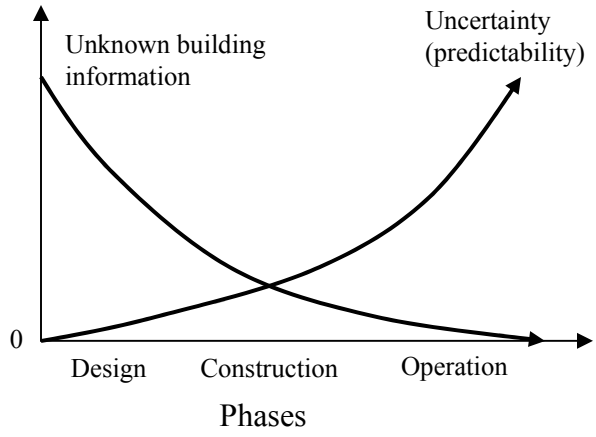

Figure 5.1 Uncertainties and building project phases

The second obstacle is that most computational simulation tools focus on the design context and use only design-specific information in the evaluation. When an unexpected event occurs in the operational stage, it often cannot be explained with the idealized representation of the building. A good example of such an event is mold infestation. A deterministic assessment of mold growth in the design stage cannot provide reliable results due to the deviation between design specification and actual building realization, such as construction errors and operation schedule change. The identification and processing of uncertainty associated with the building performance evaluation (mold growth risk analysis) is the main topic in this chapter.

To deal with such uncertainties, safety factors are usually introduced in the performance evaluation. For example, one safety factor related to HVAC system design calculation could require a 20 to 30% oversized plant for heating and cooling. Heating load calculations often use higher values of major parameters with the assumption of the worst case, which leads to the design of oversized cooling systems. The influence of

oversized heating and cooling systems on mold growth has not been studied. However, excessive cooling from a HVAC system increases the moisture content of the air in a conditioned space(Shah 2001), which may increase the risk of mold. Another well-known danger is the fact that on/off cooling leads to longer off-times in oversized systems. This can lead to high moisture during the longer off period.

Parameters that are important in heating and cooling load calculation are relatively well understood and identified, such as heat conductivity and the surface convection coefficient. Although a set of important parameters can be identified from previous knowledge of load calculations, the users of simulation models still have to find the "best guess" value for each parameter. Most simulation tools provide a database from which the user can select a value for each parameter. Some tools even suggest a default value for use. However, inappropriate selection of values for important parameters leads to an unreliable evaluation of building performance.

In mold growth analysis, the selection of important parameters and their values is even more complex, as it is unclear which parameters play a significant role in a potential increase of the mold growth risk. Furthermore, negative/positive correlations between the dominant parameters and mold risk are case dependent, depending on building geometry, climate conditions, the location of trouble spots, and many other factors. For example, unwanted infiltration can increase or decrease mold growth risk in the same buildings located in different climate zones, as described in Figure 2.12. By introducing uncertainty in the mold growth analysis, we can track the explicit influence of "what we are not certain about" and use this to develop a probabilistic performance indicator and overcome the limitations of the current deterministic use of simulation tools.

In the field of building simulation, several studies have been devoted to uncertainty in building performance simulation (most of them concern the energy and thermal performance of a building). Most related research can be found in Lomas and Eppel (1992), Jensen (1993), Macdonald and Clarke (1999), and DeWit (2001). These studies focused on the application of uncertainty analysis for a specific aspect of building performance (e.g., thermal comfort) using a simulation tool. Uncertainties related to natural variability, e.g., material properties and building dimensions, are relatively well covered.

Uncertainties in hygrothermal simulation within an envelope system have recently been studied as the models have become steadier and more robust. Holm (2002; 2001) has studied the effect of uncertain material properties on the drying-out behavior of an autoclaved aerated concrete (AAC). He was able to determine the most influential material properties using differential sensitivity analysis (DSA) and Monte Carlo analysis (MCA). Uncertain material properties in a multi-layered wall structure were studied in Salonvaara and Karagiozis (2001), who concluded that variations of each material property could result in higher variations in moisture content in the wall. These studies were restricted to hygrothermal material properties only. In mold growth analysis, however, other factors, such as human activity and indoor moisture generation rate, infiltration, thermal bridge, and bad workmanship, may also play important roles.

5.1.2 Sources of uncertainty in a building performance evaluation

Uncertainty in the assessment of a performance evaluation can arise from various sources. Four sources of uncertainty are identified in the mold growth analysis based on

earlier research on uncertainty analysis in building simulation (De Wit 2001; Macdonald 2002). These sources of uncertainty are identified in Figure 5.2 as (1) scenario uncertainty, (2) building behavior and operation uncertainty, (3) model uncertainty, and (4) numerical errors.

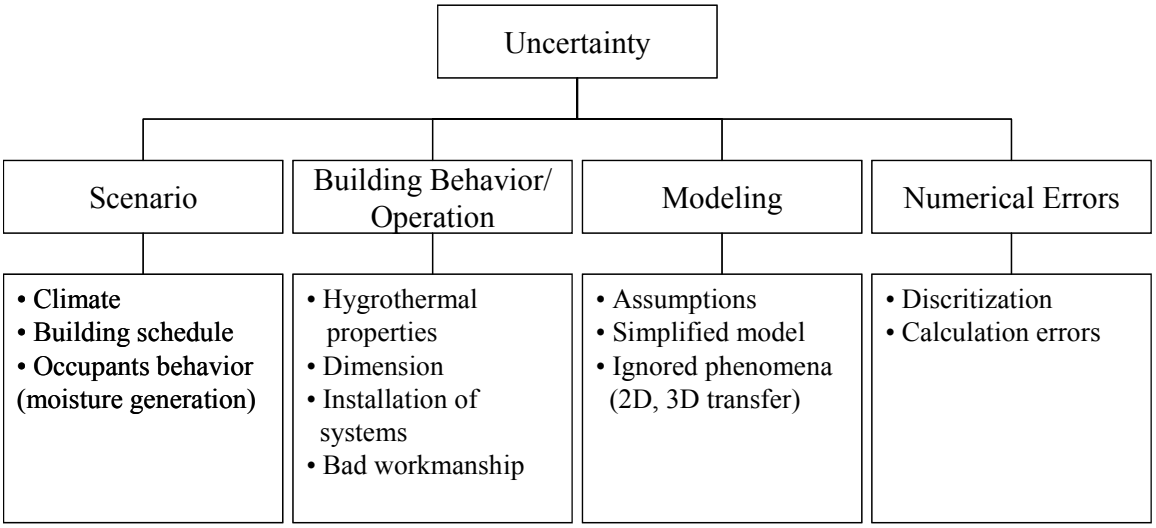

Figure 5.2 Sources of uncertainty in a performance evaluation for mold growth risk

The scenario contains information that is known about the environment and the use of the building. It specifies the external conditions to which the building model is exposed over time and contains climate data, the number of occupants, internal moisture generation, a building usage schedule, HVAC system operation and set points, building cleaning and maintenance policies, and so on. Uncertainty involving external conditions is referred to as "scenario uncertainty." Scenario uncertainty is always present since the actual in-use scenarios differ from the average use profiles assumed in the design stage. For example, actual climate conditions around the building can differ from the typical meteorological year (TMY) climate data which represents a long time average. The

uncertainty associated with internal moisture load and outdoor climate conditions was studied by Holms (2002). His study used three different values of interior moisture load (i.e., high, normal, and low) and different outdoor climate conditions (coldest, hottest) in the uncertainty analysis. The result showed a comparable range of water content in the AAC roofs due to different climate conditions at the same location and due to uncertainties in material properties. In our mold risk analysis study, we also focus on the uncertainty associated with indoor moisture generation in the case studies since it is one of the most sensitive parameters in mold growth. In the current study, scenarios are fixed and variation of mold risks over scenarios is only studied by looking at specific scenarios. In a follow-up study, scenario uncertainty could be studied in a more generic way by including a set of scenario parameters. However, quantification of these uncertainties in some schedules, such as micro climate data and building schedule parameters is a daunting study.

The second main source of uncertainty arises from the deviation between the design specification and design idealizations and the real building at the operating stage. As discussed before, this deviation is the main source of uncertainty in the mold risk analysis conducted in this study. We refer to this type of uncertainty as "building behavior and operation uncertainty." A good example of this type of uncertainty is the natural variation of material properties. Usually a building design specifies a type of building materials, not exact properties, such as "red bricks." Within the same type of building materials, actual material properties may vary significantly depending on the manufacturers, the product batches, the raw materials, and the maintenance and storage before delivery. In porous materials, the pore size of the materials differs from product to

product which in turn, and can lead to differences in hygrothermal properties such as porosity, density, vapor diffusion resistance. Such uncertainty in material properties has been relatively well studied compared to other sources of uncertainty. The uncertainties resulting from construction process on the other hand have not been studied explicitly. In this research, the focus is on this type of uncertainty and we deal with all uncertainties resulting from building behavior and operation.

The third type of uncertainty source is "modeling uncertainty" that results from certain modeling choices in the physical model development. In the representation of a physical phenomenon through mathematical equations, assumptions and simplifications are made by necessity. For example, most building energy simulation models assume a complete mixing of air in a space. However, air temperature stratification plays a role and should be considered in the assessment of specific problem cases for reliable outcome, such as the use of natural ventilation for comfort control. In specific cases, a certain phenomenon is intentionally ignored due to the computer capacity and run time constraints. This leads to geometry reductions, e.g. 1-D or 2-D simplifications of 3-D geometry. These simplification and assumptions introduce uncertainties in the performance assessment. The normal approach to representing modeling uncertainty is to add a set of surrogate parameters in the simplified model. It also requires additional simulation models in some cases. For example, De Wit (2001) demonstrated an example of the quantification of modeling uncertainty by introducing a heuristic air temperature distribution model in a thermal comfort assessment. The modeling uncertainty should be included in the uncertainty analysis only when a certain model simplification accounts for a major uncertainty of the model output (dominant parameters). A proper way to study

this is to add a surrogate parameter for the model uncertainty and make a reasonable guess of its magnitude. After the uncertainties have been propagated through the model a parameter screening process (to be introduced later) will reveal whether the surrogate parameter is among the dominant parameters. If that is the case, the analysis of the modeling uncertainty should be refined. This leads in fact to an iterative uncertainty refinement process. Although modeling uncertainty is an important part of uncertainty analysis, this thesis does not attempt to do this. It defers modeling uncertainty to a future follow-up study which should only be performed if the MRI that results from our study does not calibrate and validate well on actual cases. But even if the MRI predicts realistic mold growth risk, the further refinement of model uncertainty should be performed in every specific building cases where the sensitivity of model assumptions is expected to be dominant.

The last source of uncertainty comes from the errors due to the numerical methods and the discretization techniques used in the solution process with a computer. This "numerical error uncertainty" is a characteristic of solution techniques and the precision capacity of a computer. Thus, it is not a quantifiable uncertain parameter in most cases. The effect of numerical errors is considered to be small enough to be ignored compared to the other sources of uncertainty. This study does not deal with numerical error uncertainty.

5.1.3 Building model data and scenarios

The assessment of building performance entails the use of descriptive building information as input. This information consists of a building model (e.g., geometry,

material data, HVAC configuration) and a "scenario." Building model data describe an abstraction of the building design (the specifications). The scenario describes the experimental conditions in which the building is tested, as discussed earlier. In this study, we assume scenario information to be fixed, i.e., having no associated uncertainty. The only scenario uncertainty that is included in our study is the internal moisture generation. The uncertainty analysis is confined to the uncertainties in the parameters of the building simulation models.

We separate the building model data and the scenario explicitly in our mold growth analysis. This separation allows the analysis of a building for a variety of plausible scenarios and the study of potential mold growth risks in each scenario (Figure 5.3). In uncertainty analysis, model parameters are assigned to uncertain parameters or fixed parameters. These surrogate parameters will represent a building model and a scenario. The next section discusses how to identify uncertain parameters in mold growth analysis.

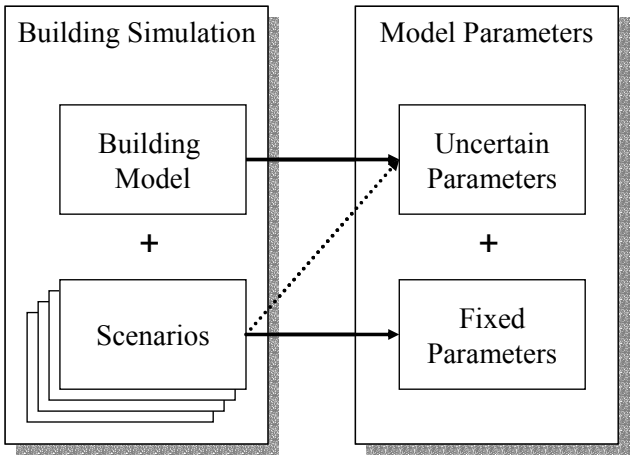

Figure 5.3 Building model and scenarios in building simulation

5.2 UNCERTAIN PARAMETERS IN MOLD GROWTH ANALYSIS

Uncertainty in the building model parameters is captured as probability distributions of model parameters. The distributions express the estimates of the deviations between "as-designed" values and actual "in-use" values of the parameters. Deviations arise from the normal spreads of the building component properties, common defects in construction, unknown effectiveness of cleaning and maintenance operations, errors in operation set points, drifts in thermostats, and so forth. Other deviations between the idealized simulation and reality are systemic to the simulation itself, i.e., attributable to the simplifying modeling assumptions that underlie the simulation. The normal approach to represent modeling uncertainty is to use a set of surrogate parameters contained in the simplified model. Uncertainty analysis studies the combined effects of all the above deviations on the physical states of a building by performing simulations for all the combinations of realizations of the uncertain parameters. Uncertainty in the parameters is thus propagated through the simulation. As a result, the expected (uncertain) behavior of the building can be aggregated as a probability distribution.

An important first step in the uncertainty analysis is the identification of uncertain parameters and the quantification of their uncertainty. Previous research on mold growth in buildings have suggested several important causes and mechanisms related to this phenomenon (Burge 2002; Shakun 1992). These studies and many other case studies of mold problems are important sources for the identification of uncertain building parameters in mold growth. Uncertain building parameters should be derived from

physical mechanisms governing local environmental conditions for mold growth, which are heat, air, and moisture transfer in porous building materials and within a building.

Heat, moisture, and air transfer can be divided into more detailed mechanisms. Heat transfer includes conduction, convection, and radiation. Air transfer in buildings involves macroscopic and microscopic airflow. Macroscopic airflow depends on two potentials: temperature and air pressure (Hens and Sneave 1991). Full modeling should solve the Navier-Stoke equations for the conservation of momentum and add a turbulence model. This particular study focuses on airflow within a building and infiltration (crack flow, large openings, and mechanical ventilation). Moisture transfer in porous building materials involves vapor and liquid transport. Detailed mechanisms and driving potentials for moisture transport used in the WUFI program are described in Table 5.1.

Table 5.1 Moisture transport mechanisms in porous building materials (Holm 2001)

Transport	**Mechanism**	**Driving potential**
Vapor transport	Effusion	Vapor pressure
	Gas diffusion	Vapor pressure
	Solution diffusion	H_2O concentration
Liquid transport	Capillary conduction	Capillary depression
	Surface diffusion	Relative humidity
	Seepage flow	Gravitation
	Hydraulic flow	Total pressure
	Electro-kinetics	Electrical fields
	Osmosis	Ionic concentration

Physical mechanisms for local environmental conditions and the cause categories developed in Chapter 4 can be used to derive uncertain parameters for mold growth

analysis, as shown in figure 5.4. The first cause category, spore availability, is mainly related to spore transportation. Since spores are assumed to exist in all building environments, spore transportation will not be considered in this study.

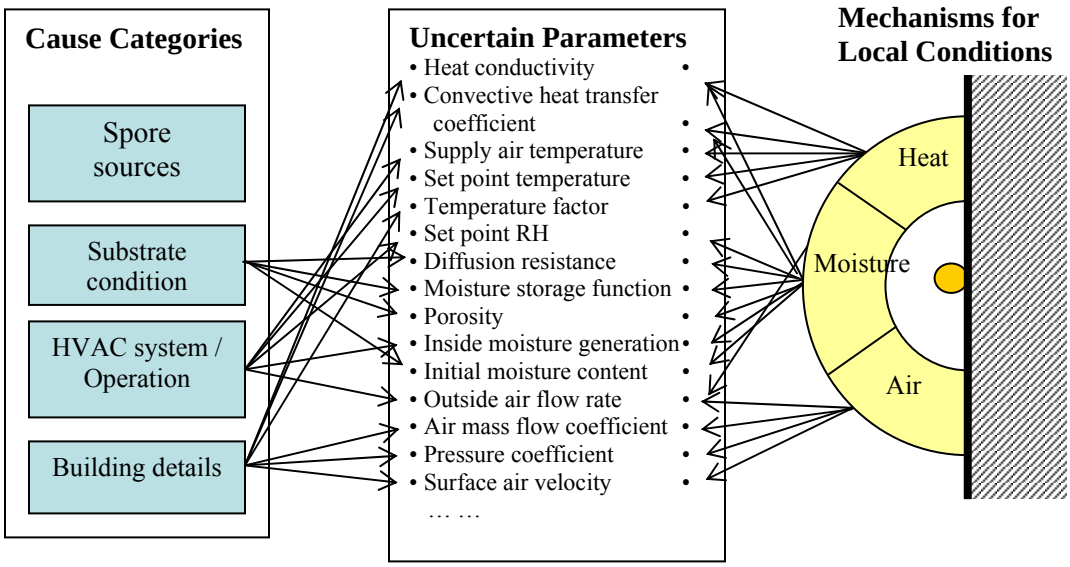

Figure 5.4 Identification of uncertain parameters by considering cause categories and mechanisms for local environmental conditions for mold growth

The causes for mold growth that are frequently mentioned in this study are outdoor air infiltration through cracks, indoor moisture sources, deficient building detailing, and improper HVAC operation. A list of uncertain parameters has been compiled for each building case and discussed in case studies later. The next step in the analysis is the quantification of uncertainty.

5.3 QUANTIFICATION OF UNCERTAINTY

Each cause/mechanism may require the introduction of uncertainty in one or several physical parameters. Infiltration, for example, is linked to the combination of the pressure difference and crack flow through façade components. The governing (external) parameters in this case are the wind pressure coefficient at critical areas of the facade and the mass flow coefficient through the type of cracks that are known to occur in the given façade. Based on theoretical models and/or data analyses from available literature, the uncertainty of each parameter is described as upper/lower values with a probability distribution. Figure 5.5 shows an example of uncertainty quantification with a normal distribution.

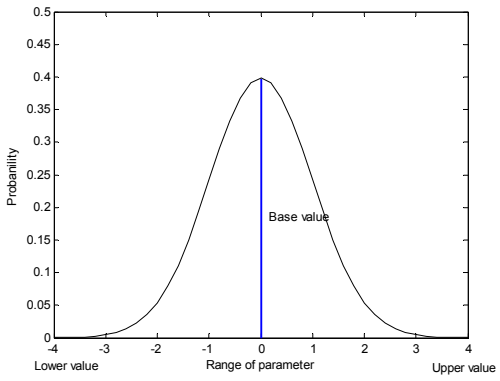

Figure 5.5 Example of uncertainty quantification with lower/upper/base values and a normal distribution

For a comparison of deterministic and probabilistic performance indicators, base values are introduced for each parameter. A base value represents a deterministic value that a designer or engineer would use for standard idealized simulation based on sound engineering judgment. In most cases, mean values of parameters are commonly accepted.

When no information on the distribution of uncertain parameters is available, the users of the simulation tool may choose to use a default value from the database in the tool.

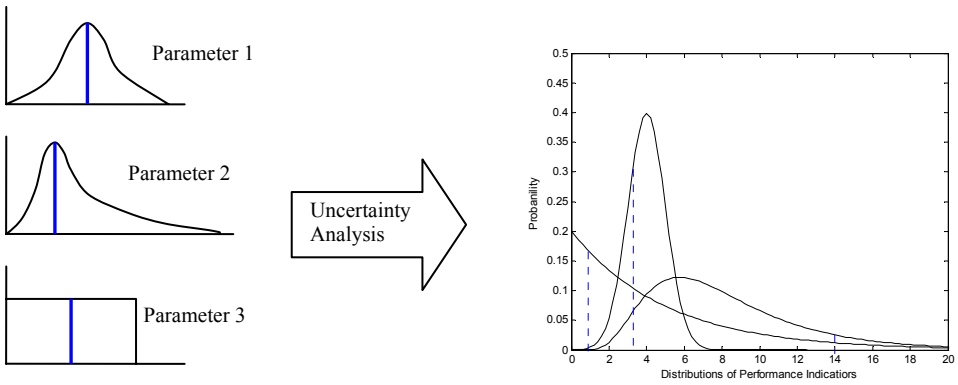

Figure 5.6 Distribution of performance indicators with probability distribution of the parameters in the uncertainty analysis

The simulation with these base values as input produces a deterministic outcome of mold growth conditions. However, the effect of each parameter on the total variance in mold growth risk is significantly different. The values of the dominant parameter, which is sensitive to the result of the evaluation, will lead to the discrepancy between the result of the base case and the distribution of the performance indicator under uncertainty. Even the use of simple mean values for all parameters produces a deviation from the mean of the simulation result distribution, as shown in Figure 5.6. This is supported by studies of the influence of stochastic building parameters on moisture content in a wall system (Holm, Kuenzel 2001; Salonvaara, Karagiozis 2001). These studies showed that the variations of the uncertainty analysis shifted upward around the deterministic solution. It also confirms that the moisture simulation results do not follow the probability distribution of the parameters (i.e., material properties). Therefore, uncertainty analysis is

particularly important in a phenomenon that involves intrinsic complexity and non-linearity among the parameters, such as moisture and mold growth risk analyses. The following sections describe important uncertain parameters that are discussed in this study. A general process to quantify the range of each uncertain parameter is introduced. A complete list of uncertain parameters and the range is shown in each case study.

5.3.1 Air mass flow coefficient

Air infiltration is unintentional airflow from the outside into building zones through crack flow. Airflow through cracks in building envelopes depends on the pressure difference and the air mass flow coefficient. The power law is widely used to calculate the amount of airflow in crack flows (Feustel 1998; Feustel and Raynor-Hooson 1990):

$$Q = C_S \left(\Delta P\right)^n \tag{5.1}$$

$$Q = C_{sd} \nu^{1-2n} \rho^{-n} \left(\Delta P\right)^n \tag{5.2}$$

where, Q : air mass flow [kg/s]

C_S : air mass flow coefficient [$kg^3/s \cdot Pa^n$]

C_{sd} : duct shape coefficient [$kg^3/s \cdot Pa^n$]

n : air mass flow exponent [-]

ν : viscosity [m^2/s]

ρ : air density [kg/m^3]

The modified power law equation (5.2) accounts for the influence of air properties (i.e., temperature and density) and the airflow rate, which differ from the measurement conditions for constructing the power law equation. Since the types of cracks vary according to workmanship, building material defects, and degradation of the façades, defining the exact dimensions of cracks and shapes is difficult. Cracks are usually classified by the building components, such as window and door frames, and walls.

The air mass flow coefficient (Cs) can be calculated by adding all length of cracks and use the coefficient from literature i.e., the AIVC leakage database (Orme, Liddament 1994). Another method is to use building pressure test data at a specified pressure (usually 50 Pa or 75 Pa). This test produces leakage air change rates in the buildings. By assuming that the cracks are uniformly distributed on the facades, the Cs coefficient can be calculated using equation (5.2) with known leakage air change rates (Schild 2003b).

ASHRAE published air leakage data in residential buildings with the air mass flow exponent of 0.65, which ranges from 0 to 50 ACH in U.S. houses. The air leakage test data for commercial buildings are not as prevalent as the data for residential buildings. Persily (1998)collected air leakage data from a review of the published literature for commercial and institutional buildings around the world. Commings and Withers (1995)investigated 68 commercial buildings to identify uncontrolled air flow and pressure imbalances in Florida. Table 5.2 summarizes the field test data in the unit of air change rate at 50 Pa from various literature sources. The conversion between different air tightness ratings in buildings was conducted based on a sample building with a volume of 108 m^3 (6×6×3m). Table 5.3 shows the calculation results of Cs in exterior walls for a U.

S. office and a house using COMISexcel (Schild 2003a) based on the air leakage test results in Table 5.2. The lower and upper boundaries of the Cs values will be interpreted as a central 95% confidence interval for the uncertainty analysis.

Table 5.2 Air leakage test results at 50 Pa (ACH) for U.S. residential and commercial buildings

Category	**Min.**	**Max.**	**Mean**	**SD**	**Distribution**	**References**
U.S. Houses	0	50	8 (most frequent)	N/A	N/A	(ASHRAE 2001e)
U.S. offices (30)	2.0 (3.9)	63.7 (124.5)	15.6 (30.48)	N/A	N/A	(Persily 1998)
Canadian offices (8)	2.51 (4.9)	11.52 (22.5)	5.43 (10.6)	5.4	N/A	(Persily 1998)
U.K. offices (10)	5.53 (10.8)	21.35 (41.7)	11.93 (23.3)	11.9	N/A	(Persily 1998)
Florida offices(22)	2.97 (5.8)	63.73 (124.5)	18.43 (36.0)	28.6	N/A	(Persily 1998)
New York schools(13)	1.38 (2.7)	7.53 (14.7)	4.35 (8.5)	4.4	N/A	(Persily 1998)
Florida schools(7)	5.58 (10.9)	27.59 (53.9)	12.54 (24.5)	15.4	N/A	(Persily 1998)
Canadian schools(11)	9.01 (17.6)	22.58 (44.1)	14.49 (28.3)	8.4	N/A	(Persily 1998)
Florida retail (6)	2.05 (4.0)	38.44 (75.1)	16.89 (33.0)	24.9	N/A	(Persily 1998)
Florida retail (8)	3.9	31.2	13.0	N/A	N/A	(Cummings, Withers 1995)
Canadian retail(10)	10.55 (20.6)	36.50 (71.3)	25.24 (49.3)	19.6	N/A	(Persily 1998)
Florida hotel (1)	N/A	N/A	7.6	N/A	N/A	(Cummings, Withers 1997)
Florida retail (69)	0	50+	16.7	N/A	Bi-polar	(Cummings, Withers 1996)

* Values in () are air leakage at 75Pa, $m^3/h.m^2$

Table 5.3 Cs (wall) calculation example for a U. S. office and a house using COMISexcel

Category	Range	Mean	Remarks
US offices	0.00017 ~ 0.0054	0.0013	Based on Air leakage test results in table 5.2 (US offices)
US houses	0.000003 ~ 0.0014	0.0002	Based on Air leakage test results in table 5.2 (US houses)

* Building size (6×6×3m)

5.3.2 Wind pressure coefficient

The wind around a building generates pressure differences on the building surfaces. The pressure distribution is expressed by the wind pressure coefficient and the dynamic pressure on the undisturbed airflow. The wind pressure coefficient represents the relationship between the building surface pressure and the local dynamic pressure at a given reference level, as shown in equation (5.3) (Feustel 1998).

$$c_p = \frac{p_s}{p_{dyn}(z)} = \frac{p(x,y,z) - p_o(z)}{p_{dyn}(z)}, \tag{5.3}$$

where c_p = pressure coefficient [-]

p_s = the difference between building surface pressure and local outdoor atmospheric pressure

$p(x,y,z)$ = surface pressure at coordinates x,y,z [Pa]

$p_o(z)$ = atmospheric pressure at height z [Pa]

$p_{dyn}(z)$ = dynamic pressure in the undisturbed flow at height z [Pa]

Literature and data on the wind pressure coefficient are available based on the previous wind tunnel studies with various shape of buildings and wind profile velocity profiles. Tabulated values for simple building shape (i.e., low-rise, box shape building) have been published from AIVC (Orme, Liddament 1994) and ASHRAE (2001b). These tabulated values are widely used under different assumptions (i.e., length to width ratio, shielding conditions), but they give averaged pressure coefficients and have limited applications. Multi-zone airflow models use a module to calculate the averaged surface pressure coefficients, including COMIS and CONTAMW (Persily and Ivy 2001). A few computer models have been developed for detailed pressure coefficient calculations at specific locations of building surfaces, including CPCALC+ (Grosso 1995) and the Cp generator (Knoll, Phaff 1995).

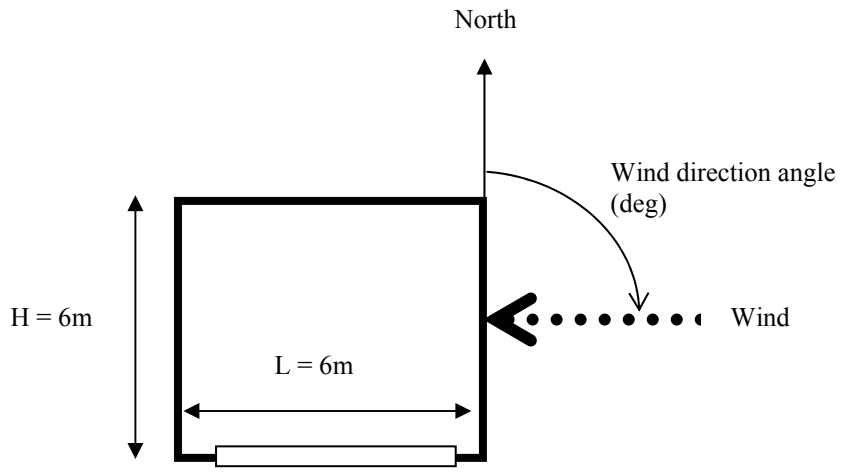

Figure 5.7 Plan view of the example building and wind direction angle.

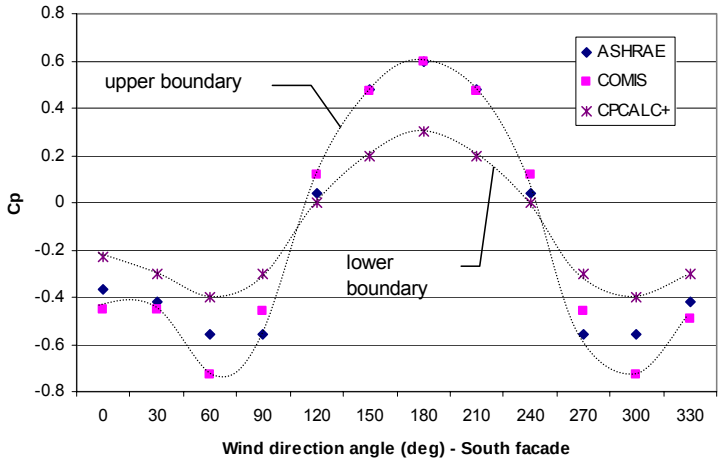

Figure 5.8 Wind pressure coefficients as a function of wind direction angles – south facade

In this study, the scatter of the values from the published data and the output from computer models are used to quantify an uncertain range of the pressure coefficients. Figure 5.7 and 5.8 above show an example case and resulting wind pressure coefficients as a function of wind direction angles. The upper and lower boundaries are shown in the figure as well. In uncertainty analysis, an absolute value of each pressure coefficient at different wind direction angle is considered to be positively correlated.

5.3.3 Wind velocity profile exponent

The wind profile in the direction of each building façade can be different depending on the surrounding environment. For example, building façades facing a city center or a large open space without obstacles experience a different wind profile and wind speed. The wind velocity profile around buildings depends on the roughness of the terrain, obstacles on the ground, and the surrounding buildings. Wind speed increases as

the height above the ground increases. With an assumption that wind flow is isothermal, horizontal, and no direction change results from differences in terrain, the wind velocity profiles can be approximated by the power law equation (Feustel 1998):

$$v_z = v_{z_0}\left[\frac{z}{z_0}\right]^{\alpha}, \tag{5.4}$$

where v_z = wind speed at height z [m/s]

v_{z_0} = wind speed at reference height z_0 [m/s]

α = wind velocity profile exponent [-]

The value of the wind velocity profile exponents is a function of terrain roughness. In the estimation of wind velocity using meteorological data, different values of the exponents are introduced. The wind velocity profile exponents for each type of terrain around the building can be found in the literature, such as in Feustel and Raynor-Hooson (1990), Orme and Liddament (1994), Feustel (1998), and ASHRAE (2001b). Table 5.4 summarizes the results of these studies.

Table 5.4 The wind velocity profile exponents as a function of terrain from available literature sources

Terrain Category	**Description**	**Exponent**
1	Large city centers	0.33 ~ 0.4
2	Urban and suburban areas	0.22 ~ 0.28
3	Open terrain	0.14 ~ 0.2
4	Flat, unobstructed areas	0.10 ~ 0.17

5.3.4 Discharge coefficients

Airflow through openings (i.e., doors and windows) in buildings are proportional to a cross-sectional opening area and an empirical discharge coefficient. The discharge coefficient accounts for the fractional airflow loss due to the shape of the openings (e.g., sharp-edged or trumpet shaped). The relationship can be expressed by using the Bernoulli equation with an assumption of incompressible flow in steady state, as shown in equation (5.5) (ASHRAE 2001b):

$$Q = C_d A\sqrt{2\Delta p / \rho} \ , \tag{5.5}$$

where Q : airflow rate [m^3 / s]

C_d : discharge coefficient [-]

A : cross-sectional area of opening [m^2]

ρ : air density [kg / m^3]

Δp : pressure difference [Pa]

Feustel (1990) concluded that reasonable values for the discharge coefficients lie between 0.6 and 0.75 for the Bernoulli equation in a building airflow calculation based on the experimental results of Van der Mass (1989). De Wit (2001) came to the same conclusion of an uncertain range of the discharge coefficient for windows and door openings. Thus, in the case studies of this research, the same uncertain range [0.6, 0.75] will be used for uncertainty and sensitivity analyses.

5.3.5 Moisture sources

Moisture sources are important in mold growth analysis and vary significantly, depending on building type, occupants' behavior, and building operation. While outside humidity is the most important moisture source in humid climates, indoor moisture source is the most important factor for room relative humidity in cold climates. Since most regions require both heating and cooling systems to meet thermal comfort level, moisture sources from both the inside and the outside should be carefully examined.

Moisture can intentionally be added to room air through the use of humidifiers, or unintentionally through normal activities by occupants or by equipment. It can also be added from ground moisture that migrates through walls of the foundation and the basement, or the floors of the crawl space from the surrounding soil. Obvious sources of moisture in some existing buildings are pipe leaks and rain penetration. All of these sources of moisture can be categorized as follows:

Indoor moisture sources:

- Humidifiers
- Human activities (e.g., cooking, cleaning, washing, shower)
- Open water surfaces (e.g., swimming pools, interior ponds)
- Equipment (e.g., refrigerator, medical equipment)
- Construction sources (e.g., initial moisture contents)

Outdoor moisture sources:

- Ground soil (e.g.,foundation walls, basement, crawl space)

- Leaks (e.g.,piping, rain penetration)
- Humid outdoor air (e.g.,ventilation and infiltration)

Moisture migration from outdoor sources, such as ground soil or leaks, can be a significant source of indoor relative humidity. However, research in this area is limited and the quantified moisture generation data are not sufficient for this particular study. Research related to moisture migration from a foundation, a basement, and a crawl space can be found in Trethowen (1994), Carmody and Anderson (1997), Straube (2002). This particular study concentrates on indoor moisture sources and outdoor humid air through ventilation and infiltration. As described in Chapter 4, moisture migration from any catastrophic event (e.g., leaking pipes, failure to waterproof a roof) is beyond the scope of this study.

The amount of indoor moisture sources varies significantly, depending on the type, use, and a configuration of a building. The literature shows a large variation among moisture generation rates, even within the same building type, i.e., residential buildings (Yik, Sat 2004). Table 5.5 summarizes moisture source data from several studies. In the case studies, the author collects data from table 5.5 for each moisture source and takes additional building type specific considerations as discussed below.

Table 5.5 Moisture sources from interior space

Source of Moisture		L/day	g/h	References
People	Light activity	0.03~0.06 (L/h)	30 ~ 60	(Christian 1994; Harriman 1990)
		0.75	31.25	(Straube 2002)
		0.72~2.88	30~120	(Trechsel 2001)
	Medium activity	0.12~0.2 (L/h)	120~200	(Christian 1994; Harriman 1990)
	Hard work	0.2~0.3 (L/h)	200~300	(Christian 1994; Harriman 1990)
		5	208	(Straube 2002)
Humidifier		2 ~ 20 +	83 ~ 833	(Straube 2002)
		0 ~ 120 + (or 2.08 L/h)	0 ~ 2080	(Angell 1988)
Washing floors etc.		0.147 (L/m2)	147 (g/m2)	(Hansen 1984)
		0.15 L/m2	150 (g/m2)	(Angell 1988)
		-	100 ~ 150 (g/m2)	(CIBSE 1999)
		-	180 (g/m2)	(Lstiburek 1993)
Frost-Free Fridge		0.5	20.8	(Straube 2002)
		1.03	43	(Angell 1988)
Plants	small plant	0.04 ~ 0.1	1.6 ~ 4.2	(Straube 2002)
	small plant	0.1	4.2	(Christian 1994)
	-	0.02	0.83	(Hansen 1984)
	medium size	0.17 ~ 0.5	7.1 ~ 20.8	(Christian 1994)
	-	0.8	33.3	(CIBSE 1999)
	-	0.5	20.8	(Lstiburek 1993)
Firewood, per Cord		1 ~ 3	41.6 ~ 125	(Straube 2002)
Dishwashing		0.5	20.8	(Straube 2002)
		0.45	18.7	(Hansen 1984)
Cooking	Three meals for four people	0.9 ~ 2 (3 with Gas range)	38.3 ~ 83.3 (125 with Gas range)	(Straube 2002)
		0.92 ~ 2.1	38.3 ~ 87.5	(Hansen 1984)
		2.4	100	(Christian 1994)
	Breakfast	0.17(plus 0.28 if gas cooking)	7.1 (plus 11.6 if gas cooking)	(Christian 1994)
	Lunch	0.25(plus 0.32 if gas cooking)	10.4 (plus 13.3 if gas cooking)	(Christian 1994)
	Dinner	0.58(plus 0.75 if gas cooking)	24.2 (plus 31.3 if gas cooking)	(Christian 1994)

Table 5.5 (continued)

Bathing/Washing per person	Typical	0.2 ~ 0.4 ea.	8.3 ~ 16.7 ea.	(Straube 2002)
		0.6 ea.	25 ea.	(Erhorn and Gertis 1986)
	Shower (ea.)	0.5 ea.	20.8 ea.	(Straube 2002)
		0.23 ea.	9.6 ea.	(Hansen 1984)
		0.25/5min	10.4	(Angell 1988)
		0.22/5min	9.16	(Erhorn and Gertis 1986)
	Bath (ea.)	0.1+ ea.	4.166 + ea.	(Straube 2002)
		0.05 ea.	2.08 ea.	(Hansen 1984)
		0.06 ea.	2.5 ea.	(Angell 1988)
Gas Appliance		0.15 kg/KWh for Natural Gas		(Straube 2002)
		0.18	7.5	(Angell 1988)
Clothes drying (unvented)		11.97	-	(Hansen 1984)
			2660 ~ 3520 per load	(Lstiburek 1993)
			2200 ~ 2920 per load	(Trechsel 2001)
Clothes washing (unvented)		1.96	-	(Hansen 1984)
		0.5 ~ 1.8	-	(CIBSE 1999)
Seasonal desorption (or new materials)		3 to 8 depends on the house construction	125 to 333	(Straube 2002)

Residential Buildings

The *ASHRAE Handbook* states that a family of four produces an average of 320 g/h of moisture (ASHRAE 2001d). Christian (1994) suggested that, from assorted references, the range of internal moisture loads from single family residences varies from a low of 179g/h to a high of 958 g/h (or 4.3 to 23 L/day). The upper range can be significantly exceeded by unvented clothes dryers, extensive use of unvented kerosene heaters, attached greenhouses or swimming pools, and interior fire wood storage. Angell

(1988) provided some typical total moisture loads in North American residential buildings and Hansen (1984) estimated that an average family of four generates 291.7 to 500 g/h of water on an average day.

The total moisture loads from residential buildings are a strong function of family size and household activity profiles. Yik and Sat (2004) collected moisture load data from Chinese houses in Hong Kong and showed a big difference between these houses and western residential buildings.. Erhorn and Herbak (1991)conducted a case study of 67 flats affected by mold growth and collected moisture production rates from them. A mean moisture production was 3 $g/h \cdot m^3$.

Hotels

The moisture sources of hotel rooms are similar to those of residential buildings, except cooking and laundry sources. However, the total area of a hotel suite is smaller than most residential buildings and ventilation through open windows influences total moisture loads differently, particularly in resort areas.

A study on moisture sources in hotels showed a maximum of 2.3 L/day in a hotel room, including people, showers, plants, cleaning, and wet clothes. A typical motel generated an average of 2.27 L/day(95 g/h), which is less than the typical residential building (Shakun 1992).

Commercial Buildings

A large quantity of water is used in cleaning, particularly in commercial buildings such as grocery stores, where the floors are wet mopped every day. Any water left in the

shower or sink, or on the floor or walls will evaporate and add moisture to the conditioned space.

In the case of an indoor swimming pool or open water surface, such as ponds in shopping malls and landscaped interior spaces, evaporation is directly proportional to the difference in vapor pressure between the wet surface and the air, and the heat transfer rate to the water surface film. For this case, refer to Harriman (1990), Christian (1994). In the case of malls, special consideration should been made for the large number of oversized plants, which generate a lot of moisture in indoor air.

To include moisture sources in a building simulation, moisture sources need to be converted to latent heat energy in units of watts. The latent energy required in a humidifying process can be calculated if the rate at which water is being vaporized and the enthalpy of vaporization (latent enthalpy) are known (McQuiston and Parker 1994). The relation can be expressed as

$$\dot{q}_l = i_{fg}\, \dot{m}_w \quad , \tag{5.6}$$

where $\dot{q}_l =$ rate of latent heat addition, [W]

$i_{fg} =$ enthalpy of vaporization, [J/kg]

$\dot{m}_w =$ rate at which water is vaporized, [kg/s]

5.3.6 Initial moisture content

Most building materials in a new building contain high moisture content, releasing a substantial amount of water vapor into indoor air during the first two to three years of a building's life. This moisture source plays an important role in the heating season when indoor relative humidity is relatively low. A study showed that normal concrete contains about 200 kg of water per cubic meter and releases half of them as vapor (Straube 2002).

Table 5.6 Typical built-in moisture (Karagiozis, Desjarlais 2002)

Material	**Water content [kg/m^3]**
Fresh concrete Free water	175
Concrete – 28 days old (at 70% hydratation) Bounded water Dried water Free water	 85 25…45 65…45
Concrete – 3 to 6 months old (at 90% hydratation) Bounded water Dried water Free water	 105 35…50 35…20
Gas concrete	180…220
Clay brick masonry	100..150
Calcium silica brick masonry	100..120

Accurate simulation of moisture transport should consider initial moisture content. However, initial moisture content may vary dramatically, depending on how the materials are processed in the plant and maintained in the construction sites (Moon and Augenbroe 2004). Unfortunately, precise data of typical building moisture conditions are unavailable

(Holm 2001). Holm suggested that if an "air dried" condition is expected at the beginning of the calculation, the humidity of 80% relative humidity is appropriate for all layers of the constructional element. In case studies, Holm used 80% relative humidity, but in the case of newly-constructed buildings, the initial water content of each building component must be used. Some of typical cases of built-in moisture are presented in Table 5.6.

5.3.7 Hygrothermal material properties

5.3.7.1 Diffusion resistance factor

The diffusion of moisture molecules in the air depends on the water vapor partial pressure difference and can be derived from Fick's law as follows:

$$g_v = -\delta \Delta p \,, \tag{5.7}$$

where $g_v \left[kg / m^2 s \right]$ = water vapor diffusion flux density

$\delta \left[kg / msPa \right]$ = water vapor diffusion coefficient in air

$p \left[Pa \right]$ = water vapor partial pressure

The water vapor diffusion coefficient in the air can be calculated with the ambient temperature and the air pressure as follows:

$$\delta = \frac{2.0 \times 10^{-7} \times T^{0.81}}{P_L}, \tag{5.8}$$

where $T \left[K \right]$ = ambient temperature

$P_L\,[Pa]$ = ambient air pressure

The water vapor diffusion in the pores of building materials can also be described by introducing a water vapor diffusion resistance factor (μ), which is independent of temperature and pressure. Each building material has a unique μ value and constant as long as the temperature is below 40°C (Kunzel 1995). The vapor diffusion flux density for building materials can be expressed with a water vapor diffusion resistance factor (μ) as follows:

$$g_v = -\frac{\delta}{\mu}\Delta p\,, \tag{5.9}$$

or,

$$g_v = -\delta_p \nabla p\,, \tag{5.10}$$

where $\mu[-]$ = water vapor diffusion resistance factor

$\delta_p\,[kg/msPa]$ = water vapor permeability of a building material

The water vapor diffusion resistance factor is the ratio of the diffusion coefficients of the water vapor in the air and in the building material, which represents the reduction of the accessible cross-section, water vapor by the tortuosity of the pore paths and adsorption at the pore walls (Kunzel, Karagiozis 2000). The two basic measurement methods include the “desiccant method (dry cup)” and the “Water method (wet cup).”

The procedures of both test methods are described in Kumaran (1998), ASTM (2000), and Holm (2001).

The measurement data of the water vapor diffusion resistance factor are available from the WUFI software material database and literature, including Seiffert (1970), IEA (1996b), and Kunzel and Holm (2000). Table 5.7 shows the measurement data of the diffusion resistance factor for various building materials from the literature.

Table 5.7 lists μ values for some common materials

Materials	**Vapor diffusion resistance factor (μ)**		**References**
	Dry cup (3-50% RH)	Wet cup (50-93% RH)	
Cellular concrete	7.7	7.1	(Kunzel 1995)
Lime silica brick	27	18	
Solid brick	9.5	8.0	
Gypsum board	8.3	7.3	
Concrete (B25)	110	150	
Cement-lime plaster	19	18	
Lime plaster	7.3	6.4	
Sander sandstone	60	28	
Baumberger sandstone	20	17	
Worzeldorfer sandstone	38	22	
Mineral fiber insulation	1.5		(IEA 1996a)
Lime mortar rendering (1:3)	9.1		(Seiffert 1970)
Cement rendering (1:1)	32.0		
Foamed polystyrene	21 ~ 74		
Mineral wool board	2.7		
Baked brick	15 ~ 20		

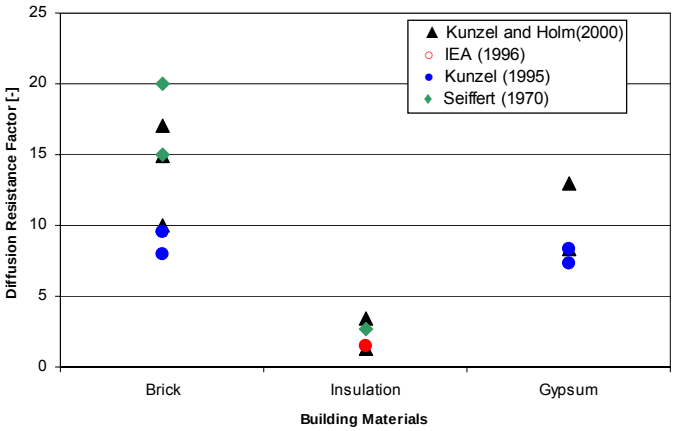

Figure 5.9 The range of the diffusion resistance factors for building materials used in the virtual case study.

Figure 5.9 shows the water vapor diffusion resistance factors for building materials used in the first case study. The upper and lower bounds for each building material are derived from this figure.

5.3.7.2 Moisture storage function

Porous building materials can absorb moisture, depending on the relative humidity of ambient air and temperature. However, temperature, ignored in the field of building physics, plays only a minor role in most building materials. The relationship between ambient relative humidity and water content in a building material are represented as a sorption isotherm in the hygroscopic range of humidity (0 ~ 95%). The curve of soil moisture tension represents the relationship in the super-hygroscopic range of humidity (95% ~ free water saturation). These two functions are combined to make the moisture storage function in the whole range of relative humidity through the Kelvin-relation (Holm 2001). The sorption/desorption and pressure plate measurements for each

region are described in Kumaran (2002). Figure 5.10 shows a theoretical moisture storage function with two moisture regions.

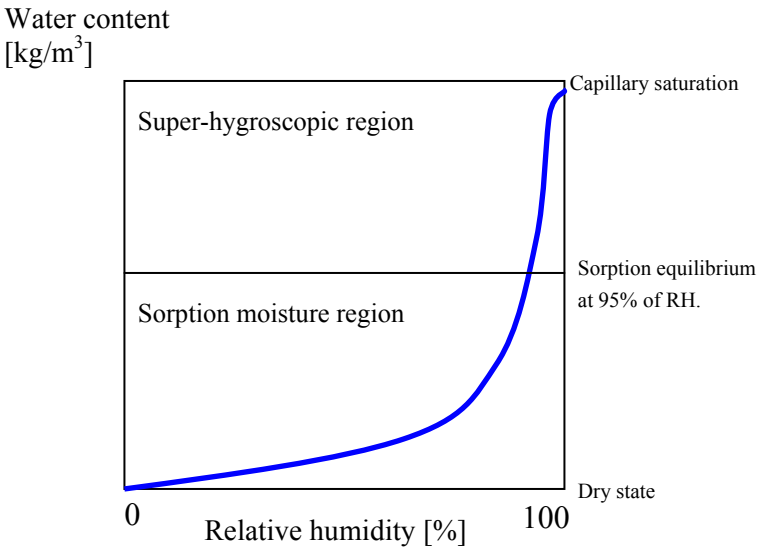

Figure 5.10 A schematic drawing of the moisture storage function with two moisture regions (modified from (Kunzel 1995))

The moisture storage function of non-hygroscopic materials (essentially insulating materials, but air layers as well) is theoretically more or less zero in the region of relative humidity 0 to 100% (Kunzel, Karagiozis 2000).

Due to natural variations of pore structures in porous building materials, a wide range of hygrothermal properties can easily be found between specimens even in the same materials. Experimental data of the moisture storage function for building materials are available from various studies and databases, including Kumaran (1996; 2002), and Kunzel and Karagiozis (2000). Although experimental data of hygrothermal properties have been kept updated, not all building materials are available yet.

Figure 5.11 shows moisture storage functions for building materials used in the first case study with upper and lower boundaries. For insulation material, base values for the moisture storage function correspond to the lower boundary moisture storage function.

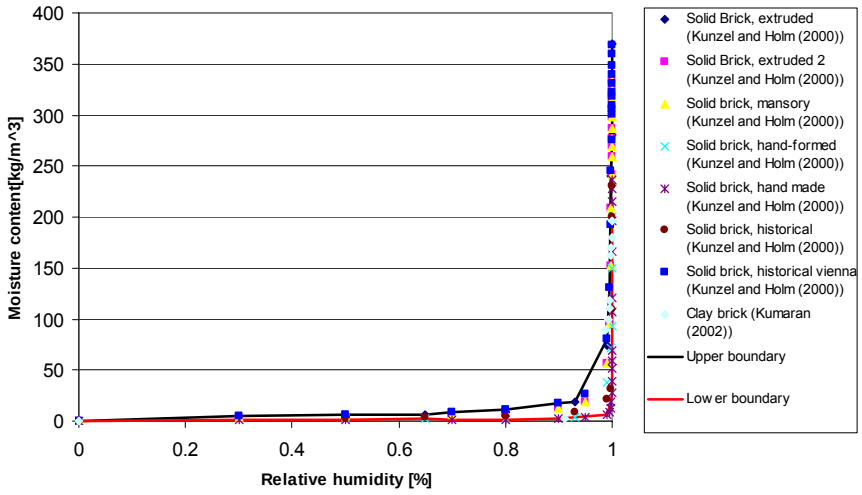

(a) Brick

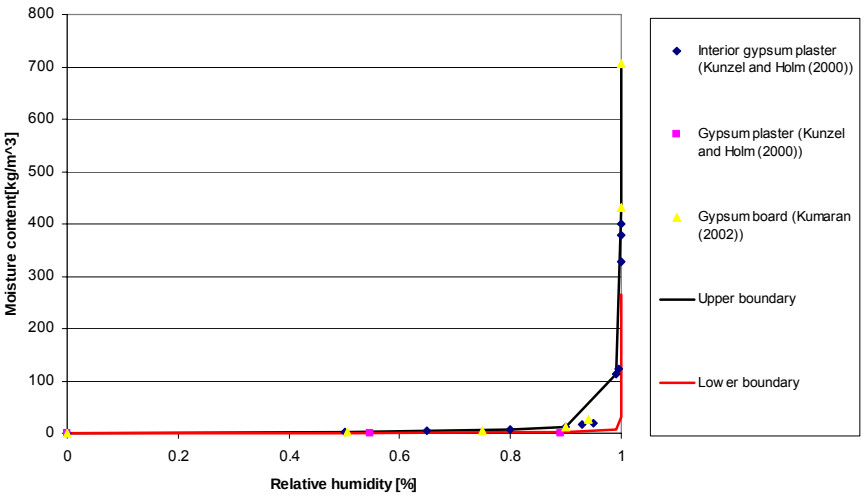

(b) Gypsum board

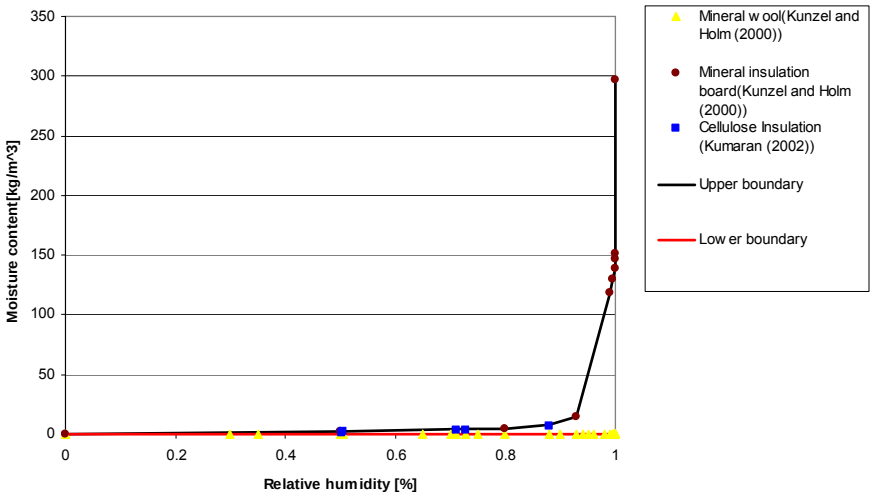

(c) Insulation

Figure 5.11 Moisture storage functions for building materials with upper and lower boundary

Table 5.8 Upper boundary and lower boundaries for building materials used for the virtual case with base values.

	Brick			**Insulation**			**Gypsum board**		
	Base	Lower boundary	Upper boundary	Base	Lower boundary	Upper boundary	Base	Lower boundary	Upper boundary
Density [kg/m^3]	1650	1100	2150	60	8	190	850	618	850
Porosity [m^3/m^3]	0.41	0.11	0.41	0.95	0.25	0.95	0.65	0.305	0.65
Heat capacity [J/kg K]	850	830	920	850	837	850	850	837	870
Heat conductivity [W/mK]	0.6	0.397	1.08	0.04	0.0303	0.045	0.2	0.152	0.23
Diffusion resistance [-]	9.5	8	17	1.3	1.3	3.4	8.3	7.3	13
Moisture storage function (at 100% RH)	370	192.06	370	0	0	297	400	264.4	707.5

Table 5.8 summarizes the basic building material properties from data collected and used in the first case study with upper and lower boundaries and base values (De Wit 2001; DOE 2004a; Kumaran 1996; Kumaran 2002; Kunzel, Karagiozis 2000).

5.3.8 Temperature factor for a thermal bridge and bad workmanship

As discussed in the previous chapter, the temperature factor can be used to account for the thermal bridge effect and bad workmanship. However, very little field measurement data are available regarding the temperature factor and bad workmanship in specific building construction technology, which is a cavity wall in this particular study. The presence of the thermal bridge effect was established from the analysis of trouble spots in buildings with a similar type of facade as that in the test case. In these walls, vertical line joints at the exterior wall corners constitute inherent thermal bridges due to the differences in the surface areas of interior and exterior walls. The author conducted field measurements and linked the results with KOBRA simulations to derive the uncertainty in the severity of the selected thermal bridge type.

Three buildings with cavity wall construction, each building showing slightly different building materials and dimensions, as shown in table 5.9 were selected in Atlanta.. The table includes the first case study building along with three test buildings. The KOBRA calculation results for the temperature factor with specified construction are represented as well. Within each test building, two or three external corners are identified (a total of seven corners) and the surface temperature was measured at the interior corners between 40cm above the floor and below the ceiling to remove the 3D thermal bridge

effect. The measurements were taken in the heating season with a temperature difference of about 20°C. The highest surface temperature and lowest temperature values on the corners were monitored.

Table 5.9 Corner wall components and KOBRA results

Buildings	**Building Materials**	**Thickness (cm)**	**KOBRA Results**
Building A	Face Brick	10	0.87 (undisturbed wall: 0.93)
	Air cavity	1.2	
	Rigid Insulation	3.8	
	CMU	20	
Building B	Face Brick	10	0.85 (undisturbed wall: not recorded)
	Air cavity	2.5	
	Rigid Insulation	2.5	
	CMU	20	
	Plaster	2	
Building C	Face Brick	10	0.81 (undisturbed wall: 0.92)
	Rigid Insulation	2.5	
	CMU	20	
	Brick	10	
The first case study building (office)	Brick	20	0.86
	Air cavity	5	
	Insulation	5	
	Gypsum board	4	

Figure 5.12 shows the field measurement results and calculated values using KOBRA with a linear relationship at the corners and the plain wall surfaces. The measured temperature factors are much lower than the calculated values. Within the same wall component, surface temperature differences were 1°C to 4°C, leading to a spread of temperature factors in the figure. This scattering of temperature factors represents the

combined uncertainty of the deterministic thermal bridge effect of the line joint and potential bad workmanship that may exacerbate the effect.

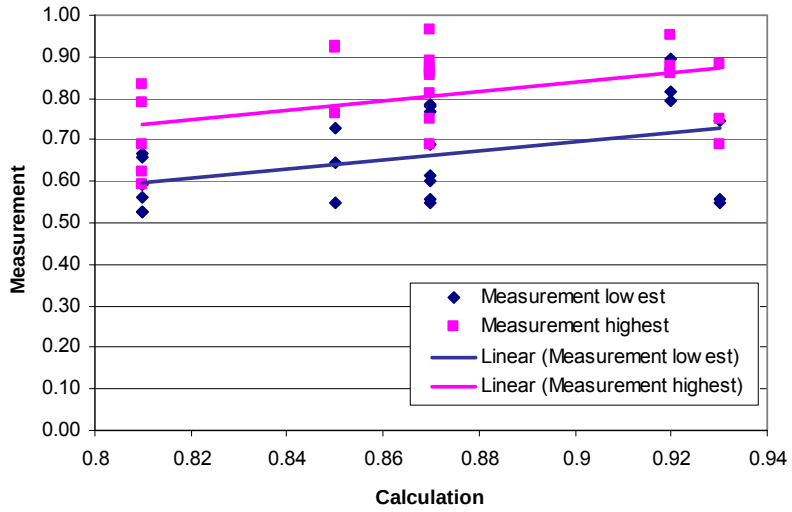

Figure 5.12 Temperature factor measurement and calculation results including plain walls and corners

Figure 5.13 shows the measurement and calculation results of the temperature factors only in the corner walls with 95% confidence intervals. The range of measurement values is used for the uncertainty analysis at a calculated temperature factor. For example, in the reference case that is used for the first case study, the KOBRA result for the corner (0.86) leads to actual values between 0.68 and 0.78 with uncertainties due to bad workmanship and the thermal bridge effect.

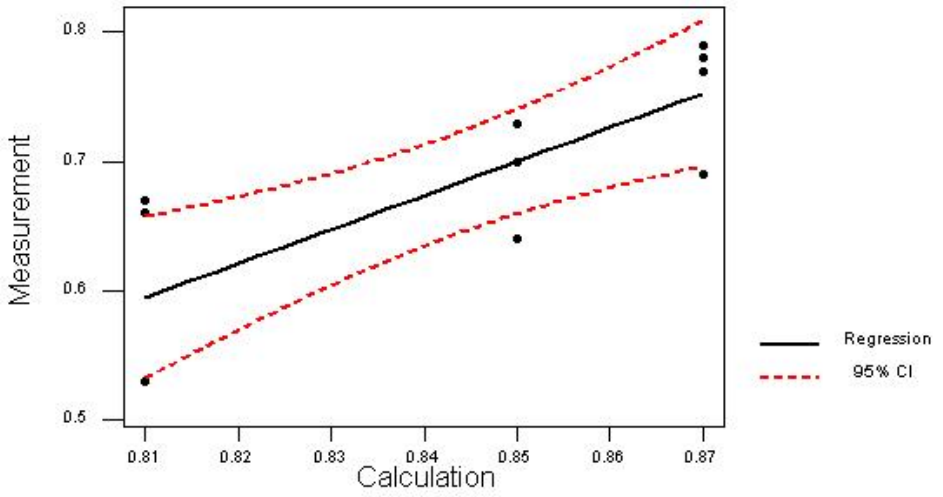

Figure 5.13 Regression results of the corner walls with 95% confidence intervals

This section described the quantification process of some of important uncertain parameters in mold growth analysis. The selection of uncertain parameters and the range of uncertain parameter values depend on each specific building and the trouble spots of interest. As a next step, the quantified uncertainties of each parameter are propagated in uncertainty analysis.

5.4 PROPAGATION OF UNCERTAINTY

Earlier chapters discussed an extended simulation engine, a new post processing method based on the mold germination graphs, and identification of uncertain parameters and quantification of uncertainty in mold growth analysis. All three are essential steps toward the intended MRI under uncertainty. The quantified uncertainty is propagated to generate the probabilistic mold growth risk in a specific location of concern in a given building. The schematic drawing of this process is presented in Figure 5.14. This section describes the uncertainty propagation method used in the MRI.

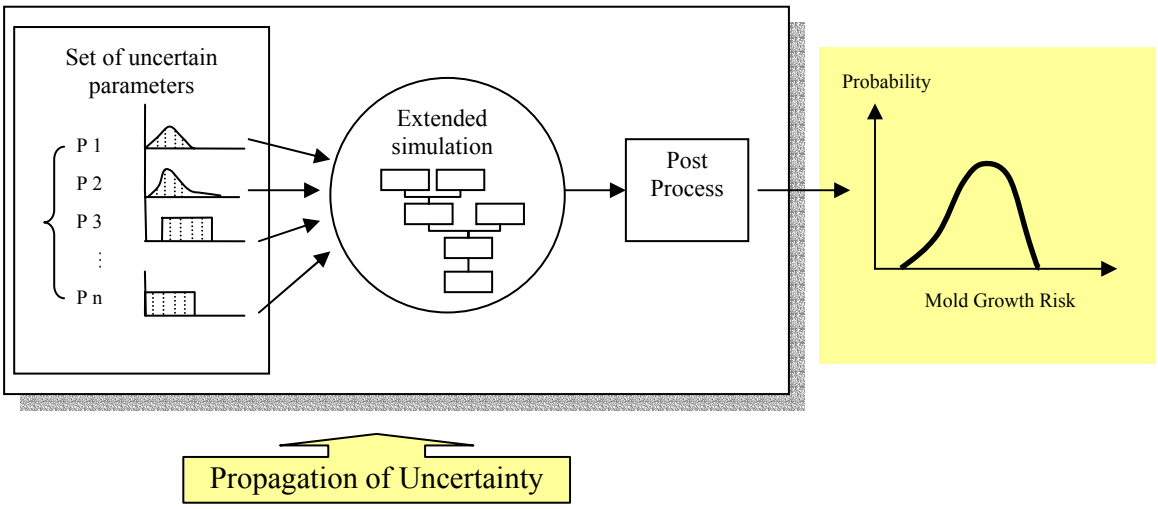

Figure 5.14 Uncertainty propagation in mold risk analysis

The propagation of uncertainties can be performed using various uncertainty analysis techniques. The purpose of uncertainty analysis is to determine the uncertainty in estimates for dependent variables of interest, see references (European Commission - IPSC 2004; Iman and Helton 1988; Saltelli, Andres 1993; Saltelli, Tarantola 2004). Since

mold growth risk mainly depends on various physical and biological parameters whose variations are significant, it is important to evaluate the risks based on the uncertainties of input parameters.

One of the most widely used means for uncertainty analysis is the Monte Carlo method. This method involves random sampling from a distribution of inputs and successive model runs until a statistically significant distribution of outputs is obtained. Since Monte Carlo analysis requires a large number of samples (or model runs), its applicability is sometimes limited to simple models. In case of computationally intensive models, the time and resources required by this method could be prohibitively expensive.

The Latin Hypercube Sampling is one such widely used variant of the standard Monte Carlo method (Wyss and Jorgensen 1998) that is particularly suited to our needs. This approach was well described in the work by De Wit and Augenbroe (2002) and demonstrated to be suitable in building simulation. In this method, the range of probable values for each uncertain input parameter is divided into ordered segments of equal probability. Thus, the whole parameter space, consisting of all the uncertain parameters, partitioned into cells with equal probability and sampled in an "efficient" manner in that each parameter is sampled once from each of its possible segments. The advantage of this approach is that the random samples are generated from all the ranges of possible values, thus providing insight into the extremes of the probability distributions of the outputs. A detailed description of the implementation of LHS is presented in (1999). Some commercial software that utilizes the algorithm for LHS includes Crystal Ball (Decisioneering), @RISK, RISKMAN, and MonteCarlo. Matlab(MathWorks) also has statistical functions (i.e., lhsdesign, lhsnorm) for Latin hypercube sampling methods. In

this study, parameter samples were generated using an LHS algorithm in SIMLAB version 2.2 (European Commission - IPSC 2004).

5.5 IDENTIFICATION OF DOMINANT PARAMETERS

In addition to uncertainty propagation, a related method can be used to provide knowledge about dominant parameters, i.e. those parameters that have a major influence on the uncertainty in the mold risk. The method to do this is a parameter screening technique as shown in Figure 5.15. A brief description explains he main points of the method.

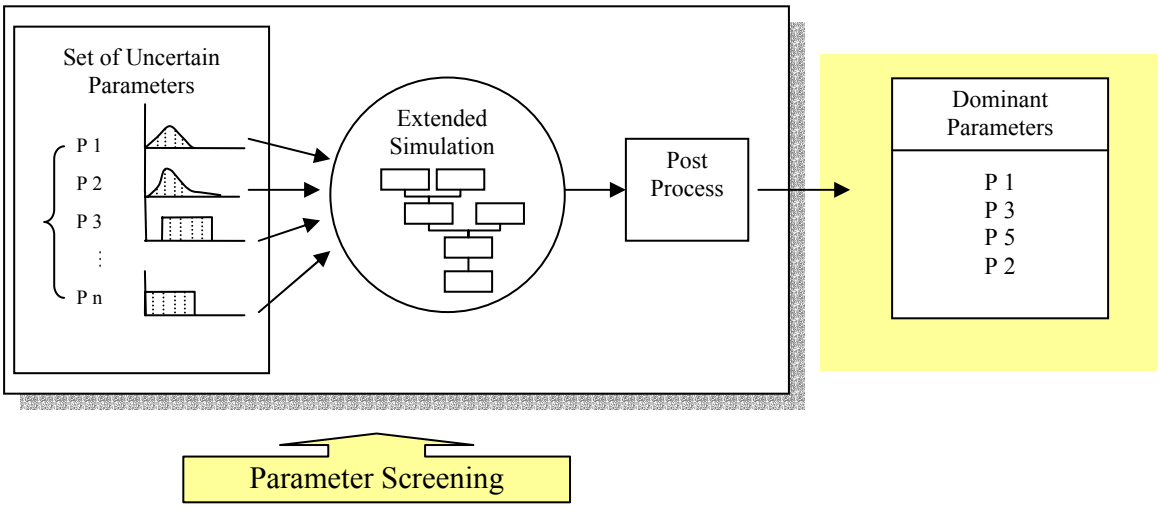

Figure 5.15 Parameter screening in mold risk analysis

In this study, the identification of dominant parameters is performed using a parameter screening technique suggested by Morris (1991). This method has been proven to be adequate for parameter screening in complex building simulation (De Wit 1997).

This technique is economical for models with a large number of parameters, as it does not depend on any assumptions about the relationship between parameters and model output (such as linearity), and the results are easily interpreted in a lucid, graphical way. The factorial sampling technique also allows for the exploration of non-linearity and the interaction effects in the model and ranks parameters in order of their importance, i.e., their individual contribution to the uncertainty in the model output based on elementary effects. An elementary effect of a parameter is the change in the model output as a result of a change Δ in that parameter, while all other parameters are kept at a fixed value. If the variation Δ is chosen for each parameter as a fixed fraction of its central 95% confidence interval, the elementary effects become a measure of parameter importance. If the model is non-linear in the parameters, or if the parameters interact, the value of the elementary effect of a parameter may vary according to the point in the parameter space where it is calculated. When the elementary effect of a parameter at a number of randomly selected points in the parameter space is calculated, a sample of elementary effects is obtained. A large mean value or a large standard deviation of this sample indicates "overall" importance of the corresponding parameter on the output. A large standard deviation indicates an input whose influence is highly dependent on the values of the parameters, i.e., one that is involved in interactions or whose effect is nonlinear. The results of the sensitivity analysis can be examined from a figure in which the sample mean and the standard deviation of the elementary effects are plotted for each of the parameters. The exemplary results of the sensitivity analysis are presented in Figure 5.14.

In the application of the Morris method, each parameter (x_i) will be assumed to be scaled to take on values in the interval [0, 1]. Each parameter, the region of interest is

discritized in a p-level grid, where each xi may take on values from [0, 1/(p-1), 2/(p-1), 3/(p-1),….,1]. Then, the elementary effect of the *i* th input can be defined as (De Wit 2001):

$$d_i(\mathrm{X}) = \frac{y(x_1, x_2, x_3, ..., x_{i-1}, x_i + \Delta, x_{i+1}, ..., x_k) - y(\mathrm{X})}{\Delta} \quad , \qquad (5.11)$$

where X is a subset of the region of interest, except that $x_i \leq 1 - \Delta$ and Δ is a predetermined multiple of 1/(p-1).

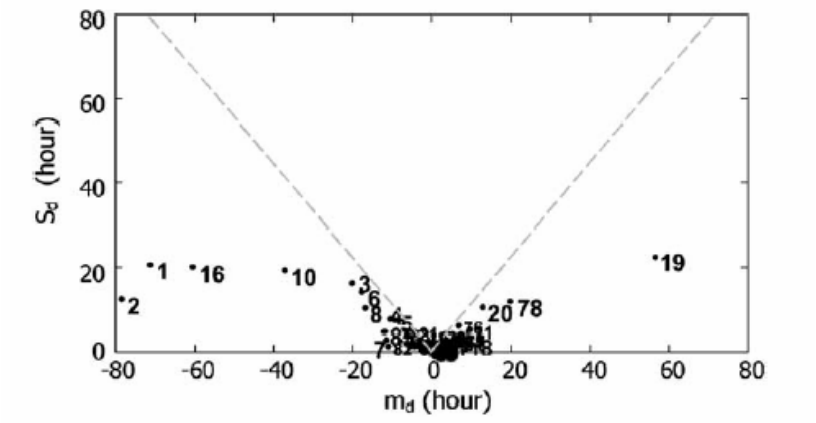

Figure 5.16 Example of the estimated means (m_d) and standard deviations (S_d) of the distributions of elementary effects. The dotted lines are correspond to $m_d = \pm 2 s_d / \sqrt{r}$ (from (deWit and Augenbroe 2002))

In the next chapter, the analysis explained above will be applied to three building cases in order to test the merit of the MRI in design, operation and remediation.

CHAPTER 6

CASE STUDIES

In this chapter, three case studies that test the developed probabilistic performance indicator for the mold growth indicator are conducted. The first case is a virtual office building, the second a federal office building, and the third a dormitory building. The objective of the case studies is to determine the distribution of mold growth risks and identify the dominant parameters that contribute to the mold growth risk at specific trouble spots. Each trouble spot represents a separate case as its location will determine which uncertainties need to enter the simulation and how these can be quantified.

In all three studied buildings, only one trouble spot was chosen all located in similar location, i.e. at the interior surface at the corner of an exterior wall. The MRI is quantified for the chosen trouble spot using the approach from the previous chapter. For each case the mixed simulation is set up by had preparing the input file. Detailed descriptions and analytical results are provided for the first case study. The remaining cases follow the same analytical methods and procedures.

6.1 CASE 1: INTERIOR CORNER SURFACE IN A REFERENCE OFFICE BUILDING

The first case is a virtual office building with a trouble spot at the interior surface of an exterior wall corner. The objective of this case study is to find how the environmental conditions provided by the building systems affect to mold growth risk on this specific location of building, as shown in figure 6.1. The reason to choose this

location is that exterior corner has been reported as mold occurrence places in many studies and has inherent thermal bridge effects due to the difference of surface areas between interior and exterior wall. The mixed simulation approach described in figure 4.2 is used to generate the environmental conditions for the mold growth risk assessment.

Building parameters and appropriate range of each parameter's values are derived as explained in the previous chapters. The building model, building design and operation data are described in the following sections.

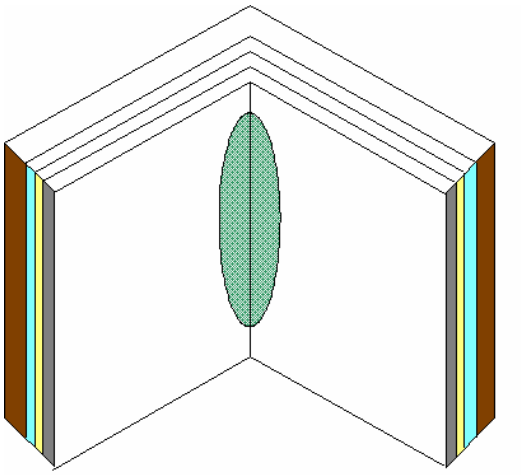

Figure 6.1 Exterior wall section and the location of concern (i.e., interior surface of the corner in exterior wall)

6.1.1 Building model and scenario

The selected reference building is a one-story office building located in the city center of Miami, which has hot and humid climate (according to the DOE proposed climate zone[1]). The reference area has a typical urban setting with surrounding buildings

[1] www.energycodes.gov/implement/pdfs/IECC_code_change_Mar03.pdf

(average height of 15m). The density of surrounding buildings over the reference area is 20% and no significant difference exists between windward and leeward side. This building is composed of four office rooms (6m×6m×3m) and one corridor (12m×2m×3m). Each room has one operable window (4m×1m) in the exterior facade. Figure 6.2 shows the plan of the reference building, and location of concern for mold growth. Table 6.1 summarizes the building construction and material data.

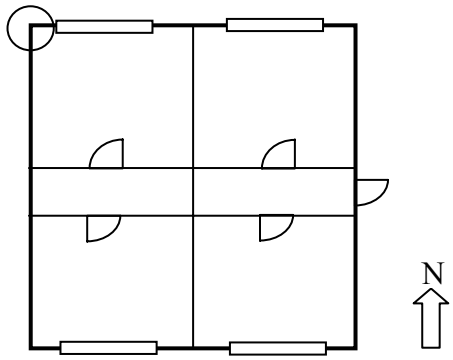

Figure 6.2 Plan of the reference building and location of concern for mold growth

The exterior walls are composed of brick, air gap, insulation, and gypsum board. Four persons are assumed to be working in each room during normal office hours (8:00 – 18:00). In the scenario that is reported below, the HVAC system is operated during the occupied hours, and only during weekdays. In the simulation, the HVAC system with Variable Air Volume (VAV) is controlled to meet the set temperature of 20°C (±2°C) and minimum 45% RH (±10%).

Table 6.1 Construction and materials

Building components	**Layers**	**Roughness**	**Thickness (m)**
Exterior wall (width=0.54m)	Brick	Rough	0.3
	Air gap	Very smooth	0.1
	Fiber glass	Very rough	0.1
	Gypsum board	Smooth	0.04
Floor	HW Concrete	Medium	0.2
Roof (width=0.21)	Roofing Shingle	Rough	0.01
	HW Concrete	Medium	0.2
Partition (0.243m)	Plaster/Gypsum board	Smooth	0.02
	Clay tile	Smooth	0.203
	Plaster/Gypsum Board	Smooth	0.02
Door	Solid core	Smooth	0.349
Window	Single pane		0.003

In this reference case, an abstracted HVAC system is used to study the parameter sensitivity in terms of the mold growth risk. The system is composed of a heating coil, a cooling coil, a humidifier, and a supply fan to provide supply air with the specified set temperature and relative humidity. VAV system is adopted to control the required airflow volume rate. In this particular case, the air loop components, plant loop components, and the air handling unit are assumed to be designed and performed well to cover heating, cooling, and humidity requirement ideally. Figure 6.3 shows a schematic drawing of the abstracted HVAC system.

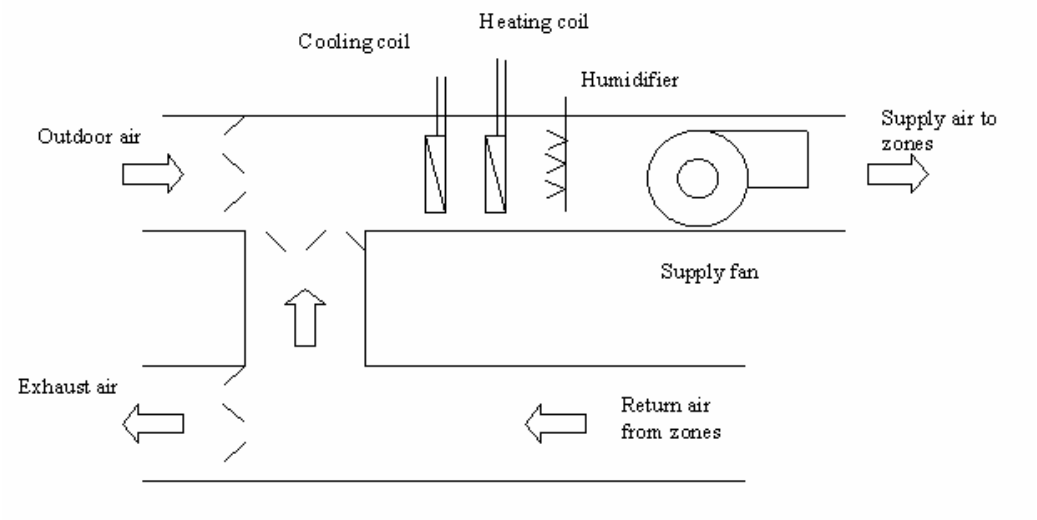

Figure 6.3 Schematic drawing of the abstracted HVAC system

In this case study, each room is assumed to have indoor moisture sources, which are four office workers with light activities, regular wet cleaning of the floor, one frost-free fridge, and two small plants per room. Table 6.2 shows the range of indoor moisture loads for each moisture source based on the study in chapter 4. Latent heat from people is calculated along with sensible heat gain from metabolic rate. Figure 6.4 shows hourly upper and lower boundary profiles of total indoor moisture loads for the case study. For the base values of the case, mean values of the parameter range will be used as shown on the figure.

Table 6.2 Indoor moisture loads for the case study

Moisture sources	**Moisture generation**	**Hourly profile**	**Remarks**
4 persons (light activity)	120 ~ 240 [g/h]	Same as occupancy schedule	30~60 [g/h · person]
Washing floor [36 m^2]	149.8 ~ 270 [g/h]	Weekdays at 6 PM.	100 ~ 180 [g/ m^2 · day]
Frost-free fridge	20.8 ~ 43 [g/h]	24 hours	
Plants 2 ea.	3.2 ~ 8.4 [g/h]	24 hours	1.6~4.2 [g/h]

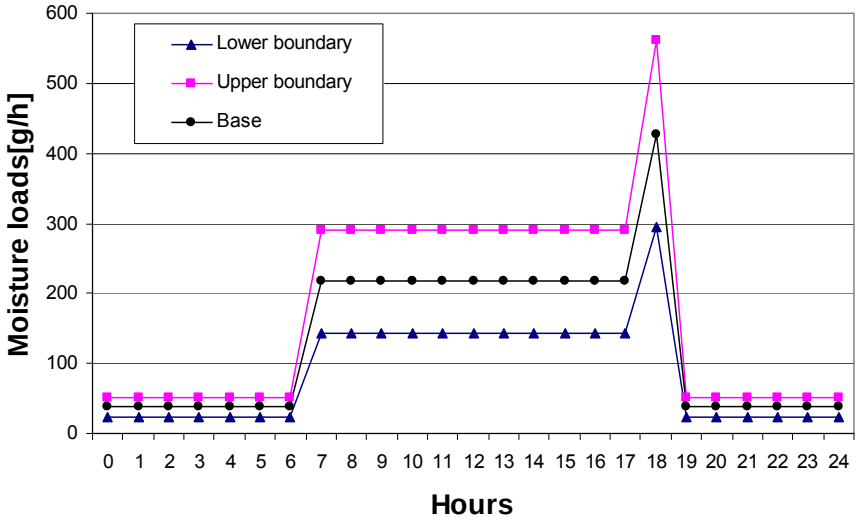

Figure 6.4 Maximum and minimum total moisture loads for a room in the case study

6.1.2 Uncertain parameters and their ranges

A set of uncertain parameters in this case study are constructed based on the required input parameters for each flow equation and causes for mold growth in buildings as described in the previous chapter. In this case at hand, heat, moisture transport within a wall, and airflow (i.e., infiltration and ventilation) are considered the governing physical mechanisms. After constructing the input model for this reference case, all relevant uncertain building parameters are identified and their level of uncertainties can be quantified with similar techniques, as described early. Table 6.3 shows the selected 33 parameters with base values and the lower and upper values that quantify the uncertainty.

A base value represents the deterministic value that a designer or engineer would use for standard idealized simulation based on sound engineering judgment. Values for the base case are acquired from the design conditions, the specification of the building

components, default values of simulation tools, or mean values from lower and upper value of the parameter range. The base case that uses base values for all parameters will result in a deterministic value for mold growth risk analysis. The result of the base case will be compared with that of uncertainty analysis.

The lower and upper values of uncertain parameters are derived from the study of each parameter in Chapter 5. The range of uncertainty of each parameter depends on the building case (building description and scenario). As described in an earlier chapter, uncertainties of parameters may arise from different sources of uncertainty. Uncertainties from "building behavior and operation" and "scenario" (indoor moisture generation) are included in the uncertainty analysis. The flowchart of mixed simulation is followed for implementation (Figure 4.5).

Table 6.3 Uncertain parameters and their upper and lower values

	Parameters	**Base**	**Min**	**Max**	**Remarks**
1	Outside air flow rate (m^3/s)	0.16	0	0.16	* 16 person with ASHRAE outdoor air requirement (ASHRAE 2001a)
2	Zone set point temperature control deviation (°C)	0	0	2	See Appendix A
3	Minimum RH delta (%)	0	0	10	See Appendix A
4	Supply air temperature(°C)	14.5	13	16	Typical values from (ASHRAE 1999b)
5	External convective heat transfer coefficient(W/m^2K)	18	9	27	At 2 m/s of the surface-parallel flow velocity (De Wit 2001)

Table 6.3 (continued)

6	Internal convective heat transfer coefficient(W/ m^2K)	2.4	1.59	3.21	at $\Delta T = 2°C$ (De Wit 2001)
7	Air mass flow coefficient (Cs) (Crack, Wall)	0.001 * COMIS default	0.00017	0.0054	See table 5.3
8	Discharge coefficient for opening factor (-)	0.675	0.6	0.75	See Ch. 5.3.4 Infiltration
9	Cp value (South façade)	-0.37	-0.6	-0.1	Base values from ASHRAE (2001b) See Appendix A for upper/lower values (Values at 0 degree)
10	Cp value (North façade)	0.6	0.02	0.9	
11	Cp value (West façade)	-0.56	-0.9	-0.23	
12	Cp value (East façade)	-0.56	-0.9	-0.23	
13	Wind velocity profile exponent (-)	0.33	0.33	0.4	Table 5.4
14	Moisture source (moisture generation, g/h)	37.7 (26.2)	24 (16.7)	51.4 (35.7)	see figure 6.4 Values at unoccupied hours Values in ( ) with unit of W/h
15	Brick: density (kg/m^3)	1650	1100	2150	See table 5.8
16	Brick: porosity (m^3/m^3)	0.41	0.11	0.41	
17	Brick: heat capacity (J/kg K)	850	830	920	
18	Brick: heat conductivity (W/m K)	0.6	0.397	1.08	
19	Brick: diffusion resistance (-)	9.5	8	17	See figure 5.7

Table 6.3 (continued)

20	Brick: moisture storage function (kg/m^3)	370	192.06	370	See figure 5.7 Value at RH = 1
21	Insulation: density (kg/m^3)	60	8	190	See table 5.8
22	Insulation: porosity (m^3/m^3)	0.95	0.25	0.95	
23	Insulation: heat capacity (J/kg K)	850	837	850	
24	Insulation: heat conductivity (W/m K)	0.04	0.0303	0.045	
25	Insulation: diffusion resistance (-)	1.3	1.3	3.4	See figure 5.7
26	Insulation: moisture storage function (kg/m^3)	0	0	297	See figure 5.7 Value at RH = 1
27	Gypsum board: density (kg/m^3)	850	618	850	See table 5.8
28	Gypsum board: porosity (m^3/m^3)	0.65	0.305	0.65	
29	Gypsum board: heat capacity (J/kg K)	850	837	870	
30	Gypsum board: heat conductivity (W/m K)	0.2	0.152	0.23	
31	Gypsum board: diffusion resistance (-)	8.3	7.3	13	See figure 5.7
32	Gypsum board: moisture storage function (kg/m^3)	400	264.4	707.5	See figure 5.7 Value at RH = 1
33	Temperature factor (-)	0.86	0.68	0.78	See figure 5.11 Base value is a result of KOBRA

In the mixed simulation, the building zone was set up for a yearly simulation with the Miami climate. The simulation was conducted in Monte-Carlo style to analyze the mold growth conditions at the trouble spot under uncertainty. In order to translate the conditions into an aggregated mold risk factor, two alternative methods were used. Both methods are based on a count of the yearly average number of "risky days for mold growth" (a value between 0 and 365). The first method is based on the germination graph method developed in chapter 3. The second is based on the 80% RH criterion recommended by IEA (1991)as a threshold for preventing mold germination(IEA 1991). This method counts a day as risky if the daily average surface relative humidity exceeds 80% of RH. Both approaches can be viewed as leading to the quantification of a "mold performance indicator."

6.1.3 Distribution of the performance indicator

The propagation of the parameter uncertainties leads to a statistical distribution of mold growth conditions in the specific building case. The parameter ranges in table 6.3 are interpreted as central 95% confidence intervals. Due to the lack of explicit information on the parameter distribution, normal distributions were assumed for all parameters.

The Latin Hypercube Sampling (LHS) method was used for the uncertainty propagation as discussed in the previous chapter. Parameter samples were generated using an LHS algorithm in SIMLAB version 2.2 (European Commission - IPSC 2004). A total of 60 samples were generated and propagated through the mixed simulation toolset.

The number of samples generated are well above the minimum required value ($4k/3 = 44$).

Each sample was fed into a series of models as described in figure 4.2. Results from each step are presented below.

Based on the scenario information and uncertain parameters, building energy and airflow simulation was conducted first using EnergyPlus and COMIS. Indoor air temperature and relative humidity calculation results from the this step were used as a boundary condition in a hygrothermal envelope model, i.e., WUFI. 60 simulation runs were conducted for the exterior wall in northwest zone. This simulation gives wall level surface temperature and relative humidity. Temperature factors and associated uncertainties were calculated using KOBRA and the field measurement results presented in Figure 5.13.

The results from WUFI and temperature factor parameters were used to calculate local surface level of mold growth risk at the corner of the exterior wall. The results of the propagation of 60 samples are shown in figure 6.5 and 6.6 for the germination graph method and 80% RH criterion method, respectively. The distribution (dotted line) was found for each case by using fitting techniques. Cumulative density functions are drawn for each case as well.

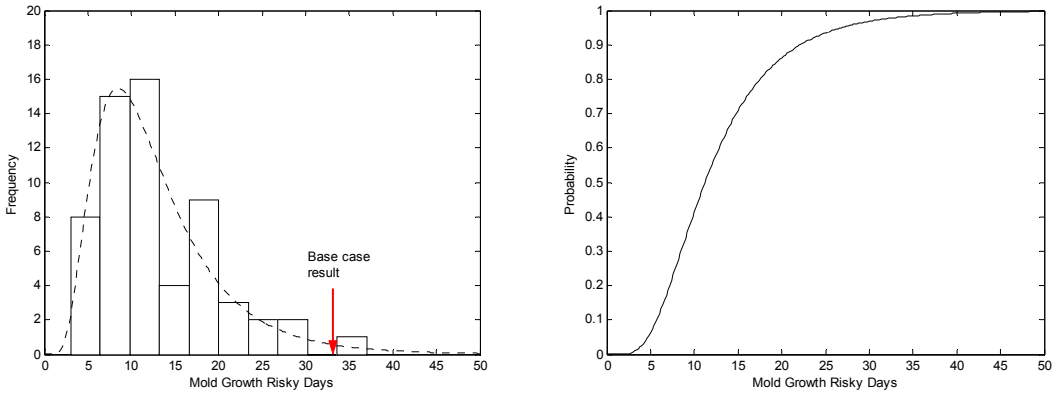

(a) (b)

Figure 6.5 (a) Histogram of the performance indicator for the chosen trouble spot using the germination graph method with Latin Hypercube sample size of 60. (b) Cumulative density function with the germination graph method

In the case of the germination graph method (figure 6.5), the mean value of risky days is 12.9 and the standard deviation is 7.35 with a variance of 54.0. In this analysis, variation is significant as the coefficient of variation ($C_v = \sigma/\overline{X}$) is around 0.57. A lognormal distribution was found as the best fit for the distribution of risky days, which has a long, gradually decreasing tail as X-axis values increase.

The uncertainty propagation results showed mold growth risks in all 60 samples, which predict, theoretically, some level of mold growth in all possible combinations of uncertain parameters in this particular case. It is plausible that only if the number of yearly risky days is above a certain threshold, harmful, visible mold growth will actually occur. In order to find this threshold value, we need to calibrate the outcomes of figure 6.5 for a large set of building cases with established mold problems in those buildings. This is an area of important follow-up research.

It should be noted that in this particular case, the distribution in figure 6.5 shows median value of 11 and a long tail that indicates possible severe mold occurrence with relatively low probability. The analysis with the base parameter values resulted in 34 risky days, which is at the upper end of the distribution, i.e., in this case a deterministic simulation with average guess values would predict a relatively high mold risk, which has relatively low probability of occurring in the actual building. It is atypical that the deterministic simulation produces a risk value that is considerable higher than the median of the distribution that results form an uncertainty analysis. In this particular case, the base value for the air mass flow coefficient was selected from the default value in COMIS. As it happens, this parameter proves to have a dominant influence on the mold growth (as shown below). As table 6.3 shows, the base value is close to the lower bound of the uncertainty range of the parameter.

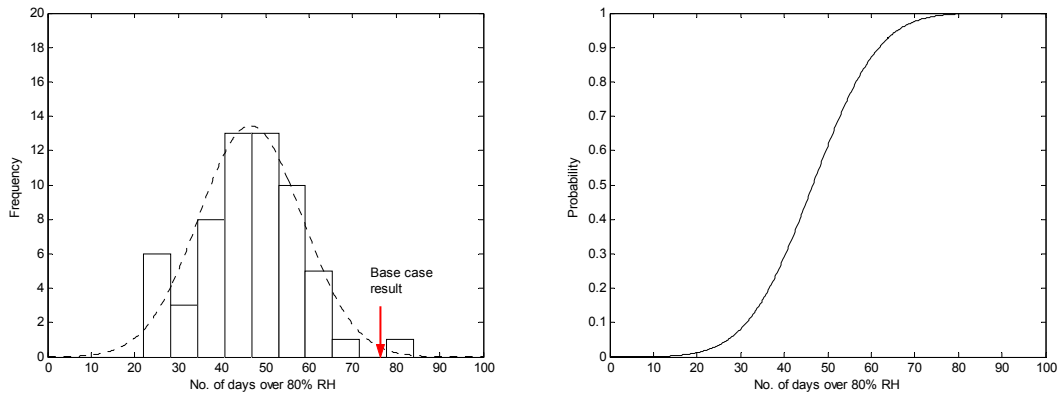

(a) (b)

Figure 6.6 (a) Histogram of the performance indicator using 80% RH criterion from the Latin Hypercube sample size of 60 (b) Cumulative density function for 80% criterion

Figure 6.6 shows the results of the same uncertainty analysis now using the 80% RH criterion with a mean value of 46.5 and standard deviation of 11.8. The normal distribution was found as the best fit in this case. Using 80% RH criteria gives much higher mean mold risks but low of coefficient of variation ($C_v = \sigma/\overline{X} = 0.254$). It should be noted that the 80% RH criterion only accounts for the surface relative humidity without considering the effect of temperature and nutrition of building material to mold growth. The deterministic simulation with base values now results in 76 risky days. Again, and in line with what we found above, the resulting value is to the high end of the risk, with relatively low probability due to same reason above.

It should be noted that the number of risky days using the two criteria differs substantially. Little significance can be attributed to this as the "scale" of both distributions has only relative meaning. Future research will have to establish the correlation between the risky days in either distribution and actual occurring mold. Both criteria could be used for this purpose, but it is expected that the germination graph will show a stronger correlation due to the better representation of the fundamental mold growth mechanism.

6.1.4 Identification of dominant parameters

The identification of dominant parameters is performed using the Morris method as described in the previous chapter. In our test case, the 33 parameters were discretized on a 6-level grid (p=6) and the predefined elementary step Δ was chosen to be 3/5. Samples were generated by using the Morris method algorithm in SIMLAB. A total of 5 independent samples of the elementary effects were assessed in 170 simulation runs. The

parameters that explain about 80% of total variance are considered the dominant parameters.

Figure 6.7 and table 6.4 show the result of identification of dominant parameters using the mold germination graph method. Only the identified dominant parameters are shown in the figure. An elementary effect above the wedge line ($m_d = \pm 2S_d / \sqrt{r}$) indicates parameter interaction or non-linear effect. In the study of the elementary effects for each parameter, five dominant parameters were identified. The top two parameters (air mass flow coefficient and indoor moisture source) accounted for about 72% of the total variance.

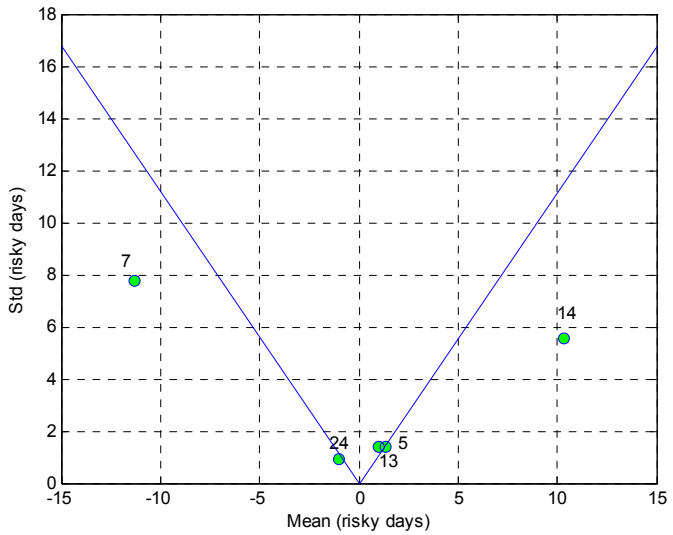

Figure 6.7 Ranking results for top 5 dominant parameters using the mold germination graph method (Parameters 33 Run 5)

Table 6.4 Top 5 dominant parameters using the mold germination graph method

Ranking	Parameters	Index
1	Air mass flow coefficient (Cs) (CRACK)	7
2	Moisture source	14
3	External convective heat transfer coefficient	5
4	Wind exponent	13
4	Insulation conductivity	24

Similar results can be found in the case of 80% RH criteria as well, as shown in figure 6.8 and table 6.5. The 6 dominant parameters were found and three parameters were same from the previous result, i.e., air mass flow coefficient, moisture source, and wind exponent, although the ranks are slightly different. The reason of the different ranks is that the 80% RH criteria consider only relative humidity and excludes the effect of temperature, and exposure time.

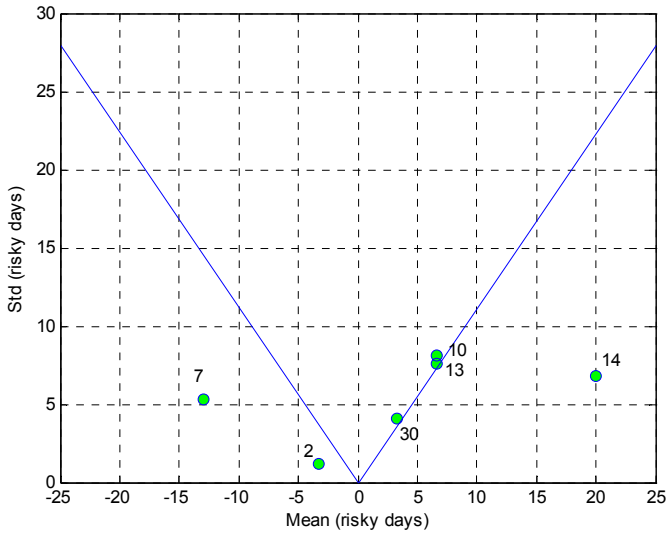

Figure 6.8 Ranking results for top 6 dominant parameters for 80% RH Criteria (Parameters 33 Run 5)

Table 6.5 Top 6 dominant parameters using the 80% RH Criteria

Ranking	Parameters	Index
1	Moisture Source	14
2	Air mass flow coefficient (Cs) (CRACK)	7
3	Pressure coefficient (North)	10
3	Wind Exponent	13
5	Set temperature delta	2
5	Gypsum conductivity	30

The identified dominant parameters can be used to design for a reduced mold risk in the building case. Figure 6.9 shows a schematic drawing of the transition of the distribution of mold growth risk (solid line) to the reduced mold risk case (dotted line). This is achieved with a better management of uncertainties in the dominant parameters. Depending on the positive or negative correlation between each dominant parameter and resulting mold risk, appropriate building operation schemes and an A/E/C procurement contract can be suggested.

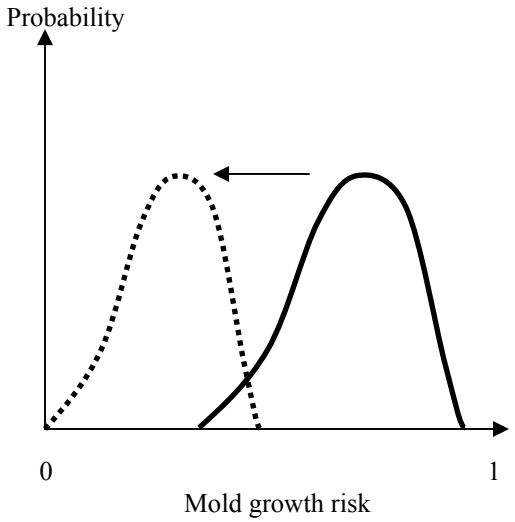

Figure 6.9 Reducing mold growth risk based on knowledge of dominant parameters

In the above results of the dominant parameters (Figure 6.7 and 6.8), the moisture source (moisture generation rates inside the room) and the air mass flow coefficient account for most of the uncertainty of mold risk. For the parameter representing the moisture source, it shows a positive correlation with mold risk, which indicates that an increased moisture generation rate leads to higher mold risk. Furthermore, increased uncertainty of the moisture source (a broader range of the parameter) results in a wide distribution of resulting mold risk. Thus, it is clear that one needs to lower the moisture generation rate (the mean value for a normal distribution) and reduce the uncertainty associated with the moisture generation rate to reduce mold risk. However, this requires a change of scenario and the refinement of uncertainty associated with moisture generation. For example, it would require removing moisture generating equipment, or reducing the number of occupants and thus would require a new MRI quantification for a changed scenario.

Additional study would be required to refine the uncertainty, such as the ones based on expert judgment study (Cooke 1991). This case study only has performed a "first pass" assessment and does not deal with the uncertainty refinement.

It is interesting to note that the air mass flow coefficient shows a negative correlation with mold growth risk, i.e., the minus mean value. This reveals that a decreased infiltration rate increases mold growth risk. This is because in the studied scenario, the HVAC system works only on weekdays, i.e., not on weekends or on holidays. As it happens, most mold growth risks occur during the system off period. In general, HVAC system turn-off with continuous moisture sources in rooms during weekends contributes to higher indoor humidity ratios than outdoors and thus constitutes

a substantial risk for mold growth. However, higher infiltration of outside air mitigates this risk! This explains the unexpected high risk that was found in deterministic base case simulation in which the mitigating effect was underestimated. This “post analysis” shows the power and versatility of the uncertainty analysis, as it helps to indicate those factors that need to be controlled and procured in a way to keep mold risk under acceptable levels. It should also be noted that for this particular building in this particular location, the risk analyses for different scenarios reveals that the chosen HVAC operation leads to unacceptable risks, and a HVAC shut down is not acceptable.

6.2 CASE 2: INTERIOR CORNER SURFACE IN A FEDERAL OFFICE BUILDING

A second case study has been conducted for an existing office building (Figure 6.10). This seven-story massive-blocked structure was constructed in 1931-1933 for the postal service and is now used as an office building. Mold problems have occurred in a zone of the building located on the ground floor (Figure 6.10 (b) and Figure 6.11). Office workers were evacuated and an investigation was conducted to identify the possible causes and remediation method. It was concluded that the main cause was water leaking from the ceiling of the office rooms. The water penetrated from the side walk due to lack of water intrusion prevention on top of the ground. The developed performance indicator was applied to this building case to check whether mold growth risks would persist after fixing the water leakage.

(a) View of the office building

(b) Location of the room with mold problems

Figure 6.10 Pictures of the federal office building in Atlanta

Figure 6.11 Example of mold and moisture problems in the office building

6.2.1 Building model and design conditions

The building is located in the city center of Atlanta, which has mixed humid climate according to the new DOE proposed climate zone. The reference area has a

typical urban setting with surrounding buildings. Figure 6.12 shows the location of the room on the ground floor targeted for the analysis (6m×6m×3m). Again, the MRI is applied to a trouble spot, an interior wall corner. The location of concern for mold growth is indicated in the figure as well. Table 6.6 summarizes the building construction and material data.

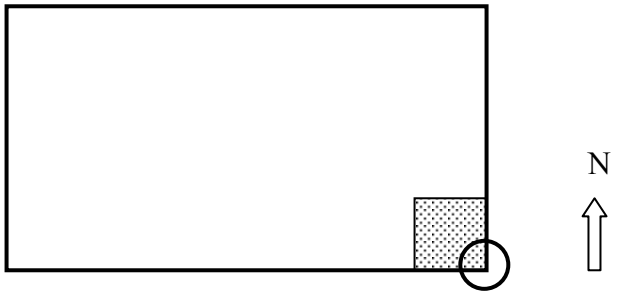

Figure 6.12 Schematic drawing of the target room in the office building located in ground floor

The exterior walls are composed of concrete, insulation, gypsum board, and wallpaper. Four people are assumed to work in the office room during normal office hours (8:00 – 18:00). From the operation data of the building, the HVAC operation schedule could be determined. The HVAC system is operated during working hours (8:00 – 18:00), five days a week. HVAC runs for return air setback during off working hours and weekdays. In the mixed simulation, the HVAC system with VAV is controlled to meet the set temperature of 24°C (±1.5°C) and minimum 55% RH (±10%). Indoor moisture sources include four office workers with light activity, and one small plant in the room. A detailed description can be found in Appendix B.

Table 6.6 Construction and materials of the federal office building:

Building components	**Layers**	**Roughness**	**Thickness (m)**
Exterior wall	Concrete	Rough	0.4
	Fiber glass	Very rough	0.1
	Gypsum board	Smooth	0.04
	Wall paper	Smooth	-
Floor	HW Concrete	Medium	0.2
Roof	Roofing Shingle	Rough	0.01
	HW Concrete	Medium	0.2
Partition	Plaster/ Gypsum board	Smooth	0.02
	Clay tile	Smooth	0.203
	Plaster/Gypsum board	Smooth	0.02

6.2.2 Values of parameters for the base case and range

The target room is located on the ground floor and only one façade is exposed to the external condition (i.e., south façade). Thus, no infiltration or crack flow is considered in this case analysis. Heat and moisture transport within a wall are considered the main governing physical mechanisms. At the chosen trouble spot, the KOBRA simulation produces a result of the temperature factor of 0.87 inside surface of the exterior corner wall. This value corresponds to an uncertain range of 0.67 ~ 0.81 (see figure 5.13). Table 6.7 shows the 26 selected uncertain parameters with base values and the lower and upper values that quantify the uncertainty from the study of quantification of uncertainty as described in previous chapters. Uncertainties associated with wallpaper are ignored due to a lack of information about its hygrothermal properties. The fixed values of the hygrothermal properties of wallpaper are found on the WUFI database and used in the

mixed simulation approach (see Appendix B). The mixed simulation ran for a one year period in the Atlanta climate. The same statistical analysis was conducted as the first case study to analyze the mold growth conditions at the chosen trouble spot.

Table 6.7 Uncertain parameters and their upper and lower values

	Parameters	**Base**	**Min**	**Max**	**Remarks**
1	Outside air flow rate (m^3/s)	0.04	0	0.04	* 4 person with ASHRAE ventilation requirement
2	Zone set point temperature delta T (C)	0	0	1.5	See Appendix B
3	Minimum RH delta (%)	0	0	10	See Appendix B
4	Supply air temperature (°C)	14.5 * median	13	16	Typical values from (ASHRAE 1999b)
5	External convective heat transfer coefficient (W/m^2K)	18 * median	9	27	At 2 m/s of the surface-parallel flow velocity (De Wit 2001)
6	Internal convective heat transfer coefficient (W/m^2K)	2.4 * median	1.59	3.21	at $\Delta T = 2°C$ (De Wit 2001)
7	Moisture source (g/h)	2.9 (2)	1.6 (1)	4.2 (3)	See Appendix B Values at unoccupied hours Values in () with unit of W
8	Concrete: density (kg/m^3)	2200	2100	2300	See Appendix B
9	Concrete: porosity(m^3/m^3)	0.18	0.15	0.18	

Table 6.7 (continued)

10	Concrete: heat capacity (J/kg K)	850	837	940	
11	Concrete: heat conductivity (W/m K)	1.6	1.16	2	
12	Concrete: diffusion resistance (-)	92	92	248	
13	Concrete: moisture storage function (kg/m^3)	175	147	175	Value at RH = 1 See Appendix B
14	Insulation: density (kg/m^3)	60	8	190	See table 5.8
15	Insulation: porosity (m^3/m^3)	0.95	0.25	0.95	
16	Insulation: heat capacity (J/kg K)	850	837	850	
17	Insulation: heat conductivity (W/m K)	0.04	0.0303	0.045	
18	Insulation: diffusion resistance (-)	1.3	1.3	3.4	See figure 5.7
19	Insulation: moisture storage function (kg/m^3)	0	0	297	See figure 5.7 Value at RH = 1
20	Gypsum board: density(kg/m^3)	850	618	850	See table 5.8
21	Gypsum board: porosity (m^3/m^3)	0.65	0.305	0.65	
22	Gypsum board: heat capacity (J/kg K)	850	837	870	
23	Gypsum board: heat conductivity (W/m K)	0.2	0.152	0.23	
24	Gypsum board: diffusion resistance	8.3	7.3	13	See figure 5.7
25	Gypsum board: moisture storage function (kg/m^3)	400	264.4	707.5	See figure 5.7 Value at RH = 1
26	Temperature factor	0.87	0.67	0.81	See figure 5.11 Base value is a result of KOBRA

6.2.3 Distribution of the performance indicator

The uncertainty analysis was conducted with 60 simulation runs using the Latin Hypercube Sampling method, introduced earlier. Although the MRI uses the germination graph method as a post process, the analysis was also conducted with the 80% RH criterion for comparison purpose. The results of the distribution of mold risk are presented below.

In the case of the germination graph method, the uncertainty analysis results showed no mold growth risk in all possible combinations of uncertain parameters in this particular case. As discussed in Chapter 4, our analysis method does not cover the effect of a catastrophic breakdown of functionality, i.e., water leakage in this case. It can be concluded, however, that the building will not have mold growth risk under normal operation. If the problem of water leakage from the ceiling is fixed correctly, the building should not experience mold problems.

The profile of surface relative humidity showed a number of risky days over 80% during the course of one year. An uncertainty analysis using the 80% RH criterion was conducted to get the full picture. Figure 6.13 shows the results with a mean value of 26.8 and a standard deviation of 5.87. In this case, a low coefficient of variation ($C_v = \sigma/\bar{X} =$ 0.215) and a normal distribution were found as the best fit in this case. The simulation with the base values now results in 9 risky days, shown in Figure 6.14(a) has a low probability to occur. Again, the deterministic simulation result does not represent the mold phenomenon correctly.

Although the mold germination graph method did not show mold growth risk, the results of the 80% RH criterion generate a high number of risky days. After the water

leakage problem was fixed, no mold occurrences were observed in the federal building. It could be concluded that it is plausible that the mold germination method gives better estimation of mold assessment than the 80% RH criterion.

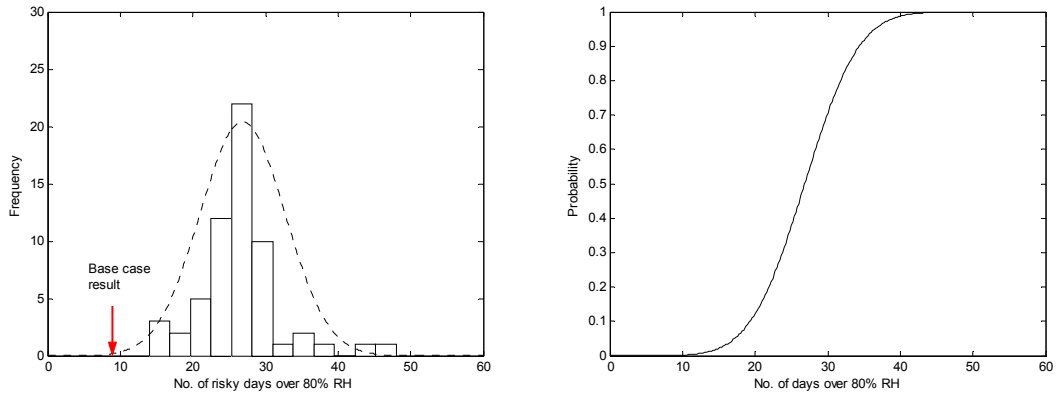

(a) (b)

Figure 6.13 Uncertainty propagation result for the federal building using the 80% RH criterion (a) Distribution of the performance indicator from the Latin Hypercube sample size of 60. (b) Cumulative density function of the performance indicator

6.2.4 Identification of dominant parameters

Since the mold germination graph method did not result in any risk, the 80% RH criterion was used for the identification of dominant parameters using the Morris method and procedures. For each parameter, five independent samples of the elementary effects were assessed. Figure 6.14 and Table 6.8 show the top four dominant parameters from the sensitivity analysis, which account for over 80% of total variance. These four parameters accounted for about 84% of the total variance.

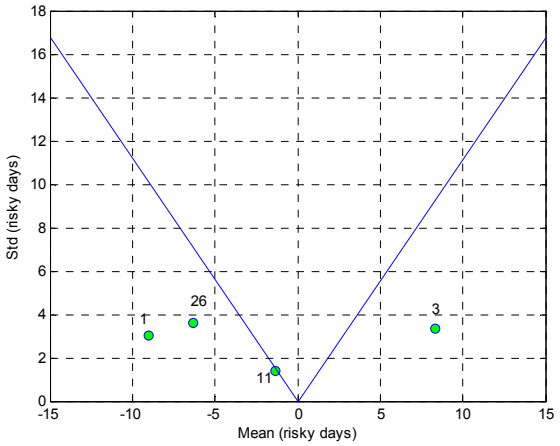

Figure 6.14 Ranking results for top 4 dominant parameters using 80% RH criterion in the federal building case (Parameters 26 Run 5)

Table 6.8 Top 4 dominant parameters which explain 80% of the total variance using the 80% RH criterion in the federal building case

Ranking	**Parameters**	**Index**
1	Outside air flow rate (m^3/s)	1
2	Minimum RH delta (%)	3
3	Temperature factor	26
4	Concrete: heat conductivity	11

The results show that three dominant parameters (i.e., the outside air flow rate, the temperature factor, and the concrete heat conductive coefficient) have a negative correlation with mold growth risk. From information about the dominant parameters and each correlation in this particular case, suggestions for reducing mold risk can be made. First, the temperature factor is one of the dominant parameters with a negative correlation, which means poor thermal insulation increases the total variance of mold risk. Thus, one needs to design the building with higher performance of thermal insulation at the corners

to reduce thermal bridge effects. Second, introducing higher outside air flow rates through the HVAC system will also reduce mold growth risk. In this particular case, appropriate levels of outdoor air supply should be introduced. Obviously, it is also confirmed, from the minimum relative humidity delta, that the building should be maintained at a lower relative humidity setting with a small offset.

6.3 CASE 3: INTERIOR CORNER SURFACE IN A DORMITORY BUILDING

The third case is an existing dormitory building that was constructed in 1972 as shown in Figure 6.15. This building has experienced mold infestation on the surface of exterior corner walls for many years. Although the building management team removes mold on the walls by using a spray application, mold has occurred in heating season and cooling season repeatedly. Corner rooms have shown most extreme mold growth, while the middle rooms have not. Figure 6.16 shows a picture of mold infestation in one of the corner room. The developed mold growth analysis method was tested for the heating season (October to March) to see whether it shows increased mold growth risk in this particular mold problem case.

Figure 6.15 Picture of the dormitory building in Atlanta

Figure 6.16 Mold infestation in the dormitory building

6.3.1 Building model and design conditions

The building is located on a university campus in Atlanta which has a mixed humid climate. Figure 6.17 shows the room (3.4m×5m×3m) of the building that was modeled. The location of concern for mold growth is highlighted. Table 6.9 summarizes the building construction and material data. The exterior walls are composed of brick, air gap, and concrete block without insulation. Two persons share the room. Due to the lack of an occupancy profile in the dormitory environment, it is assumed that two people occupy the room from 18:00 to 9:00 and one occupies it during the daytime. A common space is located in the center of the floor, where a shower facility, a kitchen, and the bathrooms are located.

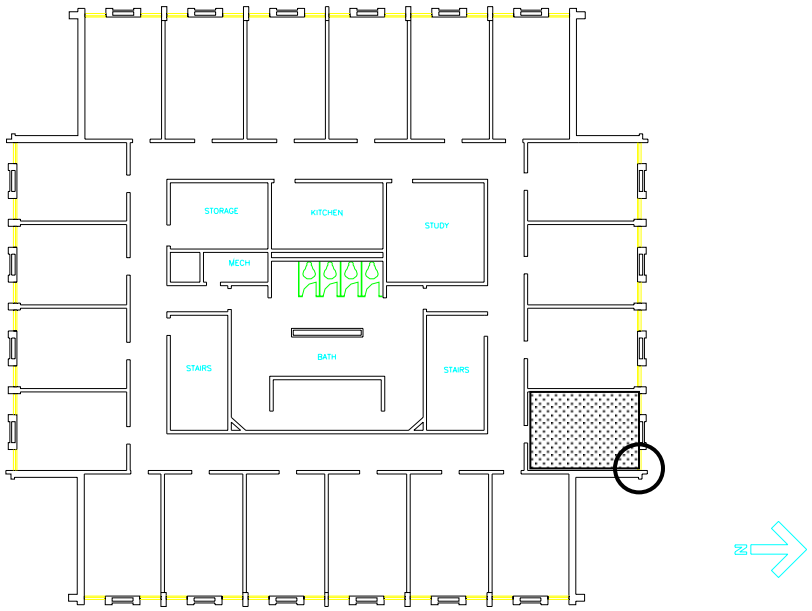

Figure 6.17 Plan of the building and the room under consideration

Table 6.9 Construction and materials

Building components	**Layers**	**Roughness**	**Thickness (m)**
Exterior wall	Brick	Rough	0.1
	Air gap	Very Smooth	0.05
	Concrete Block	Medium Rough	0.152
Floor	HW Concrete	Medium	0.2
Roof	Roofing Shingle	Rough	0.01
	HW Concrete	Medium	0.2
Partition	Concrete Block	Medium Rough	0.152

The room is equipped with a fan coil unit (FCU) that provides heating in winter and cooling in summer. The FCU is a two-pipe system so that the supply temperature cannot be adjusted. Although users can turn on or off the system, the university provides either hot or cold water by the season. The FCU is designed to provide 300 CFM without

introducing outdoor air. Since no thermostat control is available, the schedule of the FCU operation was derived from an interview with the manager of the building. As a result, it is reasonable to assume that the users run the FCU according to the occupancy schedule. A two-pipe FCU system was modeled in EnergyPlus.

In this specific case study, the only indoor moisture source in each room is limited to the occupants. Shower activity in the common space is modeled as a moisture source in the mixed simulation. A detailed description of the building data and an hourly profile of the occupancy schedule can be found in Appendix C.

6.3.2 Values of the parameters for the base case and range

Infiltration and crack flows are considered in the analysis along with heat and moisture transfer. The calculation results for the air mass flow coefficient (Cs) and wind pressure coefficient are presented in Appendix C in detail. The KOBRA simulation gives a result of the temperature factor of 0.81 at the inside corner of the exterior wall (the trouble spot). This value corresponds to an uncertain range of 0.53 ~ 0.67 as shown in Figure 5.13. Table 6.10 shows the 21 selected parameters with base values and the lower and upper values that quantify the uncertainty from the study of the quantification of uncertainty as described in previous chapters. Due to the lack of available data for porosity, diffusion resistance, and the moisture storage function of concrete blocks, these parameters were not included in the uncertainty analysis.

The mixed simulation runs for six months during the winter season in the Atlanta climate. The mold growth conditions at the trouble spot were analyzed under uncertainty similar to that in the other case studies.

Table 6.10 Uncertain parameters and their upper and lower values

	Parameters	**Base**	**Min**	**Max**	**Remarks**
1	External convective heat transfer coefficient(W/m^2K)	18	9	27	At 2 m/s of the surface-parallel flow velocity (De Wit 2001)
2	Internal convective heat transfer coefficient(W/m^2K)	2.4	1.59	3.21	at $\Delta T = 2°C$ (De Wit 2001)
3	Air mass flow coefficient (Cs) (Crack, Wall)	0.001 * COMIS default	0.0009	0.0048	Based on school buildings in table 5.2
4	Discharge coefficient for opening factor (-)	0.675	0.6	0.75	See Ch. 5.3.4 Infiltration
5	Cp value (South façade)	-0.37	-0.37	-0.08	Base values from ASHRAE (2001b) See Appendix C for upper/lower values (Values at 0 degree)
6	Cp value (North façade)	0.6	0.31	0.6	
7	Cp value (West façade)	-0.56	-0.56	-0.17	
8	Cp value (East façade)	-0.56	-0.56	-0.17	
9	Wind velocity profile exponent (α)	0.18 *COMIS default	0.22	0.28	Table 5.4
10	Moisture source room (g/h)	29 (20.02)	27 (18.68)	31 (21.36)	See Appendix C Values at 0:00 AM Values in () with unit of W
11	Moisture source: common space (g/h)	83.25 (57.9)	41.5 (28.3)	125 (86.8)	See Appendix C Values at shower Values in () with unit of W

Table 6.10 (continued)

12	Brick: density (kg/m^3)	1650	1100	2150	See table 5.8
13	Brick: porosity (m^3/m^3)	0.41	0.11	0.41	
14	Brick: heat capacity (J/kg K)	850	830	920	
15	Brick: heat conductivity (W/m K)	0.6	0.397	1.08	
16	Brick: diffusion resistance (-)	9.5	8	17	See figure 5.7
17	Brick: moisture storage function (kg/m^3)	370	192.06	370	See figure 5.7 Value at RH = 1
18	Concrete block: density (kg/m^3)	664	609	1362	See Appendix C
19	Concrete block: heat capacity (J/kg K)	850	837	850	
20	Concrete block: heat conductivity (W/m K)	0.14	0.14	1.037	
21	Temperature factor (-)	0.81	0.53	0.67	See figure 5.11 Base value is a result of KOBRA

6.3.3 Distribution of the performance indicator

In the uncertainty analysis, Latin Hypercube Sampling with a sample size of 60 was conducted in the mixed simulation approach. Figure 6.18 shows the results of the distribution of the performance indicator for the heating season using the germination graph method. The maximum available value for mold growth risky days is 182 (October to March). The mean value of risky days is 33.7 and the standard deviation is 88.7, with

median value of 11.5. In this analysis, variation is significant as the coefficient of variation ($C_v = \sigma/\bar{X}$) is around 2.63.

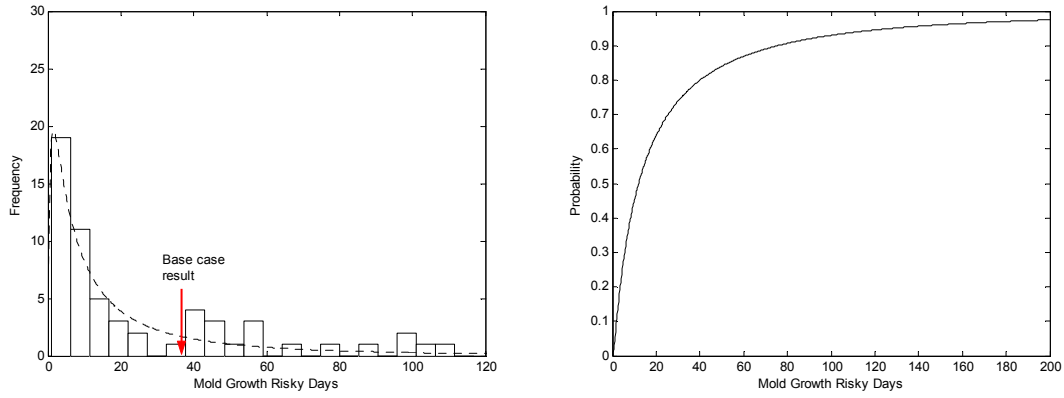

(a) (b)

Figure 6.18 (a) Histogram and (b) cumulative density function of the performance indicator using the germination graph method with Latin Hypercube sample size of 60.

The uncertainty propagation results showed mold growth risks in all 60 samples, ranging from 1 to 110, which predict, theoretically, some level of mold growth in all possible combinations of uncertain parameters in this particular case. As in the reference office building case, the distribution in Figure 6.18 shows a long tail that indicates possible severe mold occurrence. The possibility of severe mold occurrence is much greater than the reference office building case. The analysis with the base parameter values resulted in 38 risky days, which is close to the mean value but considerably higher than the median of the distribution that resulted from the uncertainty analysis.

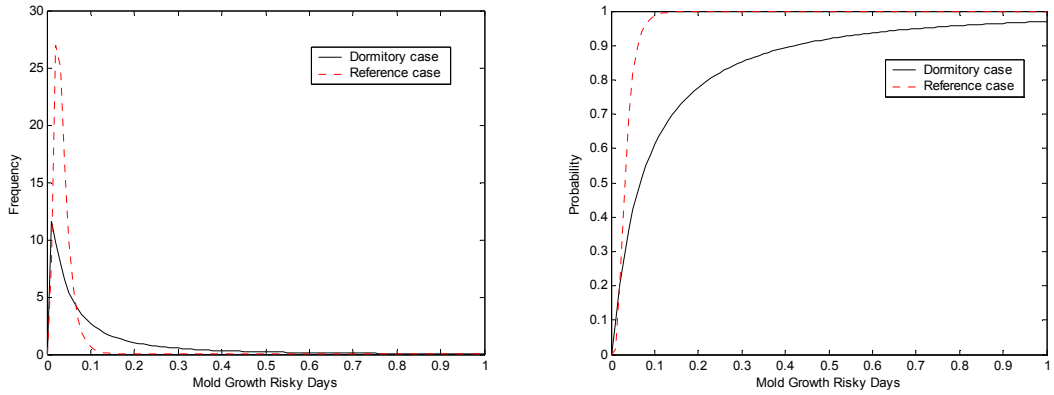

(a) (b)

Figure 6.19 (a) Distributions and (b) cumulative density functions of the normalized performance indicator for the dormitory case and the reference office building case

Figure 6.19 shows the distribution of the performance indicator for the two building cases that showed some levels of mold growth risk, which are the dormitory case and the reference building case (the first case study). The normalized performance indicator [0, 1] is used to compare the both results. From the figures above, the dormitory case shows much higher probability of possible severe mold occurrence than the reference building. The results of the cumulative density function show that the reference case will not exceed 0.1 of the normalized performance indicator in all possible combination of uncertain parameters. However, in the dormitory case, severe mold growth risk that reaches to 1.0 exists with low possibility. This analysis provides a plausible explanation for why the dormitory building had experienced mold problems persistently.

Although a concrete block wall in the dormitory building is not a good nutrient source for mold growth, contamination of dust on the surfaces and other deposits provide enough nutrient sources for mold spore to germinate. This may delay actual mold

occurrence in the problem spot, but mold can eventually recur if no changes to the building systems or building usage are made. The effect of different scenarios can be tested against the building model to find appropriate building operation schedules or retrofit.

6.3.4 Identification of dominant parameters

Figure 6.20 and table 6.11 show the result of the sensitivity analysis using the mold germination graph method. The top three dominant parameters were identified and shown in the figure including air mass flow, temperature factor, and a pressure coefficient. All three dominant parameters show negative correlations with mold risk.

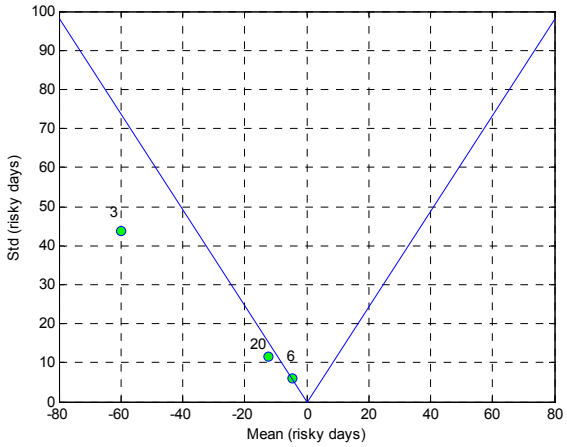

Figure 6.20 Ranking results for the top three dominant parameters using the mold germination graph method in the dormitory case

Table 6.11 The top three dominant parameters using the mold germination graph method in the dormitory case

Ranking	Parameters	Index
1	Air mass flow coefficient (Cs) (CRACK)	3
2	Temperature factor	20
3	Cp north	6

The results of the dominant parameters reveal that a lower infiltration rate (due to a negative correlation with the air mass flow coefficient) account for a significant amount of total variance of mold risk. The effect of air mass flow coefficient can be reduced by introducing direct outside air into the room. Opening windows can be an efficient way to reduce mold growth risk. After the building has experienced mold infestation, it was observed that the occupants intentionally open windows based on their experiences. The developed performance indicator indeed confirms that opening windows helps to reduce mold growth risk. However, rooms with closed windows during the heating season (e.g., an empty room) will still have increased mold growth risk.

The temperature factor is also one of the dominant parameters, which has a negative correlation with mold growth risk. Since the exterior wall does not have insulation inside the cavity, it contributes to mold growth during the heating season, especially at thermal bridge locations. Putting insulation material on the interior surface of the exterior wall may reduce the mold growth risk. However, special care should be taken to select and locate insulation materials.

Similar results can be found in the case of 80% RH criterion as well, as shown in figure 6.21 and table 6.12. Same three dominant parameters were identified from the previous result with same ranking.

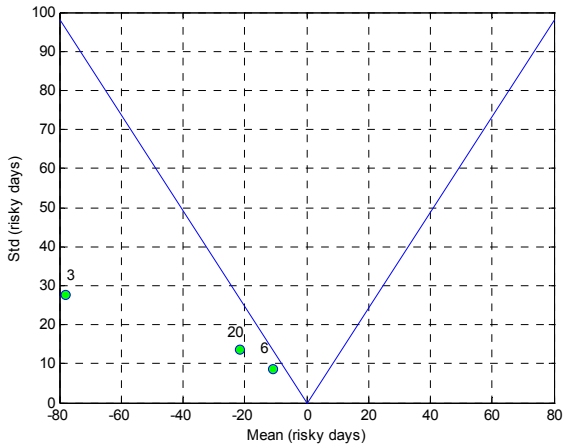

Figure 6.21 Ranking results for the top three dominant parameters using 80% RH criterion in the dormitory case

Table 6.12 The top three dominant parameters using 80% RH criterion in the dormitory case

Ranking	Parameters	Index
1	Air mass flow coefficient (Cs) (CRACK)	3
2	Temperature Factor	20
3	Cp north	6

6.4 DISCUSSION AND PRACTICAL IMPLICATIONS

The new probabilistic mold risk indicator (MRI) was applied to three case studies. In each case, the MRI was capable to explain (partly unexpected) mold growth occurrences in buildings based on its probability over mold growth risky days. Moreover, it identified the parameters with dominant effects on the increase of uncertainty of the result (mold risk). The latter provides crucial information for designers and engineers to

guarantee better building performance. A number of conclusions from the case studies can be drawn:

1) The MRI approach looks promising as a more realistic prediction of mold risks going beyond the deterministic assessment. The deterministic evaluation was shown to fail to give conclusive indication for mold growth risk. The probabilistic evaluation under uncertainty provides relatively significant mold growth risks for the case where there is indeed a mold problem (the dormitory case).

2) The similarity of the resulting dominant parameters using two different mold risk criteria is encouraging. Both the germination graph and 80% RH criteria was able to identify similar dominant parameters with similar ranks for the cases with mold problems. Although further calibration of both distributions on a larger set of real cases is required, the mold germination graph method provided more power to explain mold growth risk with bigger variation and lognormal profile. The 80% RH criterion can be used as a surrogate method to identify dominant parameters in case no mold risk is observed using the MRI (the federal office case).

3) The identification of the parameters that have a major influence on mold risk can provide useful information for early mold risk control, i.e. during design, commissioning and A/E/C procurement. This post analysis helps to indicate the factors that require additional attention to reduce mold growth risks. Each building case has different building parameters, since the results of the dominant parameters are very case specific, i.e. specific to the chosen trouble spot, particular building, locations, HVAC operation schedule, and so on. The developed approach was able to make

recommendations for each case based on the identified dominant parameters and their correlations with the mold growth risk that was found.

Table 6.13 Summary of the results and recommendations for each case study

	Case 1 **(a reference office building)**	**Case 2** **(a federal office building)**	**Case 3** **(a dormitory building)**
Trouble spot	Interior corner wall	Interior corner wall	Interior corner wall
Mold problems	Unknown	No (without water leakage)	Yes
MRI results	Relative mold risk	No	Yes (relative mold risk)
Dominant parameters and correlation	Air mass flow coefficient (-) Moisture Source (+) External convective heat transfer coefficient (+) Wind exponent(+) Insulation conductivity (-)	* Outside air flow rate (-) * Minimum RH delta (+) * Temperature Factor (-) * Concrete: Heat conductivity (-)	Air mass flow coefficient(-) Temperature factor (-) Cp north (-)
Recommendations	Change HVAC operation schedule (no HVAC shutdown)	N/A	Open windows Add insulation in the exterior walls

* Results using 80% RH criterion

Table 6.13 summarizes the analysis results and recommendations made for each case. In the cases 2 and 3, the MRI results show good agreement with actual mold problems at the trouble spot. The identified dominant parameters are different in all three cases. This confirms that mold growth risk is very case specific depending on the location of concern (the trouble spot), building specifications, and the scenario. Thus, the recommendations are made differently for each case as well, based on the identified dominant parameters and correlations.

The case studies have conducted uncertainty analyses with a crude range of uncertainty for each parameter. For a more rigorous uncertainty analysis, an iterative process should be applied in the MRI quantification. The identified dominant parameters are the best candidates for refining uncertainty further, i.e. through a deeper analysis of the source of uncertainty or by studying randomly selected samples. However, this thesis does not attempt to refine the uncertainty of dominant parameters at this stage of the research. Before we establish an iterative process, the MRI results under uncertainty should be calibrated against real mold cases, using statistical techniques to provide confidence intervals related to false negatives and false positives of the MRI.

CHAPTER 7

EVALUATION

7.1 EVALUATION

In the building industry, neither a performance indicator nor performance criteria for mold growth risk have been established. This study has taken a radically different approach by establishing a mold risk indicator expressed as a probability distribution. This approach holds promise to lead to a performance criterion for mold that could be enforced throughout the life cycle of a facility. The mold risk indicator can be regarded as a major step forward, since all buildings and subsystems have some extent unexpected behavior and deviation from design specifications are unavoidable, thus contributing to unexpected behavior in a building.

This study treats mold as a risk related to a limit state phenomenon, the limiting criterion being defined as the moment that mold germination occurs. The probability that this occurs is expressed as the number of risky days. Mold germination graphs are used for this purpose as they identify the number of mold growth risky days using environmental conditions that are determined by hygrothermal simulations as input. A comparative study using the mold limitation curves in ESP-r showed that the mold germination graph method could provide quantitative evaluation results in terms of mold growth risk.

The current standard simulation functionality was extended to account for additional mechanisms that affect the mold growth phenomenon. Based on the identified

four cause categories, this study utilized a mix of existing "best of breed" simulation tools, each specialized in a particular domain of heat, air, and moisture transport. By mixing the temperature factor at certain building details in the mixed simulation approach, the mold growth risk can be approximately represented at any chosen trouble spot.

Using uncertainty analysis, the new mold risk indicator (MRI) accounts for the effect of the uncertainty in a large set (theoretically the entire set) of building and operation parameters on the mold risk. This requires the quantification of uncertainties in these parameters, in fact quantifying the chance that a certain deviation between the "as-designed" values and the actual "in-use" values of the parameters will occur. The uncertainty of each building parameter is expressed as upper/lower values with a probability distribution based on theoretical models and/or data analyses from the available literature. The uncertainty associated with the temperature factor, which accounts for the thermal bridge effect and bad workmanship in a particular building construction technology, was investigated by establishing an empirical relationship between an idealized thermal bridge and potential bad workmanship. This study focused on a cavity wall construction technique and an exterior wall corner as a thermal bridge.

This approach is the first to produce a probabilistic performance indicator for mold growth risk that evaluates relative mold risk at any chosen trouble spot in a specific building case. In three case studies, the MRI successfully determined relative mold risks. Moreover, by using the Morris method for the identification of dominant parameters, the MRI provides a long-awaited breakthrough for early mold risk control, i.e., during design, commissioning, and A/E procurement. The developed MRI also provides a foundation for developing a normative performance indicator for mold growth risk and could lead to

eventually establishing a building performance criterion that prevents mold in different types of buildings.

In current practice, mold risk evaluation is rarely performed in the design stage or in the operation stage of a building as the only standard available method is to use deterministic hygrothermal models without consideration of uncertainty in building parameters. Introducing the developed MRI in practice could lead to a substantial breakthrough in so called performance contracting. The MRI and the knowledge about dominant parameters enable building partners to verify these minimum levels of performance to keep mold risk below allowed levels. Performance-based contracts can consequently make specific provisions that a building component performs to a certain minimum level. These provisions in performance contracts would not only govern the A/E/C procurement but would also be an ideal instrument to settle litigation when mold occurs. Once the performance criterion is defined, the performance of building components or materials can be assessed and selected in the design process to meet the goal. For example, in the case that an air mass flow coefficient is identified as a dominant parameter with positive correlation, the designer can ask a certain façade system that ensures the minimum level of crack flow with small uncertainty. The developed MRI will enhance and facilitate performance-based approach in building industry.

7.2 LIMITATIONS

Although the MRI has successfully been tested in three building cases and is able to explain unexpected and non-deterministic mold growth occurrences at a specific trouble spot, certain restrictions apply:

- The MRI evaluates mold risk based on the worst case of mold germination: Fungal spores require different minimum environmental conditions to germinate, depending on mold species (e.g., xerophilic or hygrophilic). Some fungi species are involved in producing mycotoxins, and considered toxic to occupants. This study does not consider the classification of fungal species based on requirements or health effects, and it always assumes the worst case, which indicates that mold germination in buildings should be treated as a risk regardless of the type of fungal spores. After all, in building practice, one cannot simply guess which type of fungi species exists in a building. Even fungal species that are neither toxic nor harmful to occupants can damage structures and decrease the economic value of the building. Although nutrients on the substrates are a critical condition in which mold germinates and grows, the required surface contaminations and deposits are in reality almost always possible and sufficient for mold to grow. By using the standard mold germination graph based on the optimum media, which represents the worst case, the MRI provides conservative results for mold risk and therefore prompts preventive actions that reduce mold growth and its impact on human health.

- The mold germination graph method does not account for all fungal species: The fungal species that germinate and grow outside the favorable

conditions of the standard germination graph cannot be accounted for with the current approach. The standard germination graph represents only common indoor fungal species. If specific species are of concern in the mold growth analysis, one can replace the standard germination with one developed for that specific fungal species and the specific building materials substrate that is present at the selected trouble spot..

- The mixed simulation approach does not cover building defects: acute failures in building systems, such as a water leak from a broken pipe, are some of the main "special" causes for mold problems in existing buildings. Such defective building performance cannot be predicted in the current simulation capacity and is thus beyond the scope of this study. However, the developed performance indicator that involves practical issues, including rain penetration, pressurization of buildings, and moisture migration from a foundation, can be extended. Another way to approach catastrophic events is to introduce them through special scenarios that could be used to conduct the mold assessment. The development of these scenarios and additional mechanisms that take these issues into account remains a subject for future work.

- The MRI evaluation provides case-specific results: Each building is unique in its specific location, client and operation. Furthermore, the MRI can only be quantified for a specific trouble spot that is governed by its

detailed physical location and environmental. The use of the evaluation model is therefore always case-specific and employs a specific set of building parameters depending on the governing mechanisms for the local environmental conditions and the scenarios that impact on it. The uncertain ranges of each parameter also vary in particular building types, locations, HVAC operation schedule, and so on. Therefore, the distribution of mold risks and the results of the dominant parameters at a trouble spot relate only to the specific case that is being studied. One can rightfully ask whether it is realistic to assume whether the assessment of uncertainties and subsequent simulation and analysis is worth the effort in every specific case. It will be necessary to generate more generic recommendations, and this will be one of the thrusts for future work. It may be possible to derive generalized recommendations per combination of building type and construction technology, located in a specific climate zone with similar building usage pattern. This could for instance lead to generic recommendations for manufactured houses in a hot and humid region. This is a fruitful area of research that should be surveyed after the MRI approach has proven its usefulness on a broader set of cases and common patterns of mold risks become visible.

CHAPTER 8

CONCLUSIONS AND FUTURE WORK

8.1 CONCLUSIONS

Microbial growth in indoor living spaces is now regarded as the single greatest threat to human health and long-term building performance. This study has developed a probabilistic performance indicator for mold risk under uncertainty (MRI) and provided a foundation for the performance-based regulation of mold risk. The main achievements of this study are addressed below.

- Quantified mold growth risk assessment: The developed performance indicator is able to quantify the risk of mold growth based on extended hygrothermal models and the standard mold germination graph method. Quantified mold risks in different building cases (trouble spots) and scenarios can now be compared. This helps designers and building engineers select the most appropriate building materials, subsystems, and operation schedules that lessen the risk of mold risks and guarantee better building performance.

- Probabilistic mold growth risk beyond the deterministic assessment: The phenomenon of mold involves intrinsic complexity and non-linearity among building parameters, such as an imperfect building envelope and the details, workmanship, and natural variation of hygrothermal properties

in building materials, HVAC operation and building usage, occupants' behavior, and indoor moisture generation. The developed MRI incorporates these uncertain building parameters into the mixed simulation approach and shows the total variance of mold growth risks resulting from combinations of the uncertain parameters.

- Identification of dominant parameters: The identification of the parameters provides critical information that can be used to control early mold risk, i.e., during design, commissioning, and A/E/C procurement. This analysis indicates the factors that require additional attention in the effort to reduce the risk of mold growth.

In conclusion, the new performance indicator for mold risk can successfully determine actual mold occurrences that would remain hidden from standard deterministic assessment. The identification of the parameters that have a major influence on mold risk can provide the long-awaited breakthrough for early mold risk control. The developed performance indicator provides a foundation for establishing building performance criteria that could be regulated to prevent mold in different types of buildings.

8.2 FUTURE WORK

This thesis has provided a foundation for developing a normative risk-based performance indicator and regulation embedded performance criteria for mold risk. In

the future, a more practical MRI can be developed with simplified mechanisms and a limited set of uncertain parameters. The remaining future work is listed below:

1) Calibration of the MRI within a set of buildings

Although the MRI has been tested on three building cases, extensive calibration needs to be conducted on a set of buildings with existing mold problems and another set without mold. The application of the MRI to the selected buildings and trouble spots will reveal the distribution of mold risks in various building types (e.g., office buildings, homes, hotels), scenarios, and climate zones. Based on these results, the selection of uncertain parameters and the range of each parameter can be adjusted for correct evaluation. If further refinement is required for the quantification of uncertainty of the dominant parameters, additional methods, such as the ones based on expert judgment study, as described in De Wit (2000), will be deployed.

2) Consolidation of the mixed simulation tools

The current mixed simulation approach requires that separate modules be harnessed in a single application for better robust applicability. The separate modules in this thesis were developed based on the requirements of each step, including heat, air, and moisture transport, random sample generation and propagation, sensitivity analysis, and so on. The development of a single application that internally links the current steps will facilitate interactions between modules and will allow uncertainty analyses by non-experts. This will lead to a rapid and robust tool for uncertainty analysis of mold growth.

The module interface can be constructed by extending the current research version based on Matlab.

3) Development of performance criteria

The MRI provides relative mold growth risk rather than absolute risk. Since no clear criterion between mold-free buildings and mold-problem buildings has been established yet in terms of mold growth risky days, further research is required to set practical performance criteria (or a target value). Before the mold risk indicator can be used as the basis for new regulations, a method of associating the probability density function of the mold risk indicator with an absolute mold risk must be developed This can be done by creating a sample set of realized building cases, some of which have evidence of mold. Calibration will be used to determine the best predictors (e.g., expected mean, variance, 2^{nd} moment) of actual mold based on the ANOVA technique. These predictors will then be used to develop the mold criterion. In line with the interpretation of mold as a limit state phenomenon, the mold criterion will be developed following proven methodologies for the development of structural safety criteria. An important aspect of this phase of the research is the orthogonality test on location, building type, and scenario type. Based on this test, the validity of the absolute criterion across different climates and technologies can be determined. In each individual case, the developed criterion will then be applied to the mold risk indicator distribution. The result can be expressed as a “pass” or “fail.”

4) Development of a normative performance indicator

This thesis provides a foundation for achieving a normative risk-based performance indicator. Calibration of the MRI with selected sets of buildings will reveal the dominant parameters and uncertain ranges of building parameters for each type of building, scenario, and climate zone. Within the identified set of parameters, a deterministic value that increases mold risk most in each parameter range is selected for normative calculation procedures based on the parameter estimation study. This approach will enable direct performance evaluation by utilizing the set of parameters and predefined values. The normative PI will give an indicative performance evaluation result and enable comparison with the performance criteria in a selected level of objective.

5) Guidelines for each climate and building type

As a consequence of the above performance criteria for mold growth risk, guidelines and recommendations for designers, engineers, and facility managers can be developed to ensure a mold-free environment in different building types and climate zones. The results of identified dominant parameters for each case can be aggregated and analyzed to generalize the overall importance of building parameters in each building type and climate. Appropriate building operation schedules can be developed to reduce mold growth risks in organizational institutes, such as the P-100 of the General Services Administration (GSA) (U.S. GSA 2003).

6) Extension of simulation capacity and translation into practice

The developed performance indicator evaluation may be extended to include practical issues, including rain penetration, deviating flow calibration and pressurization of buildings, air flow patterns at specific locations, moisture migration from a foundation, and so on. However, this can only be accomplished if additional mechanisms are developed to account for these issues in the current approach. The coupling of additional mechanisms is non-trivial work. In the case of a room with furniture that is an obstacle to airflow, a CFD study may reveal the relationship between mold growth risks and airflow patterns or air velocity at a local material surface. Detailed information on airflow near walls may affect the moisture diffusion coefficient and increase or decrease the range of the coefficient. The result of the mold risk indicator can also be compared with other performance evaluations such as thermal comfort and energy consumption of a building. This study will thus make a contribution to ensuring healthy, comfortable, and energy efficient building design.

APPENDIX A

A REFERENCE OFFICE BUILDING

Scenario of the Reference Case

Table A.1 Indoor design conditions

Season	**Environmental conditions**		**Control deviation**	**References**
Heating	Temperature	20°C	±2°C	(ASHRAE 1999b; 2000; McQuay 2001)
	RH	Minimum 45%	±10%	
Cooling	Temperature	20°C	±2°C	
	RH	Minimum 45%	±10%	

Uncertain Parameters

Table A. 2 Wind pressure coefficients of the south facade from different calculation methods and literature

Calculation Methods	**Façade**	**Wind direction angle(deg)**											
		0	30	60	90	120	150	180	210	240	270	300	330
ASHRAE (ASHRAE 2001c; DOE 2004b)	North	0.6	0.48	0.04	-0.56	-0.56	-0.42	-0.37	-0.42	-0.56	-0.56	0.04	0.48
	East	-0.56	0.04	0.48	0.6	0.48	0.04	-0.56	-0.56	-0.42	-0.37	-0.42	-0.56
	South	-0.37	-0.42	-0.56	-0.56	0.04	0.48	0.6	0.48	0.04	-0.56	-0.56	-0.42
	West	-0.56	-0.56	-0.42	-0.37	-0.42	-0.56	-0.56	0.04	0.48	0.6	0.48	0.04
COMIS (Feustel 1997) *Surface-average calculation	North	0.60	0.47	0.12	-0.46	-0.73	-0.45	-0.45	-0.45	-0.73	-0.46	0.12	0.47
	East	-0.43	0.12	0.47	0.60	0.47	0.12	-0.43	-0.63	-0.33	-0.29	-0.33	-0.63
	South	-0.45	-0.45	-0.73	-0.46	0.12	0.47	0.60	0.47	0.12	-0.46	-0.73	-0.49
	West	-0.43	-0.63	-0.33	-0.29	-0.33	-0.63	-0.43	0.12	0.47	0.60	0.47	0.12

Table A.2 (continued)

Sohn & Sextro (2003)	North	0.2~0.9			-0.5~-0.9			-0.2~-0.6			-0.5~-0.9		
	East	-0.5~-0.9			0.2~0.9			-0.5~-0.9			-0.2~-0.6		
	South	-0.2~-0.6			-0.5~-0.9			0.2~0.9			-0.5~-0.9		
	West	-0.5~-0.9			-0.2~-0.6			-0.5~-0.9			0.2~0.9		
CPCALC+ (Grosso 1995)	North	0.02	0.01	0	-0.22	-0.16	-0.01	-0.1	-0.1	-0.16	-0.22	0	0.01
	East	-0.23	0	0.01	0.01	0.01	0	-0.23	-0.16	-0.1	-0.1	-0.1	-0.16
	South	-0.1	-0.1	-0.16	-0.22	0	0.01	0.02	0.01	0	-0.22	-0.16	-0.1
	West	-0.23	-0.16	-0.1	-0.1	-0.1	-0.16	-0.23	0	0.01	0.01	0.01	0

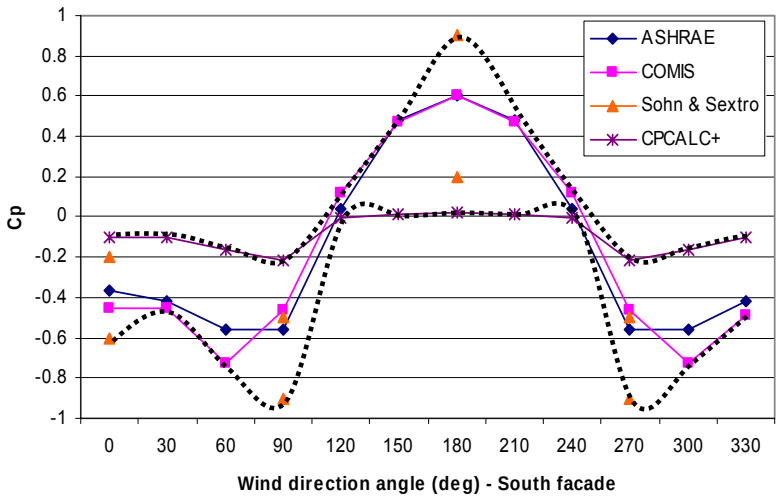

Figure A. 1 Wind pressure coefficients as a function of wind direction angles – south facade

APPENDIX B

A FEDERAL OFFICE BUILDING

Scenario of the Federal Building

Table B. 1 Indoor design condition

Season	**Environmental conditions**		**Control deviation**	**References**
Heating	Temperature	24°C	± 1.5°C	building operation data
	RH	Minimum 55%	±10%	
Cooling	Temperature	24°C	±1.5°C	
	RH	Minimum 55%	±10%	

Table B. 2 Indoor moisture loads for the case study

Moisture sources	**Moisture generation**	**Hourly profile**	**Remarks**
4 persons (light activity)	120 ~ 240 [g/h]	Same as occupancy schedule	30~60 [g/h · person]
Plants 1 ea.	1.6~4.2 [g/h]	24 hours	1.6~4.2 [g/h]

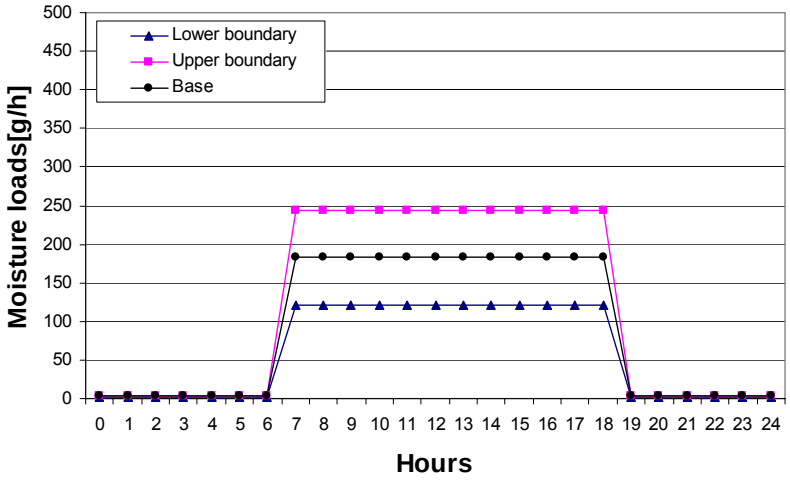

Figure B. 1 Hourly profile of the moisture generation

Uncertain Parameters

Table B. 3 Hygrothermal properties for Concrete and wall paper

Material properties	**Concrete**			**Wall paper**
	Base	Lower boundary	Upper boundary	
Density [kg/m^3]	2200	2100	2300	471
Porosity [m^3/m^3]	0.18	0.15	0.18	0.001
Heat capacity [J/kg K]	850	837	940	2300
Heat conductivity [W/mK]	1.6	1.16	2	23
Diffusion resistance [-]	92	92	248	200
Moisture storage function (at 100% RH)	175	147	175	0

* Hygrothermal property data from: (De Wit 2001; DOE 2004a; Kumaran 1996; Kumaran 2002; Kunzel, Karagiozis 2000)

Table B. 4 Moisture storage function for Concrete

Rel. Humidity	Base	Lower boundary	Upper boundary
0	0	0	0
0.33	23	23	37
0.43	26	26	45
0.63	44	44	78
0.8	53	53	90
0.93	85	85	120
1	175	147	175

* Data collected from (Kumaran 1996; Kunzel, Karagiozis 2000)

APPENDIX C

A DORMITORY BUILDING

Scenario of the Dormitory Building

Table C. 1 Indoor moisture loads for the case study

	Moisture sources	**g/h**	**Hourly profile**	**Remarks**
Room	2 persons (light activity)	60 ~ 120 [g/h]	occupancy schedule	30~60 [g/h · person]
Common space	Shower	41.5~125 [g/h]	7~9 AM 18~20 PM 5 persons/hour	8.3~25 [g/h]

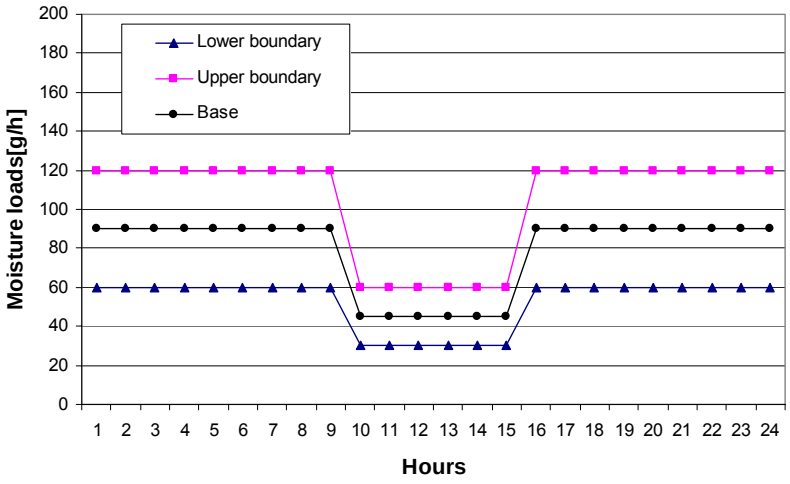

Figure C. 1 Moisture generation from a room

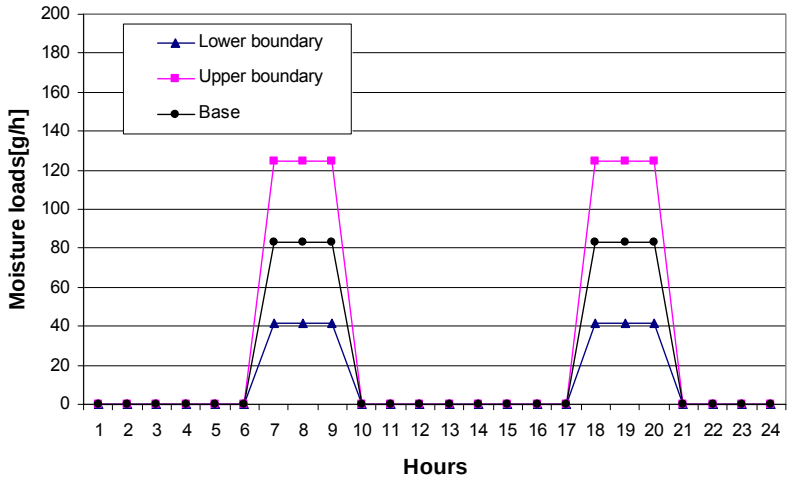

Figure C. 2 Moisture generation from the common space due to shower activity

Uncertain Parameters

Table C. 2 Wind pressure coefficients of the facades from different calculation methods

Calculation Methods	**Façade**	**Wind direction angle(deg)**											
		0	30	60	90	120	150	180	210	240	270	300	330
ASHRAE (ASHRAE 2001c; DOE 2004b)	North	0.6	0.48	0.04	-0.56	-0.56	-0.42	-0.37	-0.42	-0.56	-0.56	0.04	0.48
	East	-0.56	0.04	0.48	0.6	0.48	0.04	-0.56	-0.56	-0.42	-0.37	-0.42	-0.56
	South	-0.37	-0.42	-0.56	-0.56	0.04	0.48	0.6	0.48	0.04	-0.56	-0.56	-0.42
	West	-0.56	-0.56	-0.42	-0.37	-0.42	-0.56	-0.56	0.04	0.48	0.6	0.48	0.04
COMIS (Feustel 1997) *Surface-average calculation	North	0.60	0.47	0.12	-0.44	-0.68	-0.39	-0.36	-0.39	-0.68	-0.44	0.12	0.47
	East	-0.44	0.12	0.47	0.60	0.47	0.12	-0.44	-0.68	-0.39	-0.36	-0.39	-0.68
	South	-0.37	-0.42	-0.56	-0.56	0.04	0.48	0.60	0.47	0.12	-0.44	-0.68	-0.39
	West	-0.44	-0.68	-0.39	-0.36	-0.39	-0.68	-0.44	0.12	0.47	0.60	0.47	0.12
CPCALC+ (Grosso 1995)	North	0.31	0.26	-0.01	-0.17	-0.12	-0.08	-0.08	-0.07	-0.12	-0.17	-0.01	0.26
	East	-0.17	-0.01	0.26	0.31	0.26	-0.01	-0.17	-0.12	-0.08	-0.08	-0.07	-0.12
	South	-0.08	-0.07	-0.12	-0.17	-0.01	0.26	0.31	0.26	-0.01	-0.17	-0.12	-0.08
	West	-0.17	-0.12	-0.08	-0.08	-0.07	-0.12	-0.17	-0.01	0.26	0.31	0.26	-0.01

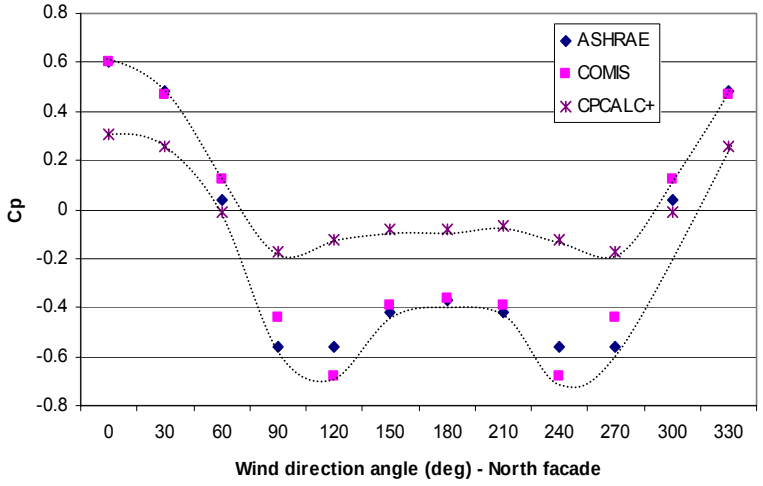

Figure C. 3 Wind pressure coefficients of the north facade from different calculation methods

Table C. 3 Upper boundary and lower boundary for building materials used for the case studies

Material properties	**Concrete Block**		
	Base	Lower boundary	Upper boundary
Density [kg/m3]	664	609	1362
Porosity [m3/m3]	0.67	0.67	0.67
Heat capacity [J/kg K]	850	837	850
Heat conductivity [W/mK]	0.14	0.14	1.037
Diffusion resistance [-]	4	4	4
Moisture storage function (at 100% RH)	175	175	175

* Hygrothermal property data collected from: (DOE 2004a; Kunzel, Karagiozis 2000)

REFERENCES

Adan, O. 1994. On the Fungal Defacement of Interior Finishes. Technische Universiteit Eindhoven, Thesis. Eindhoven, pp.233.

Angell, W. J. 1988. Home Moisture Sources, St. Paul, MN, University of Minnesota

ASHRAE. 1992. ANSI/ASHRAE Standard 55-1992, Thermal environmental conditions for human occupancy., Atlanta, American Society of Heating, Refrigeration and Air-Conditioning Engineers, Inc.

ASHRAE. 1999a. ANSI/ASHRAE Standard 52.2, Method of Testing General Ventilation Air-Cleaning Devices for Removal Efficiency by Particle Size., Atlanta, American Society of Heating, Refrigeration and Air-Conditioning Engineers, Inc.

ASHRAE 1999b. ASHARE Handbook: HVAC Applications. Atlanta, USA,

ASHRAE 2000. ASHARE Handbook: HVAC Systems and Equipment. Atlanta, USA,

ASHRAE. 2001a. ANSI/ASHRAE Standard 62-2001, Ventilation for Acceptable Indoor Air Quality, Atlanta, American Society of Heating, Refrigeration and Air-Conditioning Engineers, Inc.

ASHRAE 2001b. ASHARE Handbook. Atlanta, USA,

ASTM. 2000. ASTM E96-00, Standard Test Methods for Water Vapor Transmission of Materials,

Augenbroe, G.,Park, C.-S. 2005. Quantification Methods of Technical Building Performance. Building Research & Information.Vol. 33 (2), pp.159 - 172.

Ayerst, G. 1969. The Effect of Moisture and Temperature on Growth and Spore Germination in Some Fungi. J. stored Prod. Res.Vol. 5 pp.127-141.

Baughman, A.,Arens, E. 1996. Indoor Humidity and Human Health - Part1: Literature Review of Health Effects of Humidity-Influenced Indoor Pollutants. ASHRAE Transaction.Vol. 102 (Part 1), pp.193-211.

Becker, R. 1996. Implementation of the Performance Concept in Building-Future Research & Development Needs. Proceedings of the Applications of the Performance Concept in Building. Tel Aviv, Israel.

Ben-Nakhi, A. E. 2003. Development of an Integrated Dynamic Thermal Bridging Assessment Environment. Energy and Building.Vol. 35 pp.375-382.

BIA. 1999. Technical Notes 21A - Brick Masonry Cavity Walls - Selection of Materials, Brick Industry Association

Bornehag, C.-G., Blomquist, G., Gyntelberg, F., et al. 2001. Dampness in Buildings and Health. Indoor Air.Vol. 11 (2), pp.72-86.

BSI. 1994. BS 6676: Part 2: Thermal insulation of cavity walls using man-made mineral fibre batts (slabs) - Code of practice for installation of batts (slabs) filling the cavity, British Standards Institution

Burge, H. A. 1995. Bioaerosols. CRC Press.

Burge, H. A. 2002. An Update on Pollen and Fungal Spore Aerobiology. Journal Of Allergy and Clinical Immunology.Vol. 110 (4), pp.544-552.

Burge, H. A., Pierson, D. L., Groves, T. O., et al. 2000. Dynamics of Airborne Fungal Populations in a Large Office Building. Current Microbiology.Vol. 40 (1), pp.10 - 16.

Burnett, J. H. 1976. Fundamentals of mycology. London, Edward Arnold.

Carmody, J.,Anderson, B. 1997. Moisture in Basements: Causes and Solutions, University of Minnesota

Christian, J. 1994. Moisture Sources. Moisture Control in Buildings. H. R. Trechsel. ASTM.

CIB. 2005. PeBBu Thematic Network.(http://www.pebbu.nl/) Access: 2005/March

CIBSE (1999). Guide A: Environmental Design. Chartered Institution of Building Services Engineers.

Clark, N. M., Ammann, H. M., Brunekreef, B., et al. (2004). Damp Indoor Spaces and Health. Washington D. C., The National Academics Press.

Clarke, J. A., Johnstone, C. M., Kelly, N. J., et al. 1999. A Technique for the Prediction of the Conditions Leading to Mould. Building and Environment.Vol. 34 pp.515-521.

Clarke, J. A., Johnstone, C. M., Kelly, N. J., et al. 1997. Development of a Simulation Tool for Mould Growth Prediction in Buildings. Proceedings of the Fifth International IBPSA Conference, Vol.2, pp.343-349.

Cooke, R. M. 1991. Experts in Uncertainty. NY, Oxford University Press.

Csoknyai, T. 2001. Surface Temperature at Thermal Bridges. Journal of Thermal Envelope and Building Science.Vol. 25 pp.67-81.

Cummings, J. B., Withers, C. R., Fairey, P., et al. 1995. Indoor Air Quality Impacts of Uncontrolled Air Flow and Depressurization in Eight Commercial Buildings in Central Florida. Proceedings of the Eighth Annual Indoor Air Pollution Conference. Tulsa, OK, U.S.A.

Cummings, J. B., Withers, C. R., Moyer, N. A., et al. 1996. Uncontrolled Air Flow in Non-Residential Buildings, Cocoa, FL, U.S.A., Florida Solar Energy Center

Cummings, J. B., Withers, C. R.,Shirey, D. 1997. Controlling Ventilation and Space Depressurization in Restaurants in Hot and Humid Climates. Proceedings of the 18th Annual AIVC Conference, Vol.1, pp.153-161. Athens, Greece.

De Wit, S. 1997. Identification of the Important Parameters in Thermal Building Simulation Models. Journal of statistical computation and simulation.Vol. 57 (1-4), pp.305 - 320.

De Wit, S. 2001. Uncertainty in Predictions of Thermal Comfort in Buildings. Technische University Delft, Thesis,

De Wit, S.,Augenbroe, G. 2002. Analysis of Uncertainty in Building Design Evaluations and its Implications. Energy and Buildings.Vol. 34 pp.951-958.

Decisioneering. Crystal Ball 2000. Denver, CO.

DOE. 2004a. EnergyPlus (Datasets), LBNL

DOE. 2004b. EnergyPlus: Input and Output Reference - The Encyclopedic Reference to EnergyPlus Input and Output, LBNL

Erhorn, H.,Gertis, K. 1986. Minimal Thermal Insulation and Minimal Ventilation. Gesundheit Engineering.Vol. 107

European Commission - IPSC. 2004. SimLab 2.2 Reference Manual,

Fanger, P. O. 1970. Thermal Comfort. Copenhagen, Danish Technical Press.

FEMA 1997a. Example Applications of the NEHRP Guidelines for the Seismic Rehabilitation of Buildings (FEMA-276). Washington D.C., Federal Emergency Management Agency.

FEMA 1997b. NEHRP Guidelines for the Seismic Rehabilitation of Buildings (FEMA-273). Washington D.C., Federal Emergency Management Agency.

FEMA 2000. Prestandard and Commentary for the Seismic Rehabilitation of Buildings (FEMA-356). Washington D.C., Federal Emergency Management Agency.

Feustel, H. E. 1997. COMIS Users' Guide 3.0, Berkeley, California, LBNL

Feustel, H. E. 1998. COMIS-An International Multizone Air-Flow and Contaminant Transport Model, Berkeley, CA, U.S.A., LBNL

Feustel, H. E.,Raynor-Hooson, A. 1990. Fundamentals of the Multizon Air Flow Model - COMIS. Ineternational Energy Agency.

Fisk, W. J.,Rosenfeld, A. H. 1997. Estimates of Improved Productivity and Health from Better Indoor Environments. Indoor Air.Vol. 7 (3), pp.158-172.

Foliente, G. C., Leicester, R. H.,Pham, L. 1998. Development of the CIB Proactive Program on Performance Based Building Codes and Standards, International Council for Research and Innovation in Building and Construction (CIB)

FWCI. 2002. Mold: Cause, Effect and Response

Grosso, M. 1995. CPCALC+ Calculation of Wind Pressure Coefficients on Buildings, Turin, PASCOOL Research Programme

Hansen, A. T. 1984. Moisture Problems in Houses.(http://irc.nrc-cnrc.gc.ca/cbd/cbd231e.html) Access: 2004/June 8

Harriman, L. G. 1990. The Dehumidification Handbook. Amesbury, MA, Munters Cargocaire.

Harriman, L. G.,Nelson, B. 2001. Mold and Mildew. Humidity Control Design Guide. Harriman, Brundrett and Kittler. Atlanta, ASHRAE.

Hartwig, R. P.,Wilkinson, C. 2003. Mold and Insurance, New York, NY, Insurance Information Institute

Hens. 1999. Fungal Defacement in Buildings: A Performance Related Approach. HVAC&R Research.Vol. 5 (3), pp.265-289.

Hens, H. 1992. Moisture Problems in a Dwelling, Report 92/33, Leuven, Laboratory of Building Physics, Catholic University of Leuven

Hens, H.,Fatin, A. M. 1995. Heat-Air-Moisture Design of Masonry Cavity Walls: Theoretical and Experimental Results and Practice. ASHRAE Transaction.Vol. 2 pp.607-626.

Hens, H.,Sneave, E. 1991. Annex 14: Condensation and Energy, Final Report, International Energy Agency

Hens, H.,Sneave, E. 1996. Annex 24: Heat, air and moisture transfer through new and retrofitted insulated envelope parts, International Energy Agency

Holm, A. H. 2001. Determination of Accuracy of Instationary Hygrothermical Structural Calculation by Means of a Random Process. University of Stuttgart, Thesis,

Holm, A. H.,Kuenzel, H. M. 2002. Practical Application of an Uncertainty Approach for Hygrothermal Building Simulations - Drying of an AAC Flat Roof. Building and Environment.Vol. 37 pp.883-889.

Holm, A. H., Kuenzel, H. M.,Radon, J. 2001. Uncertainty Approaches for Hygrothermal Building Simulations - Drying of AAC in Hot and Humid Climates. Proceedings of the Performance of Exterior Envelopes of Whole Buildings VIII. Florida.

Huang, J., Winkelmann, F., Buhl, F., et al. 1999. Linking the COMIS Multi-Zone Airflow Model with the EnergyPlus Building Energy Simulation Program. Proceedings of the Building Simulation, pp.1065-1070. Kyoto, Japan.

HUD. 2004. Building Moisture and Durability: Past, Present and Future, Washington D.C., U.S. Department of Housing and Urban Development

Hukka, A.,Viitanen, H. A. 1999. A Mathematical Model of Mould Growth on Wooden Material. Wood Science and Technology.Vol. 33 pp.475-485.

ICC (2003). ICC Performance Code for Buildings and Facilities.

IEA. 1990. ANNEX 14, Condensation and Energy, Guidelines&Practice,

IEA. 1991. Annex 14: Condensation and Energy, Final Report, International Energy Agency,

IEA. 1996. Annex 24: Heat, Air and Moisture Transfer through New and Retrofitted Insulated Envelope Parts (Hamitie), International Energy Agency

Iman, R.,Helton, H. C. 1988. A Comparison of Uncertainty and Sensitivity Analysis Techniques for Computer Models. Risk Analysis.Vol. 8 (1), pp.71-90.

ISO. 1994. ISO EN 7730, Moderate Thermal Environment - Determination of the PMV and PPD Indices and Specification of the Conditions for Thermal Comfort, Geneva, International Standards Organization

ISO. 2001. ISO 13788, Hygrothermal Performance of Building Components and Building Elements (Internal surface Temperature to Avoid Critical Surface Humidity and Interstitial Condensation), ISO

Isukapalli, S. S. 1999. Uncertainty Analysis of Transport-Transformation Models. Chemical and Biochemical Engineering. Rutgers, The State University of New Jersey, Thesis. New Brunswick, New Jersey

Jennings, D. H.,Lysek, G. 1996. Fungal Biology: Understanding the Fungal Lifestyle. Oxford, Bios Scientific Publisher.

Jensen, S. O. 1993. Empirical Whole Model Validation Case Study: the PASSYS Reference Wall. Proceedings of the third International IBPSA Conference.

Jing, L., Aizawa, Y.,Yoshino, H. 2003. Experimental and CFD Studies on Surface Condensation. Proceedings of the Building Simulation 2003, pp.585-590. Eindhoven, Netherland.

Karagiozis, A., Desjarlais, A., H.M.Kunzel, et al. 2002. WUFI-ORNL/IBP Seminar: Boundary and Initial Conditions,

Karagiozis, A.,Salonvaara, M. 2001. Hygrothermal System-Performance of a Whole Building. Building and Environment.Vol. 36 pp.779-787.

Knapen, M.,Standaert, P. 1985. Experimental Research on Thermal Bridges in Different Outer Wall Systems. Proceedings of the CIB W40 meeting. Holzkirchen.

Knoll, B., Phaff, J. C.,Gids, W. F. d. 1995. Cp generator, TNO

Kowalski, W. J., Bahnfleth, W. P.,T.S.Whittam. 1999. Filtration of Airborne Microorganisms: Modelling and Prediction. ASHRAE Transaction.Vol. Part2 pp.4~17.

Krus, M., Sedlbauer, K., Zillig, W., et al. 2001. A New Model for Mould Prediction and its Application on a Test Roof. Proceedings of the Contribution to the II International Scientific Conference on "The current problems of building-physics in the rural building". Cracow, Poland.

Kuenzel, H. M., Karagiozis, A.,Holm, A. 2000. User's Guide: Windows program for WUFI ORNL/IBP Model, ORNL

Kulmala, M., Asmi, A. and Pirjola, L. 1999. Indoor Air Aerosol Model: the Effect of Outdoor air, Filtration and Ventilation on Indoor Concentrations. Atmospheric Environment.Vol. 33 (14), pp.2133-2144.

Kulmala, M., Raunemaa, T.,Tapper, U. 1987. Deposition of Indoor Aerosols as Determined by PIXE Analysis. Nuclear Instruments and Methods in Physics Research.Vol. 22 pp.337-339.

Kumaran, M. K. 1996. Final Report: Volume 3, ANNEX 24, Heat, Air and Moisture Transfer Through New and Retrofitted Insulated Envelope Parts, IEA

Kumaran, M. K. 1998. Interlaboratory Comparison of the ASTM Standard Test Methods for Water Vapor Transmission of Materials (E 96-95). Journal of Testing and Evaluation.Vol. 26 (2), pp.83-88.

Kumaran, M. K. 2002. A Thermal and Moisture Transport Database for Common Building and Insulating Materials, ASHRAE

Kunzel, H. M. 1995. Simultaneous Heat and Moisture Transport in Building Components. Fraunhofer Institute of Building Physics, Thesis,

Kunzel, H. M., Holm, A. H., Eitner, V., et al. 2000. WUFI-2D. Germany, Fraunhofer Institute for Building Physics

Kunzel, H. M., Karagiozis, A.,Holm, A. 2000. User's Guide: Windows program for WUFI ORNL/IBP Model, ORNL

Kunzel, H. M.,Kiessl, K. 1997. Calculation of Heat and Moisture Transfer in Exposed Building Components. Int. J. Heat Mass Transfer.Vol. 40 (1), pp.159-167.

Kunzel, H. M.,Sedlbauer, K. 2001. Biological Growth on Stucco. Proceedings of the Performance of Exterior Envelopes of Whole Buildings VIII. Florida.

Lee, A.,Barrett, P. 2003. Performance Based Building: First International State-of-the-Art Report, CIB

Liesen, R. J.,Pedersen, C. O. 1999. Modeling the Energy Effects of Combined Heat and Mass Rransfer in Building Elements: Part 1 - Theory. ASHRAE Transaction.Vol. 105 pp.941-953.

Lomas, K. J.,Eppel, H. 1992. Sensitivity Analysis Techniques for Building Thermal Simulation Program. Energy and Buildings.Vol. 19 pp.21-44.

Lstiburek, J. W. 1993. Moisture Control Handbook: Principles and Practices for Residential and Small Commercial Buildings. New York, John Wiley & Sons.

Macdonald, I. A. 2002. Quantifying the Effects of Uncertainty in Building Simulation. Department of Mechanical Engineering. University of Strathclyde, Thesis,

Macdonald, I. A., Clarke, J. A.,Strachan, P. A. 1999. Assessing Uncertainty in Building Ssimulation. Proceedings of the Sixth International IBPSA Conference.

Mass, J. V. D., Roulet, C. A.,Hertig, J. A. 1989. Some Aspects of Gravity Driven Air Flow through Large Apertures in Buildings. ASHRAE Transaction.Vol. 95 (Part 2), pp.573-583.

MathWorks, T. 2003. Matlab 6.5. Natick, MA

McQuay. 2001. School HVAC Design Manual, Staunton, McQuay

McQuiston, F. C.,Parker, J. D. (1994). Heating, Ventilating, and Air Conditioning: Analysis and Design. New York, John Wiley and Sons, Inc.

Meacham, B. 2001. Understanding Risk. Proceedings of the Australian Building Codes Board Conferences, Building Tomorrow's Future-International and National Partners. Canberra, Australia.

Mendes, N. 2002. A Simulation tool for hygrothermal analysis. Proceedings of the Indoor Air 2002. Monterey, USA.

Moon, H. J.,Augenbroe, G. 2003. Development of a Performance Indicator for Mold Growth Risk Avoidance in Buildings. Proceedings of the Healthy Building 2003. Singapore.

Moon, H. J.,Augenbroe, G. 2004. Future Research Needs for Mold Growth Risk Analysis. Proceedings of the CIB World Building Congress 2004. Toronto, Canada.

Morris, M. D. 1991. Factorial Sampling Plans for Preliminary Computational Experiments. Technometrics.Vol. 33 (2), pp.161-174.

Nakhi, A. 1995. Adaptive Construction Modelling Within Whole Building Dynamic Simulation. Department of Mechanical Engineering. University of Strathclyde, Thesis. Strathclyde

Nazaroff, W. W.,Cass., G. R. 1991. Protecting Museum Collections from Soiling due to the Deposition of Airborne Particles. Atmospheric Environment.Vol. 25A (5/6), pp.841-852.

Orme, M., Liddament, M. W.,Wilson, A. 1994. Numerical Data for Air Infiltration & Natural Ventilation Calculations, AIVC

Pasanen, A.-L., Juutinen, T., Jantunen, M. J., et al. 1992. Occurrence and Moisture Requirements of Microbial Growth in Building Materials. International Biodeterioration and Biodegradation.Vol. 30 pp.273-283.

Pasanen, A.-L., Kasanen, J.-P., Rautiala, S., et al. 2000. Fungal Growth and Survival in Building Materials under Fluctuating Moisture and Temperature Conditions. International Biodeterioration & Biodegradation.Vol. 46 (2), pp.117-127.

Persily, A. K. 1998. Airtightness of Commercial and Institutional Buildings: Blowing Holes in the Myth of Tight Buildings. Proceedings of the Thermal Performance of the Exterior Envelopes of Buildings VII, pp.829-837. Clearwater, FL, U.S.A.

Persily, A. K.,Ivy, E. M. 2001. Input Data for Multizone Airflow and IAQ Analysis, NIST

PHYSIBEL. 2002. KOBRA: User's guide, PHYSIBEL

Raunemaa, T., Kulmala, M., Saari, H., et al. 1989. Indoor Air Aerosol Model: Transport Indoors and Deposition of Fine and Coarse Particles. Aerosol Science and Technology.Vol. 11 pp.11-25.

Ritschkoff, A.-C., Viitanen, H.,Koskela, K. 2000a. The Response of Building Materials to the Mould Exposure at Different Humidity and Temperature Conditions. Proceedings of Healthy Building 2000.Vol. 3 pp.317-322. Espoo, Finland.

Robbins, C. A., Swenson, L. J., Nealley, M. L., et al. 2000. Health Effects of Mycotoxins in Indoor Air: A Critical Review. Applied Occupational and Environmental Hygiene.Vol. 15 (10), pp.773-784.

Rode, C.,Grau, K. 2001. Synchronous Calculation of Transient Hygrothermal Conditions of Indoor Spaces and Building Envelopes. Proceedings of the Seventh International IBPSA Conference, pp.491-498. Rio de Janeiro, Brazil.

Rousseau, J. 1983. Rain Penetration and Moisture Damage in Residential Construction, NRCC

Rowan, N., Johnstone, C., McLean, R. C., et al. 1999. Prediction of Toxigenic Fungal Growth in Buildings by Using a Novel Modelling System. Applied and Environmental Microbiology.Vol. 65 (11), pp.4814-4821.

Salonvaara, M., Karagiozis, A.,Holm, A. H. 2001. Stochastic Building Envelope Modeling - The Influence of Material Properties. Proceedings of the Performance of Exterior Envelopes of Whole Buildings VIII. Florida.

Saltelli, A., Andres, T. H.,Homma, T. 1993. Sensitivity Analysis of Model Output; An Investigation of New Techniques. Computational Statistics and Data Analysis.Vol. 15 pp.211-238.

Saltelli, A., Tarantola, S., Campolongo, F., et al. 2004. Sensitivity Analysis in Practice: A Guide to Assessing Scientific Models. John Wiley & Sons Ltd.

Sateri, J. 2004. Performance Criteria of Buildings for Health and Comfort, CIB, ISIAQ-CIB Task Group TG 42

Schild, P. G. 2003a. COMISexcel, Norwegian Building Research Institute

Schild, P. G. 2003b. Probabilistic Calculations by COMIS: Spreadsheet user interface and general guide, Norwegian Building Research Institute

Sedlbauer, K. 2001. Prediction of Mould Fungus Formation on the Surface of/and Inside Building Component. University of Stuttgart, Fraunhofer Institute for Building Physics, Thesis. Stuttgart, Germany

Sedlbauer, K. 2002. Prediction of Mould Growth by Hygrothermal Calculation. Journal of Thermal Envelope and Building Science.Vol. 25 (4), pp.321-335.

Sedlbauer, K.,Krus, M. 2002. Mold Growth on ETICS(EIFS) as a Result of "Bad Workmanship"? Journal of Thermal Envelope and Building Science.Vol. 26 (2), pp.117-121.

Sedlbauer, K., Krus, M.,Breuer, K. 2003. Biohygrothermal Method for the Prediction of Mould Growth: Procedure and Health Aspects. Proceedings of the Healthy Building 2003, pp.666-672. Singapore.

Seiffert, K. 1970. Damp Diffusion and Buildings: Prevention of Damp Diffusion Damage in Building Design. Essex, England, Elsevier Publishing Company.

Seppanen, O. 2001. Classification of Indoor Climate 2000. Target Values, Design Guidance and Product Requirement, Espoo, Finland, Finnish Society of Indoor Air Quality and Climate (FiSIAQ)

Shah, D. J. 2001. Effect of Mechanical Ventilation on Indoor Air Moisture Content. Proceedings of the IAQ 2001 'Moisture, Microbes and Health Effects: Indoor Air Quality and Moisture in Buildings'. San Francisco, CA.

Shakun, W. 1992. The Causes and Control of Mold and Mildew in Hot and Humid Climates. ASHRAE Transaction.Vol. 98 (pt 1), pp.1282-1292.

Shelton, B. G., Kirkland, K. H., Flanders, W. D., et al. 2002. Profiles of Airborne Fungi in Buildings and Outdoor Environments in the United States. Applied and Environmental Microbiology.Vol. 68 pp.1743-1753.

Smith, S. L.,Hill, S. T. 1982. Influence of Temperature and Water Activity on Germination and Growth of Aspergillus Restrictus and Aspergillus Versicolor. Transactions of British Mycological Society.Vol. 79 (3), pp.558-560.

Sohn, M. D., Sextro, R. G., Gadgil, A. J., et al. 2003. Responding to Sudden Pollutant Releases in Office Buildings: 1. Framework and Analysis Tools. Indoor Air.Vol. 13 (3), pp.267-276.

Strachan, P., Nakhi, A.,Sanders, C. 1995. Thermal Bridge Assessments. Proceedings of the 4th International IBPSA Conference Building Simulation. Madison.

Strand, R. K., Pedersen, C. O.,Crawley, D. B. 2001. Modularization and simulation techniques for heat balance based energy and load calculation programs: the experience of the ASHRAE LOADS toolkit and EnergyPlus. Proceedings of the Seventh International IBPSA Conference. Rio de Janeiro, Brazil.

Straube, J.,Burnett, E. (2001). Overview of Hygrothermal (HAM) Analysis Methods. Moisture Analysis and Condensation Control in Building Envelopes. H. Trechsel. West Conshohocken, ASTM.

Straube, J. F. 2002. Moisture in Buildings. ASHRAE Journal.

TenWolde, A. 2000. Mold and Decay in TriState Homes. Proceedings of the 2nd Annual Conference PATH Consortium for Wood-frame Housing in Cooperation with The Forest Products Society, pp.53-57. Madison, WI.

TenWolde, A. (2001). Manual Analysis Tools. Moisture Analysis and Condensation Control in Building Envelopes. H. Trechsel. West Conshohocken, ASTM.

Trechsel, H. R. (2001). Moisture Analysis and Condensation Control in Building Envelopes. ASTM Manual Series: MNL 40.

Trethowen, H. A. 1994. Three Surveys of Subfloor Moisture in NEW ZEALAND. ASHRAE Transactions.Vol. 1 pp.1427-1438.

U.S. Chamber Institute for Legal Reform. 2003. The Growing Hazard of Mold Litigation, U.S. Chamber Institute for Legal Reform

U.S. GSA. 2003. Facilities Standards for the Public Buildings Services, U.S. General Services Administration: Office of the Chief Architect

Viitanen, H., Hanhijarvi, A., Hukka, A., et al. 2000. Modeling mould growth and decay damages. Proceedings of the Proceedings of Healthy Buildings. Espoo, Finland.

Williams, P. R. D. (2001). The Risk Analysis Framework: Risk Assessment, Risk Management, and Risk Communication. Indoor Air Quality Handbook. J. D. Spengler, J. M. Samet and J. F. McCarthy. McGraw-Hill.

Wyss, G. D.,Jorgensen, K. H. 1998. A User's Guide to LHS: Sandia's Latin Hypercube Sampling Software, Albuquerque, NM, Sandia National Laboratories

Yik, F. W., Sat, P. S.,Niu, J. L. 2004. Moisture Generation through Chinese Household Activities. Indoor and Built Environment.Vol. 13 (2), pp.115-131.

VITA

Hyeun Jun Moon received his Bachelor of Science (1991) and Master of Science (1995) in the Department of Architecture from Hanyang University in Seoul, Korea. He has worked in Samsung Construction for five years as a researcher and has established the first large-scale experimental facility for research on Indoor Air Quality and Volatile Organic Compounds from building materials in Korea.

He started his Ph.D. in 2000 in the College of Architecture at Georgia Institute of Technology. While pursuing Ph.D., he has participated in several research projects including the Design Analysis Interface, GSA toolkit, US Courts Web. He has published 24 papers in referred journals and conference proceedings since 1994. He served as a scientific committee member in the Building Simulation conferences (2003 and 2005). He received the advanced study fellowship at the Oak Ridge National Laboratory in 2005.